ENDOCYTIC ACTIVITY IN SERTOLI CELLS OF THE RAT

by

Carlos Ramon Morales

A thesis submitted to the

Faculty of Graduate Studies and Research

in partial fulfilment of the requirements

for the degree of

Doctor of Philosophy

Department of Anatomy,
McGill University,
Montreal, Canada.

ENDOCYTIC ACTIVITY IN SERTOLI CELLS

ABSTRACT

The present study revealed that Sertoli cells were not only phagocytic cells but also active pinocytic elements which internalized by fluid-phase endocytosis tracers infused in the lumen of the seminiferous epithelium. The endocytosed tracers first reached large irregularly shaped, pale multivesicular bodies considered as endosomes, and later the tracers were seen in smaller, denser, spherical multivesicular bodies and in dense secondary lysosomes. Phagocytosis of the spermatid's cytoplasmic residual bodies appeared to be a specific process mediated by membrane-to-membrane interaction between the plasma membrane of the residual bodies and certain segments of the apical plasma membrane of the Sertoli cell. Fluid-phase pinocytosis seemed to be a constitutive process independent of microtubule polymerization and microfilament gelation, whereas phagocytosis of the residual bodies was dependent on microtubule integrity. The morphometric analysis revealed a low level of endocytic activity of Sertoli cells from stage II to stage VIII and a high level from stage IX to stage XIV, emphasizing the cyclic nature of this process. At stage IX of the cycle the secondary lysosomes fuse with phagosomes containing the cytoplasmic residual bodies. These observations clearly demonstrated a close relation of pinocytosis with phagocytosis in Sertoli cells.

Name: Carlos Ramon Morales

Title of Thesis: Endocytic activity in Sertoli cells of the rat

Department: Anatomy

Degree: Doctor of Philosophy

TABLE OF CONTENTS

Page

CHAPTER I: INTRODUCTION 1

CHAPTER II: REVIEW OF THE LITERATURE

(1) Structure and function of the Sertoli cell 3
(2) Morphometric studies on rat seminiferous tubules 8
(3) Endocytosis 9
a) - Definition - Classification - Description of the first step 9
b) - Endocytosis and membrane recycling 13
c) - Endocytosis and plasma membrane turnover 15
d) - Professional and facultative phagocytes 15
e) - Involvement of cytoplasmic contractile elements in phagocytosis 15
f) - Receptor - mediated phagocytosis 17
g) - Nonspecific receptor mediated phagocytosis 17
h) - The zipper model of phagocytosis 17
i) - Fluid-phase and adsorptive endocytosis - Marker studies . . 18

CHAPTER III: MATERIALS AND METHODS

SECTION 1: PROCEDURES FOR ELECTRON MICROSCOPY 24

(1) Tissue processing 24
a) - Fixation 24
b) - Embedding 24
c) - Sectioning and staining 25

(2) Identification of the stages of the cycle of the seminiferous epithelium 25

SECTION 2: MARKER STUDIES 29

(1) Choice of markers 29
(2) Markers to test fluid-phase endocytosis and doses used in the present study 29
(3) Preparation of HRP-colloidal gold complex 30
(4) Preparation of albumin and lactoalbumin-colloidal gold complex . 30
(5) Markers to test absorptive endocytosis and doses used in the present study 31
(6) Administration of the markers 31
(7) In vitro studies 31
(8) Non treated tissues 32

SECTION 3: EFFECT OF CYTOCHALASIN D AND COLCHICINE ON ENDOCYTOSIS IN SERTOLI CELL 32

(1) Choice of inhibitors 32
(2) Influence of colchicine and cytochalasin D on fluid-phase endocytosis 33
(3) Influence of colchicine and cytochalasin D on the phagocytosis of the spermatids cytoplasmic residual bodies 33

Page

SECTION 4: ANALYSIS OF THE DISTRIBUTION OF MICROFILAMENTS WITH SPECIAL REFERENCE TO THE PHAGOCYTOSIS OF THE RESIDUAL BODIES . . . 34

SECTION 5: CYTOCHEMISTRY 34

SECTION 6: MORPHOMETRIC AND STEREOLOGICAL METHODS 35

(1) Terminology 35
(2) Determination of volume ratios 35
(3) Sampling procedures 36
(4) Measurements 37
(5) Quantitative analysis 38
a) - Determination of the number of labelled secondary lysosomes per Sertoli cells 38
b) - True number of labelled lysosomes 39
c) - True volume of seminiferous epithelium in section 39
d) - Formula used in the computer program 40
e) - Determination of the total number of secondary lysosomes per Sertoli cells 41

(6) Corollaries 41
a) - Average volume of secondary lysosomes in Sertoli cells . 42
b) Total volume of secondary lysosomes and total volume of labelled secondary lysosomes per Sertoli cell at different stages of the cycle 43
c) - Percentage of labelled secondary lysosomes 44

(7) Correcting factors 44
a) - Thickness of the section 44
b) - Compression of the section 44
c) Magnification of the electron microscope and electron micrographs 45

CHAPTER IV: RESULTS

PART ONE

(1) Description of the apical processes of Sertoli cells 46
(2) Description of the lysosomal population and associated elements in Sertoli cells 47
(3) Distribution of the lysosomal elements in Sertoli cells during the stages of the cycle of the seminiferous epithelium 50
(4) Formation and phagocytosis of the cytoplasmic residual bodies 56
(5) Cytochemical studies 58
(6) HRP-colloidal gold complex (HRP-G), Native Ferritin (NF), Albumin, and Lactoalbumin-colloidal gold complex (Albumin-G and Lactoalbumin-G), and Concanavalin A in the presence of alpha-methyl-D-mannoside 66
(7) Cationic Ferritin (CF) and Concanavalin A-Ferritin (Con A-F) . 76
(8) Influence of colchicine on fluid-phase pinocytosis 76
(9) Influence of cytochalasin D on fluid-phase pinocytosis 78

Page

(10) Influence of colchicine on the phagocytosis of the cytoplasmic residual bodies 78
(11) Influence of cytochalasin D on the phagocytosis of the cytoplasmic residual bodies 80

PART TWO

(1) Number of secondary lysosomes per Sertoli cell 82
(2) Number of labelled secondary lysosomes per Sertoli cell . . . 83
(3) Average volume of secondary lysosomes 84
(4) Total volume of secondary lysosomes 85
(5) Total volume of labelled secondary lysosomes 85
(6) Percentage of labelled lysosomes per Sertoli cell 86

CHAPTER V: DISCUSSION 98

(1) Phagocytosis and pinocytosis in Sertoli cells; mechanism of uptake 99
a) - Phagocytosis of the cytoplasmic residual bodies 99
b) - Pinocytosis in Sertoli cells 101
(2) Intracellular pathway of the endocytosed materials 105
a) - Pinocytic pathway 105
b) - The phagocytic pathway 110
(3) Demonstration of cyclic endocytic activity in Sertoli cells . 115
a) - Number, volume and percentage of labelled lysosomes per Sertoli cell 115
b) - Total number and volume of secondary lysosomes per Sertoli cell 118
c) - Average volume of secondary lysosomes 120
(4) General summary and conclusions 121

LITERATURE CITED 123

LIST OF TABLES AND FIGURES

	Page
Table A	49
Table I	87
Table II	88
Table III	89
Table IV	90
Table V	90
Table VI	91
Figure 1	27
Figure 2	28
Figure 3	42
Figure 4	51
Figure 5	51
Figure 6	52
Figure 7	53
Figure 8	53
Figure 9	54
Figure 10	55
Figure 11	55
Figure 12	55
Figure 13	55
Figure 14	59
Figure 15	59
Figure 16	59
Figure 17	60
Figure 18	61
Figure 19	62
Figure 20	63
Figure 21	64
Figure 22	65
Figure 23	65
Figure 24	68
Figure 25	69

Page

Figure 26 69
Figure 27 69
Figure 28 70
Figure 29 70
Figure 30 71
Figure 31 72
Figure 32 73
Figure 33 74
Figure 34 74
Figure 35 74
Figure 36 74
Figure 37 74
Figure 38 74
Figure 39 75
Figure 40 75
Figure 41 75
Figure 42 77
Figure 43 77
Figure 44 77
Figure 45 79
Figure 46 79
Figure 47 81
Figure 48 81
Figure 49 81
Figure 50 81
Figure 51 81
Figure 52 81
Figure 53 92
Figure 54 93
Figure 55 94
Figure 56 95
Figure 57 96
Figure 58 97
Figure 59 112
Figure 60 113
Figure 61 114

Page

APPENDIX

Volumetric changes of Sertoli cells during the cycle of the seminiferous epithelium 140

Introduction 140

(1) Description of the ratios used in the present study 140

(2) Description of the morphometric estimations obtained by Wing and Christensen (1982) 141

(3) Estimation of the volume of Sertoli cells in relation to the stages of the cycle 144

(4) Comments on the volume of Sertoli cells reported by Wong and Russell (1983) 145

List of Tables and Figures

Table I-A 147

Table II-A 148

Figure 1-A 149

Literature Cited 150

To my wife, and to my parents

RESUME

L'utilisation de traceurs injectés dans la lumière des tubes séminifères nous a permis de démontrer que les cellules de Sertoli sont, en plus d'être des phagocytes, des cellules pinocytiques actives. Les traceurs d'abord incorporés dans de larges corps multivésiculaires pâles et de formes irrégulières, passent dans les corps multivésiculaires sphériques denses et enfin dans les lysosomes secondaires. La phagocytose des corps résiduels de spermatides est un processus qui résulte d'une interaction spécifique des membranes des corps résiduels et de la membrane des cellules de Sertoli. Alors que cette phagocytose dépend de l'intégrité des microtubules de la cellule de Sertoli la pinocytose est indépendante de l'état des microtubules ou des filaments cytoplasmiques de ces cellules. Une étude morphométrique des cellules de Sertoli au cours du cycle de l'épithélium séminifère a révélé une faible activité pinocytique du stade II au stade VIII du cycle tandis que l'activité pinocytique est élevée du stade IX au stade XIV du cycle ce qui démontre une évolution cyclique marquée du phénomène. Par ailleurs la phagocytose des corps résiduels se situe lors du stade IX du cycle au cours duquel on observe une réduction marquée du nombre des lysosomes secondaires qui paraissent se fusionner avec les phagosomes. Ces observations démontrent une relation étroite entre la pinocytose et la phagocytoses dans la cellule de Sertoli.

Nom: Carlos Ramon Morales

Titre de la thèse: Activité endocytique des cellules de Sertoli du rat.

Département: Anatomie

Diplôme: Docteur en Philosophie

ACKNOWLEDGEMENTS

I wish to sincerely thank Dr. Y. Clermont for his encouragement during this study and for his enthusiasm and valued criticism throughout the course of this investigation.

I want to express my gratitude to Dr. L. Hermo for his collaboration in the design of the experiments and for his continuous interest, and to Dr. N. J. Nadler for his help and his suggestions in many problems related to the quantitative studies.

My gratitude to Mr. A. Warshawsky for his help in computer programming and to the staff and personnel of the Electron Microscope Laboratory for their excellent technical assistance.

Many thanks to Mr. A. Graham for preparing the photographic reproductions and to Mrs. M. Oeltzschner for preparing the illustrations and graphs.

This work was supported through a grant from the Medical Research Council to Dr. Y. Clermont.

Chapter I
INTRODUCTION

Investigators interested in male fertility have given considerable attention during the last two decades to the Sertoli cells, i.e. the sustentacular cells of the seminiferous epithelium since it appears that the multiple functions of this cell permit the differentiation of spermatogonia into spermatozoa (Reviews by Fawcett, 1975; Parvinen, 1982). Amongst the several functions of these supporting cells one has been disclosed relatively soon after its discovery and description by Enrico Sertoli in 1865 and this is its capacity to phagocytose and eliminate from the seminiferous epithelium the residual cytoplasmic bodies which detach from the mature spermatids at the time of spermiation (Regaud, 1901). Thus this epithelial cell has the capacity to internalize substantial amounts of extracellular material and to efficiently and rapidly dispose of it. Although many electron microscopic descriptions of Sertoli cells have been published (Lacy, 1962; Dietert, 1966; Fawcett, 1975; Dym, 1972; Russell, 1977) the exact mechanisms of incorporation and disposal of spermatids' residual bodies and in particular the involvement of the lysosomal apparatus of these cells in this process, remains to be fully analyzed (Fawcett, 1975).

Recently, in a study of the endocytic activity of various types of epithelial cells of the male reproductive tract we have discovered that Sertoli cells are not only phagocytic cells but are also active pinocytic elements (Morales and Hermo, 1983; Hermo et al., 1983). In view of the increasing interest given to endocytosis of various cell types by cell biologists who describe a variety of mechanisms of internalization of macromolecules (fluid-phase, adsorptive, receptor-mediated; constitutive versus induced, etc.) (Reviews by Silverstein et al., 1977; Posner et al., 1982; Steinman et al., 1983), we have undertaken a detailed analysis of the

endocytic activity of Sertoli cells (both phagocytic and pinocytic) giving a special attention to the possible cyclicity of this activity in relation to the stages of the cycle of the seminiferous epithelium as a whole.

We have thus undertaken an investigation of the Sertoli cells from rat seminiferous epithelium with the electron microscope using a battery of electron dense tracers infused in the tubular lumen as well as morphometric analytical methods and a computer program to examine in detail the following problems: A) the exact mechanisms of internalization of residual bodies and of various tracers administered, B) the fate of the endocytosed material giving attention to the morphological characteristics and role of the lysosomal apparatus of these cells, C) the possible relation or integration of the phagocytic and pinocytic activity of Sertoli cells, D) the possible cyclic nature of the endocytic activity of Sertoli cells and the analysis of the significance of this phenomenon.

Chapter II
REVIEW OF THE LITERATURE

The principal aim of this review is primarily to present information on the structure and function of the Sertoli cell. Since one of the main purposes of this thesis was to evaluate the involvement of the Sertoli cell in endocytosis, it was considered of importance to present modern views on endocytosis as well and lastly to include a detailed analysis of the major progress in morphometry, an approach that will be utilized in our study of the seminiferous epithelium and of the Sertoli cell.

(1) Structure and function of the Sertoli cell

The Sertoli cell was discovered by Enrico Sertoli in 1865. This non-dividing cell is a tall element that extends from the base of the seminiferous epithelium to the lumen of the tubule. It presents numerous veil-like lateral processes that extend into the interstices between the spermatogonia, spermatocytes and spermatids. The basal portion of the cell is voluminous and is characterized by the presence of an irregularly shaped nucleus and abundant profiles of smooth endoplasmic reticulum (Fawcett, 1977). The endoplasmic reticulum is composed of interconnected tubular and flattened cisternae, some of the latter are associated to junctional complexes and subsurface specializations (Flickinger and Fawcett, 1969; Dym and Fawcett, 1970; Russell, 1977). Recently, Clermont et al. (1980) separated the endoplasmic reticulum present in the Sertoli cell cytoplasm around the heads of late spermatids (step 19) into two types: flattened cisternae and tubular cisternae communicating with each other to form a continuous network which undergoes deep structural modifications prior to spermiation. The Golgi apparatus is a juxtanuclear organelle formed by apparently separated stacks, each of which consisting of a few short, parallel saccules and associated small vesicles (Fawcett, 1975). In a more

recent work, Rambourg et al. (1979) analyzed the tridimensional structure of the Golgi complex, and by using metallic impregnation on thick sections, demonstrated communications between adjacent Golgi stacks via intersaccular connecting tubules. Lipid droplets, thin filaments, microtubules, glycogen granules, numerous spherical and elongated mitochondria are also evident within the Sertoli cell cytoplasm (Fawcett, 1975; 1977). In addition, the Sertoli cells contain clusters of membrane bound granules of different sizes and densities identified as lysosomes (Dietert, 1966; Reddy and Svoboda, 1967; Sapsford et al., 1969; Fawcett, 1975; Hermo et al., 1978; Lalli et al, 1984). The lysosomes are present in large numbers within the cytoplasm throughout the cycle of the seminiferous epithelium. These consist of large, often heterogenous, granular secondary lysosomes, multivesicular bodies and smaller or less spherical granules showing an electrodense core surrounded by a halo, believed to be primary lysosomes (Fawcett, 1975; Assaf, 1980). At most stages of the cycle the lysosomal clusters are located in the supranuclear region of the Sertoli cells next to the apex of the elongated nuclei of the late spermatids. However, at stages VI, VII and VIII (classification of Leblond and Clermont, 1952a), the lysosomes accumulate at the base of the Sertoli cell next to the plasma membrane. At stage IX some lysosomes appear to migrate toward the supranuclear region, probably merging with the residual bodies released by the late spermatids (Hermo et al., 1978).

Brokelmann (1963) described a peculiar structure between adjacent Sertoli cells located near the base of the seminiferous epithelium. These structures are called junctional specializations (Flickinger and Fawcett, 1967; Nicander, 1969). Generally the membranes of two adjacent Sertoli cells are separated by a space of 150 Å - 200 Å. However, at the level of

the junctional specializations they approach to within 20 Å of one another and form gap junctions or nexus. In addition, the plasma membrane of adjacent Sertoli cells forms tight junctions (Dym and Fawcett, 1970). Running parallel to the Sertoli cell plasma membranes in the areas of junctional specializations there are flat saccules or cisternae of endoplasmic reticulum sometimes presenting attached ribosomes. However, the outer aspect of the endoplasmic reticulum facing the plasma membrane is smooth and devoid of ribosomes (Flickinger and Fawcett, 1969). Between flat cisternae of ER and plasma membrane of adjoining Sertoli cells there are bundles of filaments which run parallel and at uniform distance of 500 Å - 600 Å. The filaments when viewed in cross section at high magnification usually exhibit a hexagonal arrangement (Flickinger and Fawcett, 1967; Dym and Fawcett, 1970). Dym and Fawcett (1970), Dym (1972) and Aoki and Fawcett (1975) demonstrated that the tight junctions of the junctional specializations formed an effective barrier that prevented the penetration of molecules of relatively large size.

The concept of the blood testis barrier was first presented in earlier physiological studies showing that when vital dyes and other substances were introduced into the blood stream they rapidly appeared in the testicular lymph but not in the fluid collected from the rete testis. Further insight was provided with the studies performed by Setchel (1967, 1969) and Setchel and Waites (1975) who demonstrated differences in protein, ionic and certain amino acid concentrations not only between the seminiferous tubules and the plasma, but also between the seminiferous tubules and the testicular lymph. With all these data it was postulated that a blood testis barrier associated with the seminiferous tubules was capable of excluding from the lumen of these tubules many substances normally present in the testicular blood and lymph (Setchel, 1967; 1969).

The precise localization of the blood-testis barrier was determined by the use of electron opaque markers such as ferritin, lanthanum, thorium dioxide, etc. (Dym and Fawcett, 1970) and more recently by the use of the enzyme horseradish peroxidase (Aoki and Fawcett, 1975). When these substances were injected interstitially or intravascularly the larger particulates were excluded by the peritubular myoid cells but the smaller ones were able to traverse clefts between myoid cells which are not closed by occluding junctions. Lanthanum and horseradish peroxidase reached the basal compartment of the seminiferous epithelium, entering the intercellular spaces surrounding spermatogonia, i.e. the interface between these germ cells and the Sertoli cells. However, these tracers were stopped by the occluding junctional complexes found between adjacent Sertoli cells (Flickinger and Fawcett, 1967). Therefore, Dym and Fawcett (1970) and Aoki and Fawcett (1975) demonstrated that the myoid layer constituted only a partial permeability barrier but that many of the cell-to-cell junctions were not closed and permitted the penetration of substances and tracers. These investigators also suggested that the junctional specialization at the interface of Sertoli cells was the most effective component of the blood-testis barrier. Thus, the ultrastructural analysis presented by Fawcett and his collaborators demonstrated in fact the exact area of exclusion of substances and macromolecules in the seminiferous epithelium. However, in physiological terms the blood-testis barrier has a more positive function than the simple exclusion of different types of macromolecules. For example, since the Sertoli cell is able to secrete fluids, proteins and ions, and the composition of the seminiferous tubular fluid is completely different from that of the plasma and lymph, one of the main functions of the blood-testis barrier is to create a special environment within the seminiferous tubules

(Tuck et al., 1970; Setchel, 1980; Lacroix et al., 1981; Wright et al., 1981; Kissinger et al., 1982; Ritzen et al., 1982; Skinner and Griswold, 1983; Wright et al., 1983). The barrier also regulates the movement of substances of endocrinological importance such as androgen binding protein (ABP) which appears highly concentrated in the seminiferous tubular fluids (Setchel 1980). However, one of the most important functions of the blood-testis barrier is to prevent the immunological system of the body from entering in contact with proteins produced by the haploid germ cells, including spermatozoa (Setchell, 1980). This is what occurs in some vasectomized men and may explain the difficulty observed in restoring fertility of these individuals even when the surgical problems are overcome (Alexander, 1977; Silber, 1978).

On the other hand, where the Sertoli cell is facing spermatogonia and preleptotene spermatocytes, the membranes of these cells run parallel at a distance of 150 - 200 Å and there are no junctional specializations (Flickinger and Fawcett, 1969; Dym and Fawcett, 1970).

Although it is obvious that the compartmentalization of the seminiferous epithelium results in the existence of a basal compartment housing the spermatogonia and preleptotene spermatocytes and an adluminal compartment housing the primary and secondary spermatocytes, and the spermatids, this compartmentalization cannot be maintained indefinitely. Thus, Sertoli cell junctions must open at certain stages of the cycle to allow the preleptotene spermatocyte to move from the basal to the adluminal compartment. With the displacement of these cells it seems likely that processes of neighboring Sertoli cells move beneath the preleptotene spermatocytes, coming in contact with each other and re-establishing the tight junctional complexes (Dym and Fawcett, 1970).

(2) Morphometric studies on rat seminiferous tubules

Morphometric information on seminiferous tubules is valuable to establish correlations between structural, physiological and biochemical findings.

One purpose of this thesis is to analyze the endocytic activity of the Sertoli cell using morphometric data. Therefore, it is necessary to review the key investigations that have contributed to the knowledge which will be utilized to tackle the present quantitative investigation.

Wing and Christensen (1982) in a very elegant and reliable investigation calculated the volume of the seminiferous epithelium of the rat per unit length of seminiferous tubule at various stages of the cycle. They found a prominent increase in volume of the whole epithelium at stage V followed by a significant diminution at stages VI and VII. The values remained low until stage XI. From stage XII the volume of the seminiferous epithelium per unit length of seminiferous tubule increased progressively and significantly, reaching a peak at stage V of the succeeding cycle. These authors also calculated the volume of the lumen per unit length of seminiferous tubule and found a significant increase between stages V and VIII, leading up to spermiation; these values were followed by a dramatic diminution in the luminal volume of seminiferous tubules which also occurred with a decrease in the tubular diameter. These observations suggested that the prominent decrease in diameter of seminiferous tubule was caused by a reduction of the luminal content rather than by the loss of the germinal cells of the epithelium, since the volume of the latter remained relatively constant over the portion of the cycle in which the tubule diameter was decreasing.

Bustos-Obregon (1970) showed that the number of Sertoli cells per given length of seminiferous tubules remained constant at stages II, IV, V and VII. From Sertoli cells counts in a whole mount of seminiferous tubule (Hermo, 1972) not only confirmed this observation but also extended it to the other stages of the cycle of the seminiferous epithelium of the rat.

Recently, Wing and Christensen (1982) calculated the number of Sertoli cells and major germ cell types per unit length of seminiferous tubule. These investigators found no significant differences in Sertoli cell number at the various stages of the cycle. Therefore, they concluded that the distribution of Sertoli cells was constant throughout the cycle in spite of the fluctuation in the size of the tubule.

The volume of the seminiferous epithelium and the number of Sertoli cell per unit length of seminiferous tubule (Wing and Christensen, 1982) were used in this investigation to calculate several ratios. Therefore, a detailed presentation of the morphometric method employed by these authors is made in the Appendix of this thesis (see page 141).

(3) Endocytosis

(a) Definition - Classification - Description of the first step.

Endocytosis is a widespread cellular function which refers to the uptake of substances into cells from the extracellular milieu by means of plasma membrane-derived vesicles (Silverstein et al., 1977; Tulkens, 1979; Posner et al., 1982; Steinman et al., 1983).

Endocytosis is usually subdivided into pinocytosis and phagocytosis (Silverstein et al., 1977; Tulkens, 1979; Posner et al., 1982). These two subclasses of endocytosis can be distinguished morphologically by the size

of the endocytic vesicle or vacuole formed (Tulkens, 1979). Pinocytosis (cell drinking) is characterized by vesicles having a diameter usually less than 1 μm, whereas phagocytosis (cell eating) involves the formation of much larger vesicles (Tulkens, 1979).

There are several physiological functions resulting from this endocytosis which include the removal of particles (e.g. bacteria and protein-aggregates), the bulk uptake of proteins and various extracellular substances and internalization of different ligands of plasma membrane receptors such as several peptide hormones, including insulin, prolactin, growth hormone, etc. (Bergeron et al., 1979; Kolb-Bachofen et al., 1982; Posner et al., 1982; Ciecnover et al., 1983).

Jacques (1969) and de Duve et al (1974) were the first to propose a theoretical model which describes the endocytosis of substances entering cells as a solute in the engulfed fluid (fluid-phase endocytosis) and/or after binding to the plasma membrane (adsorptive endocytosis). In fluid-phase endocytosis the uptake is directly related to the concentration of solute in the extracellular fluid, whereas in adsorptive endocytosis uptake depends on the number, affinity and function of the cell surface binding sites (Silverstein et al., 1977; Blok et al., 1981; Goud et al., 1981; Steinman et al., 1983; Morales et al., 1984). Adsorptive uptake is both a selecting and concentrating device whereby cells can internalize large amounts of specific solute without ingesting a correspondingly large volume of solution (Silverstein et al., 1977).

Binding of a substance to the plasma membrane may be, however, very specific, involving a limited number of sites of high affinity. Sly and Sthal (1978) proposed the distinction between receptor mediated endocytosis

and non-specific adsorptive endocytosis to call attention to the very high efficiency of the former mechanism in picking up and internalizing defined ligands. More evidence for the importance of binding sites in endocytosis has been provided by studies of receptor mediated endocytosis of different ligands such as low density lipoprotein (Brown and Goldstein, 1976; Anderson et al., 1977; Handley et al., 1983; Vasile et al., 1983), high density lipoprotein (Paavola and Strauss, 1983), alpha$_2$-macroglobulin (Pastan and Willingham, 1981; Dickson et al., 1982), asialoglycoprotein (Kolb-Bachofen et al., 1982; Tycko and Maxfield, 1982; Ciechanover et al., 1982, 1983; Geuze et al., 1983), peptide hormones (Bergeron et al., 1979, 1983; Haigler et al., 1979; Dunn and Hubbard, 1982; Cantin et al., 1982; Posner et al., 1982; Willingham and Pastan, 1982; Herzog, 1983; Willingham et al., 1983), immunoglobulins (Rodewald, 1973, 1980; Abrahamson and Rodewald, 1981; Douglas and King, 1982; King, 1982; Rodewald and Kaehenbuhl, 1982; Solari et al., 1982), transferrin (Hamilton et al., 1979; Wada et al., 1979; Galbraith et al., 1980; Zaman et al., 1980; Harding et al., 1983; Hamilton, 1983), etc.

Griffin and Silverstein (1974) and Griffin et al. (1975) demonstrated that phagocytosis of antibody coated particles by macrophages is a local event initiated by the binding of Ig to Fc receptors. Two types of particles were attached to the plasma membrane, one with a ligand that did not mediate endocytosis (e.g. complement) and another with an endocytotically active ligand (IgG). Only the latter particles were internalized. Similarly, asialofetuin adsorbed onto colloidal gold particles when incubated with freshly isolated Kupffer cells bound to the plasma membrane and later on was internalized via receptor mediated endocytosis (Kolb-Bachofen et al., 1982; Geuze, 1983). When asialofetuin was placed in the presence of N-acetyl-D-galactosamine which binds to the active sites of this ligand, the interaction

with its specific receptor and its subsequent uptake was abolished (Kolb-Bachofen et al., 1982). Based on these data, Griffin and Silverstein (1974) postulated that ligand binding generates a local transmembrane signal which activates contractile elements beneath the particle (induced endocytosis). The role of contractile elements was emphasized by the sensitivity of phagocytosis to cytochalasins (Blok et al., 1982; Steinman et al., 1983). This idea was further substantiated by results showing that di- or oligovalent ligands when incubated with lymphoid cells bound to uniformly distributed receptors on the cell surface that subsequently aggregated into "patches", collected into polar caps and finally endocytosed (Taylor et al., 1971; Geiger, 1983). It was established that patching, capping and endocytosis are temperature dependent, and the latter two were sensitive to inhibitors of metabolic energy (such as azide and dinitrophenol) and to microfilament-disrupting drugs such as cytochalasine (Taylor et al., 1971; Geiger, 1983). In contrast, fluid phase endocytosis is a constitutive activity in most cells (Steinman et al., 1983). Fluid-phase endocytosis proceeds at constant rates for long periods even in the absence of fluids in some cases (Steinman et al., 1983).

When endocytic vesicles enter the cells as coated or non-coated vesicles, they usually undergo fusion among themselves to give rise to larger, electron-lucent, smooth-surfaced vacuoles called endosomes (Abrahamson and Fearon, 1983; Jesaitis and Cochrane, 1983; Steinman et al., 1983). Endosomes are found in different cell types, even in cultured macrophages in the absence of ligand receptor interaction (Steinman et al., 1983). It has been suggested that the endosome is the principal site of receptor recycling in those cells capable of performing receptor mediated endocytosis (Wall and Hubbard, 1981). However,

there is no evidence that fusion of endocytic vesicles into larger vacuoles is required for membrane and receptor recycling, or even if most endocytic vesicles fuse with one another before fusion with other organelles such as lysosomes or Golgi apparatus (Steinman et al., 1983). Geuze et al. (1983) have chosen the term CURL (compartment uncoupled receptor ligand) instead of endosome. When the ligands have been discharged from the endosome membrane, it is suggested that the endosome has already acquired an acid pH. Endosomes are considered "pre-lysosomal" structures in the sense that they do not appear to contain acid hydrolases (Tycko and Maxfield, 1982). Several investigators have demonstrated that endosomes labelled with markers for fluid-phase endocytosis or receptor mediated endocytosis acquire acid hydrolases via primary lysosomes (Steinman et al., 1978; 1983; Van Deurs, 1978b; Wall et al., 1980; Nichols, 1982). In many instances the formation of multivesicular bodies has been described as an intermediate step between the transformation of an endosome into a typical dense acid-phosphatase rich secondary lysosome (Van Deurs, 1979a; 1979b; Van Deurs et al., 1981; Geuze et al., 1983; Morales and Hermo, 1983; Steinman et al., 1983). It appears that in some cells fusion between primary lysosomes and endosomes begins very early since it takes only 30 - 60 minutes to convert fully a pulse of endocytic vacuoles into dense, acid hydrolase-rich granules (Steinman et al., 1976; 1978; 1983).

(b) Endocytosis and membrane recycling

Although the idea of recycling of plasma membrane was initially proposed by Palade (1956), it was not until the work of Steinman et al. (1976) that evidence was provided to support this hypothesis. These authors showed that the total surface area of plasma membrane, pinocytic vesicle membrane

and secondary lysosomal membrane of mouse fibroblasts remained constant despite extensive internalization of the plasmalemma during pinocytosis. These results led Steinman et al. (1976) to propose that internalized membrane is recycled back to the cell surface. Quantitative analysis with horseradish peroxidase revealed that L-cell fibroblasts internalized the equivalent of their entire cell surface area once every 33 minutes (Steinman et al., 1976). This finding clearly indicates that the influx of membrane via pinocytic vesicles is considerable and that recycling must occur, rather than degradation and replacement of internalized plasma membrane. Muller et al. (1980; 1983) demonstrated that, when lactoperoxidase-latex vacuole membrane is radio-iodinated intracellularly, 80% of the label redistributes to the plasma membrane in 5 - 10 minutes. Recycling of asialoglycoprotein binding sites (Ciechanover et al., 1982; Tycko and Maxfield, 1982; Schwarts et al., 1982; Geuze et al., 1983) and insulin binding sites (Posner et al., 1981; Fehlman et al., 1982) requires only minutes. Despite the evidence that membrane receptors and pinocytosed solutes can recycle from pre-lysosomal compartment (receptosome, endosome, CURL, etc.) it is clear that solutes and ligands may also recycle from the lysosomal compartment (Steinman et al., 1983; Widnell and Kitson, 1983). Recently, Posner et al. (1982) have presented evidence to show the involvement of the Golgi apparatus in the endocytosis-recycling pathway.

Although the recycling is presumed to be vesicular (Silverstein et al., 1977; Posner et al., 1982; Douglas et al., 1983; Farquhar, 1983; Geuze et al., 1983; Smith and Jarett, 1983; Steinman et al., 1983), there is little evidence to support this (Douglas et al., 1983). One possible consequence of a vesicular mechanism of membrane retrieval from intracellular compartments is that some of the material in those compartments will be passively carried out

and released from the cell (Silverstein et al., 1977; Douglas et al., 1983; Steinman et al., 1983). This process has been called reflux or regurgitation (Steinman et al. 1983) and has been suggested to be mediated by exocytosis of recycling vesicles (Silverstein et al., 1977; Steinman et al., 1983).

(c) Endocytosis and plasma membrane turnover

Since endocytosis brings the plasma membrane into a degradative compartment (lysosomal compartment), it has long been suspected that this process contributes to the turnover of plasma membrane (Silverstein et al., 1977).

(d) Professional and facultative phagocytes

Ravinovitch (1968) has applied the term "professional phagocytes" to polymorphonuclear leukocytes and mononuclear phagocytes because they have made a full-time occupation of eating. However, professional phagocytes are not the only cells that internalize particles, fibroblasts, neurons and a variety of epithelial cells also ingest particles (Silverstein et al., 1977). Ravinovitch (1968) has referred to these cells as "facultative or nonprofessional phagocytes".

e) Involvement of cytoplasmic contractile elements in phagocytosis

Professional phagocytes contain actin and myosin and there is little doubt that these proteins play a central role in the phagocytic process. Microfilaments have been identified in association with the plasma membrane of amoebae and macrophages. Cytochalasin B, a compound that impairs actin gelation and microfilament function, inhibits phagocytosis (Axiline and Reaven, 1974).

The direct involvement of microtubules in phagocytosis is rather controversial (Geiger, 1983). Several authors have reported that compounds such as colchicine, which depolymerizes cytoplasmic microtubules, do not

inhibit phagocytosis and cause, at most, a small reduction of the "basal" pinocytic activity (Bhisey and Freed, 1971; Silverstein et al., 1977). However, it has been shown that microtubular organization may be modulated by capping of surface receptors with specific antibodies (Yahara and Kakimoto-Sameshima, 1978).

Recently, Fawcett and Doxey (1982) have reported that the entry of sporozoites (of Theileria parva) into cultured lymphocytes differs in several respects from phagocytosis by "professional" phagocytes. They pointed out that in a macrophage there is clear ultrastructural evidence of contractile activity as evidenced by the early appearance of a thickened zone of ectoplasm immediately subjacent to the protozoa being ingested. As the area of membrane contact enlarges, this actin-rich zone of peripheral cytoplasm spreads laterally and extends into conspicuous pseudopods that advance over the surface of the parasite until it is surrounded and finally engulfed. This local polymerization of actin and/or assembly of other cytoskeletal elements beneath the enveloping phagocyte membrane results in a prominent ectoplasmic zone from which ribosomes and membranous organelles of the cytoplasm are largely excluded. In contrast, these authors showed that in lymphocytes (a non-professional phagocyte) phagocytosis of sporozoites seemed to be a simple consequence of a propagation of the membrane-to-membrane interaction from the initial site of contact around the surface of the sporozoite, followed by fusion of the host cell membrane above the parasite to close the opening of the invagination. Thus, Fawcett and Doxey (1982) concluded that in this particular facultative phagocyte the entry process involves a sequential interaction of specific membrane receptors with ligands uniformly distributed over the surface of the parasite, which is not mediated by contractile elements.

(f) Receptor-mediated phagocytosis

Several types of pathogenic bacteria have surface structures (capsules) that inhibit their binding and phagocytosis by professional phagocytic leukocytes. On the other hand, non-pathogenic strains of the same bacteria (non-encapsulated) lack these phagocytosis-inhibiting surface structures and are readily ingested by phagocytic leukocytes (Davis et al., 1973).

The response of a host to an infection by pathogenic bacteria is characterized by the production of antibodies and complement serum proteins that coat the surface of the bacteria and promote its ingestion by professional, but not by facultative phagocytes (Ravinovitch, 1969). For example, the interaction between IgG with a specific antigenic particle stimulates its ingestion by these cells since the Fc portion of the IgG molecule is responsible for this activity. Thus the membrane of phagocytic leukocytes contains receptors that are specific not only for the Fc fragment (Fc receptors) but also for the third component of the complement and other substances (Askenase and Hyden, 1974).

(g) Nonspecific receptor mediated phagocytosis

The ingestion of particles such as zymosan, silica, latex, etc., is performed by both professional and facultative phagocytes (Silverstein et al., 1977). The cell-surface factors that mediate ingestion of these artificial particles have been called nonspecific phagocytic receptors. In the case of professional phagocytes these nonspecific receptors have been distinguished both functionally (Griffin et al., 1979) and metabolically (Michl et al., 1976) from the Fc and C_3 (third component of the complement) receptors.

(h) The Zipper model of phagocytosis

Griffin et al. (1975) have demonstrated that the initial interaction of immune ligands on the surface of a particle with receptors on the membrane

of phagocytic leukocytes does not trigger the ingestion of the particle. It merely initiates a process that requires the continuous apposition of receptors and ligands until the particle is fully enclosed within a phagocytic vacuole. Griffin et al. (1975; 1976) have termed this process the "zipper mechanism" of phagocytosis. The model proposes the following steps: a) Ligand-receptor interaction which generates a signal (perhaps the release of actin-binding protein from the membrane) that initiates the aggregation of contractile proteins and leads to the extension of pseudopods in the area of the attached particle. b) Pseudopod extension leads to further receptor-ligand interaction and this in turn leads to further aggregation of contractile proteins. c) The process may be repeated many times until the plasma membranes meet and fuse with one another, forming a phagocytic vacuole.

(i) Fluid-phase and adsorptive endocytosis - Marker studies

One of the main subjects of this thesis is the study of the endocytic behaviour of the Sertoli cell with special reference to a possible cyclical variation. A discussion of the tracers used to test fluid-phase endocytosis and adsorptive endocytosis, especially those employed in this investigation, is essential as a background for these studies. Therefore, the following section contains a brief review of the key investigations which have contributed to our present knowledge of these markers.

By definition, fluid-phase endocytic vesicles are those labelled after brief exposure to an impermeable solute that does not bind to the plasma membrane (Steinman et al., 1983). One of the most useful cytologic tracers to study fluid phase endocytosis is the enzyme horseradish peroxidase (HRP), a glycoprotein with a molecular weight of 40,000 daltons (Steinman and Cohn,

1972; Steinman et al., 1974; Silverstein et al., 1977; Simionescu and Simionescu, 1978; Blok et al., 1981; Goud et al., 1981; Raikhel and Lea, 1982; Morales and Hermo, 1983; Storrie et al., 1983; Morales et al., 1984). HRP was initially used as a tracer by Strauss (1957) at the light microscopic level to test the uptake of proteins by the epithelial cells of the proximal convoluted tubules of the kidney. Graham and Karnovsky (1966) extended the use of HRP to electron microscopic investigation by using diaminobenzidine (DAB) as an electron-donor. Morales and Hermo (1983) were the first to use HRP-colloidal gold complex prepared according to the procedure of Geoghegan and Ackerman (1977) to demonstrate the capacity of the Sertoli cell and epithelial cells of the rete testis and ductuli efferentes to take up this protein via fluid-phase endocytosis. The use of HRP-colloidal gold complex, which presents itself under the electron microscope as a uniformly dense spherical particle of regular dimension, greatly facilitates the identification and localization of the HRP labelled molecules within the cells. On the other hand, when DAB is used to demonstrate HRP, two experimental conditions are required. Firstly, the enzymatic activity of HRP has to be preserved; consequently the fixative has to be of low concentration (e.g. 1 - 2% glutaraldehyde). Secondly, since DAB can react with endogenous peroxidase, proper controls have to be performed to distinguish the peroxidases of both sources (Bainton and Farquhar, 1968; Venkatochalam et al., 1970; Anderson et al., 1975; Herzog, 1979; Anderson and Burnett, 1979; Hand, 1979). In this regard HRP-colloidal gold complex avoids the use of DAB and since the enzymatic activity of HRP does not need to be preserved, the fixatives can be used at higher concentrations (Morales and Hermo, 1983).

Native ferritin (NF) is another marker that has been shown to be incorporated by fluid-phase endocytosis (Farquhar, 1978; Peress and Tompkins,

1981; Gonella et al., 1982; Hermo et al., 1982; Morales et al., 1984). Farqhuar (1978) was the first who made the interesting observation that cationic ferritin (CF) and NF were internalized by rat anterior pituitary cells to different compartments depending on the charge of the marker. Thus, native ferritin which did not bind to the plasma membrane, was rapidly concentrated in secondary lysosomes, whereas cationic ferritin was taken up into Golgi cisternae as well as lysosomes after its internalization by adsorptive endocytosis. Similarly, immunocytochemical studies demonstrated that albumin does not bind to the plasma membrane of the hepatocyte and that it is incorporated by fluid-phase endocytosis in this cell as well as in other cell types (Besterman et al., 1983; Douglas et al., 1983; Morales et al., 1984). Concanavalin A in the presence of 0.2M of alpha-methyl-D-mannoside does not interact with the plasma membrane since this sugar binds to the active sites of the lectin (Nicolson, 1972, 1974; Goldstein, 1975; Gillouzo and Feldmann, 1977; Roth and Wagner, 1977; Brown and Hunt, 1978; Ichev and Ovtscharoff, 1981; Pinto da Silva, 1981; Welsch and Schumacher, 1983; Morales et al., 1984) and can be used to demonstrate fluid-phase endocytosis (Morales et al., 1984).

Recently, in vitro experiments performed on material fixed by perfusion with 5% glutaraldehyde, sectioned (75 μm) with a tissue chopper and then incubated with different tracers (including the above mentioned) showed that HRP-colloidal gold complex, albumin-colloidal gold complex, native ferritin and Con A-ferritin complex (Con A-F) in the presence of alpha-methyl-D-mannoside did not bind to the apical plasma membrane or to the membrane of the invaginating pits of the rat rete testis epithelium. However, in vivo intraluminal injection showed that these tracers were actively taken up by fluid-phase endocytosis (Morales et al., 1984).

In contrast, there are several other ligands which not only bind to the plasma membrane of the endocytic vesicles but are also incorporated by adsorptive endocytosis. Thus, adsorption to the endocytic vesicles membrane provides a mechanism for enhancing the efficiency with which the substrates are cleared from the extracellular space (Silverstein et al., 1977; Tulkens, 1979; Steinman et al., 1983). However, one cannot assume that simple binding to the plasma membrane is necessarily followed by uptake, since the adsorbed material must be attached to the segment of plasma membrane that is internalized (Steinman et al., 1983).

Cationic ferritin has been extensively used to test adsorptive endocytosis (Farquhar, 1978; Moller and Chang, 1978; Hewit et al., 1979; Spicer et al., 1979; Denef and Ekholm, 1980; Blok et al., 1981; Van Deurs et al., 1981; Anderson and Batten, 1982; Gronblad et al., 1982; Jersild, 1982; Van Deurs and Nilausen, 1982; Brac, 1983; McLean and Sanders, 1983; Nilsson and Van Deurs, 1983; Morales et al., 1984). CF is a polycationic derivative of ferritin useful for labelling of negative charges on cell surfaces (Danon et al., 1972; Skutelsky et al., 1977; Simionescu and Simionescu, 1978; Andrews, 1981; Jakoi et al., 1981; Peress and Tompkins, 1981; Anderson and Batten, 1982; Brac, 1983; Johanson, 1983; Marikovsky et al., 1983). It was introduced by Danon et al. (1972) by coupling horse spleen ferritin with N,N dimethyl-1,3 propanedamine (DMPA) via carbodiamide activation of the protein carboxyl groups. Thus, most of the carboxyl groups on the ferritin molecule are converted into positively charged tertiary amino groups. CF has a diameter of approximately 100 Å and it is easily identified due to its uniform electron-dense iron core.

Similarly, the lectins (sometimes called phytohemagglutinins or phyto-agglutinins) bind to specific carbohydrate containing sites on the cell surface.

Lectins were primarily used to investigate human blood groups, activation of lymphocytes, structural and functional differences of the cell surface membranes of normal and tumor cells, selective agglutination, etc. (Nicolson, 1974; Brown and Hunt,1978). In addition, some lectins such as Concanavalin A, have been used to study their internalization by adsorptive endocytosis in different cell types (Yokoyama et al., 1980; Imamura et al., 1981; Salisbury et al., 1981; Willingham et al., 1981; Leak and Sun,1983; Morales et al., 1984). Con A has been shown to bind specifically to alpha-D-mannose and alpha-D-glucose residues present on the glycocalix of several cell types (Nicolson et al., 1972; Nicolson,1974; Gillouzo and Feldmann,1977; Roth and Wagner,1977; Brown and Hunt,1978; Virtanen et al., 1978; Ichev and Ovtscharoff, 1981; Pinto da Silva et al., 1981; Chavez and Enders,1982).

In recent investigations Morales et al (1984) observed that CF and Con A were internalized by the epithelial cells of the rete testis after their binding to the plasma membrane of apical pinocytic vesicles. CF and Con A were rapidly concentrated into multivesicular bodies and dense secondary lysosomes and/or trancytosed* by transepithelial vesicular transport to lateral or basal intercellular spaces. In contrast, the tracers internalized

---

*The term "trancytosis" was introduced by Simionescu (1979) to explain the uptake of substances by means of endocytic vesicles emerging from the luminal side of capillary endothelium which in successive steps travels in the endothelial cytoplasm and finally opens in the abluminal cell front. Consequently, this process is carried out by vesicles that bypass the tight junctions and the lysosomal compartment. The process couples endocytosis and exocytosis at different plasma membrane domains (Herzog,1983). Trancytosis, however, is synonymous with the term "transepithelial vesicular transport" introduced by Palade several years before, working on transport of macromolecules by endothelial cells (Palade,1960; Bruns and Palade,1968). Trancytosis or transepithelial vesicular transport has been observed in many other different cell types such as thyroid follicle cells (Herzog,1983), intestinal epithelium (Rodewald,1973; 1980; Jersild,1982); choroid plexus epithelium (Van Deurs et al., 1981), rete testis epithelium (Morales et al., 1984), syncytial trophoblastic cells (King,1982), hepatocyte (Reston et al., 1980), etc.

by fluid-phase endocytosis, i.e., HRP and albumin colloidal gold complex, NF, and Con A in the presence of alpha-methyl-D-mannoside, were concentrated only in the lysosomal apparatus of the cell and were never seen in vesicles attached to the lateral or basal plasma membranes or in the pericellular spaces. Thus, this data confirmed the existence of two different pathways taken by the tracers via two distinct endocytic processes already demonstrated in several types of cells (Rodewald, 1973; 1970; Van Deurs et al., 1981; Jersild, 1982; Steinman et al., 1983).

Chapter III

MATERIALS AND METHODS

SECTION 1: PROCEDURES FOR ELECTRON MICROSCOPY

(1) Tissue processing

(a) Fixation

Adult male albino rats (350-450 g) were anesthetized by intra-abdominal injections of 0.2 ml of sodium pentobarbital, and their testes were fixed by perfusion through the abdominal aorta with 5% glutaraldehyde buffered in sodium cacodylate (0.1M) containing 0.5% $CaCl_2$ (pH 7.2). Fixed testes were then excised and cut into 1 mm^3 cubes which were stored in fixative for an additional 2 hours at 4°C, rinsed for 24 hours in several changes of cold buffer and post-fixed for 1 hour in ferrocyanide-reduced osmium (Karnovsky 1971), a mixture of 1% aqueous OsO_4 in 1.5% aqueous potassium ferrocyanide, prepared immediately before use.

(b) Embedding

Following post-fixation, the tissue was dehydrated through a series of ethanol dilutions increasing in concentration from 50% to 100%. The dehydrated tissue was then immersed in propylene oxide and finally infiltrated with a mixture of plastic resins consisting of 17 g Epon, 10 g DDSA, 8.5 g NMA and 0.75 ml DMP-30. This mixture will be referred to as "epon". Infiltration was performed by immersion of tissue in progressively more concentrated solutions of epon diluted with propylene oxide, and finally in pure epon. Fully infiltrated tissue cubes were then embedded in pure epon in "beem capsule" molds which were placed in a 60°C oven overnight for hardening. The resulting plastic blocks containing the tissue were trimmed on an automatic trimmer, and used for semithin and thin sectioning.

(c) Sectioning and staining

Semithin sections (0.5 µm thick) were cut on an ultramicrotome and transferred to clean glass slides which were placed on a hot plate adjusted to about 100°C. Sections were stained for 1 minute with freshly-filtered toluidine blue stain, prepared by adding 1 gm of toluidine blue and 1 gm of sodium borate to 100 ml of distilled water. These slides were used for selection of portions of seminiferous tubules suitable for observation by electron microscopy. Seminiferous tubules were selected in each stage of the cycle of the seminiferous epithelium, using the classification of Leblond and Clermont (1952). Blocks containing the chosen portions of seminiferous tubules were trimmed of excess tissue in preparation for thin sectioning.

Thin sections, with a silver interference colour, were cut on an automatic ultramicrotome, using a diamond knife, and mounted on 200 mesh copper grids. Thin sections were routinely stained for electron microscopy with 4% alcoholic uranyl acetate for 5 minutes, followed by lead citrate for 2 minutes. Lead citrate was prepared by mixing 0.03 g of lead citrate with 0.1 ml of 10N sodium hydroxide and 10 ml of distilled water.

(2) Identification of the stages of the cycle of the seminiferous epithelium

A precise identification of the different stages of the cycle of the seminiferous epithelium of the rat was performed on semithin epon sections. This was possible by using a system of classification of the germ cells which was proposed by Leblond and Clermont (1952a, b). As shown by several authors (see review, Clermont, 1972), the cycle of the seminiferous epithelium can be divided into a constant number of cellular associations or stages. The seminiferous epithelium is a renewing epithelium formed by a basal layer of stem and immature cells (spermatogonia) and several layers

of differentiating cells (spermatocytes and spermatids) at various stages of development. A steady-state system exists in which spermatogonia divide by mitosis giving rise to all of the other cells, and haploid spermatozoa are periodically released into the lumen of the seminiferous tubule. As a result of this structural arrangement, a given area of seminiferous tubule is populated by a distinct "cellular association".

In the rat, 14 stages of the cycle of the seminiferous epithelium have been characterized, each formed by several generations of germ cells where a generation is defined as a group of cells at the same step of development. As a consequence, any stage will be contributed by one generation of spermatogonia resting directly on the basal lamina adjacent to the Sertoli cell, one or two generations of spermatocytes generally located above the layer of spermatogonia, and one or two generations of spermatids found near the lumen. These specific cellular associations have constant duration (Clermont et al, 1959; Clermont and Harvey, 1965). The complete succession of cellular associations or stages in a given area of the epithelium between two successive appearances of the same cellular association has been termed the "cycle of the seminiferous epithelium" (Leblond and Clermont, 1952a, b).

Since the selection of the corresponding stages was performed on semithin sections stained with toluidine blue, in the present investigation the same criteria proposed by Clermont and Rambourg (1978) were used to classify the stages of the cycle. Accordingly, in such sections the developing acrosomic system of spermatids in the course of spermiogenesis is stained deep blue, and the steps of its formation and evolution were used to characterize the various cellular associations occurring in the rat (see

Figure 1

Drawings of the steps of spermiogenesis of the rat as seen in semithin sections of glutaraldehyde-fixed testes stained with toluidine blue or iron hematoxylin. The numbers given to the steps of spermiogenesis correspond to those proposed in the classification of Leblond and Clermont (1952).

During the Golgi and cap phases (steps 1-7) the perinuclear Golgi apparatus elaborates the cap-like acrosomic system. At the opposite pole, the centrioles give rise to the growing flagellum, and attach to the nuclear surface. The mitochondria are seen as small dots along the plasma membrane.

During the acrosome phase (steps 8-14) the nucleus elongates and progressively assumes a characteristic sickle shape. The bulk of the cytoplasm accumulates as a lobe around the flagellum which is attached to the base of the nucleus. The caudal tube or manchette, inserted around the base of the nuclear, appears in step 7 where it is seen as thin lines on either side of the flagellum. It elongates and is present throughout this phase. The Golgi apparatus leaves the nuclear region in step 8 and is subsequently located in the cytoplasmic lobule.

During the maturation phase (steps 15-19) the spermatid completes its transformation into a spermatozoon (step 19). Following displacement of the annulus, late in step 15, from the neck region to the extremity of the cytoplasmic lobe, the mitochrondria form the mitochondrial sheath around the flagellum. The caudal tube disappears in step 15. The Golgi apparatus undergoes dissolution (step 17 or 18) and clusters of lipid droplets appear in the cytoplasm. The bulk of the periflagellar cytoplasm is displaced toward the head of the spermatid and ultimately is detached to form the residual body (steps 18a and 19, RB). A small droplet of cytoplasm remains associated with the neck region (step 19).

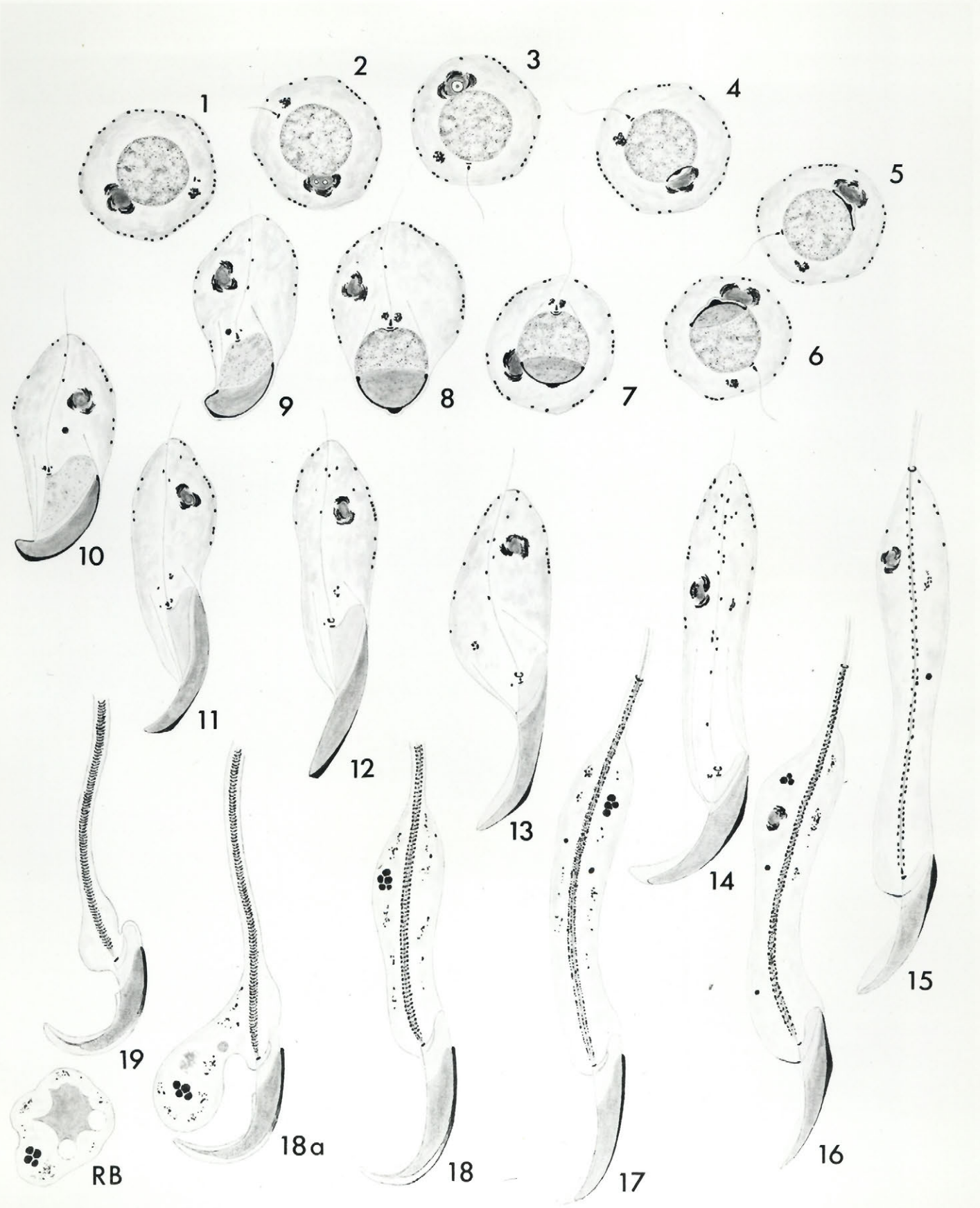
1
2
3
4
5
6
7
8
9
10
11
12
13
14
15
16
17
18
18a
19
RB

FIGURE 2

The 14 cellular associations or stages observed in the seminiferous epithelium of the rat. Each vertical column, depicted by a Roman numeral, represents a cellular association and shows the various cell types present at that stage. The stages of the cycle are identified by means of 14 of the 19 steps of spermiogenesis (numbers 1 to 19). These steps are defined by the changes observed in the nucleus and acrosomic system in semithin sections (0.5 μm thick) stained with toluidine blue.

The cellular associations or stages of the cycle succeed one another in time in any given area of the seminiferous epithelium according to the sequence indicated from left to right in the figure. Following stage XIV, stage I reappears so that the sequence starts over again. The succession of the 14 stages makes up the cycle of the seminiferous epithelium. The duration of each stage in hours is also given. The mitotic divisions of the spermatogonia are indicated by the letter M.

The germ cells present are:

A_1, A_2, A_3, A_4	- Type A spermatogonia
In	- Intermediate-type spermatogonia
B	- Type B spermatogonia
Pl	- Preleptotene primary spermatocytes
L	- Leptotene primary spermatocytes
Z	- Zygotene primary spermatocytes
P	- Pachytene primary spermatocytes
Di	- Diplotene primary spermatocytes
II	- Secondary spermatocytes
1 to 19	- Steps of spermiogenesis

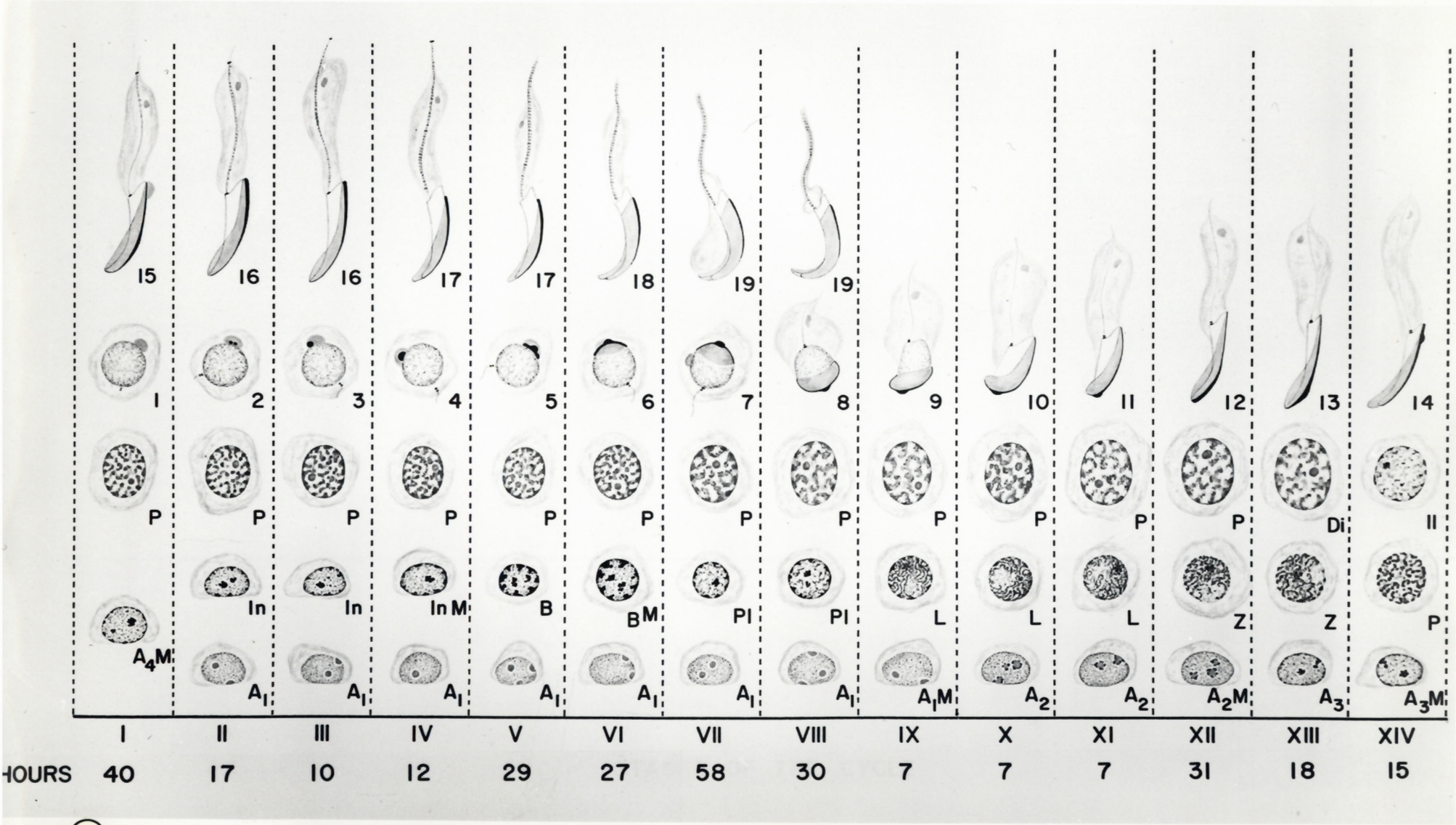
15
16
16
17
17
18
19
19
1
2
3
4
5
6
7
8
9
10
11
12
13
14
P
P
P
P
P
P
P
P
P
P
P
P
Di
II
In
In
In M
B
B M
PI
PI
L
L
L
Z
Z
P
A4M
A1
A1
A1
A1
A1
A1
A1
A1M
A2
A2
A2M
A3
A3M
I
II
III
IV
V
VI
VII
VIII
IX
X
XI
XII
XIII
XIV
HOURS
40
17
10
12
29
27
58
30
7
7
7
31
18
15

Figure 1). In order to clearly identify the different stages of the cycle of the seminiferous epithelium of the rat, other characteristics were taken into account such as the structural arrangement of the flagellar components, the orientation of the late spermatids (steps 15-19) in the seminiferous epithelium, the presence of spermatids' cytoplasmic residual bodies in the luminal aspect and within the Sertoli cells, and the appearance of the spermatocyte nucleus. The schematic representation of the 14 cellular associations observed in each stage of the cycle is shown in Figure 2.

SECTION 2: MARKER STUDIES

(1) Choice of markers

The marker experiments were designed primarily to test fluid-phase and adsorptive endocytosis by the Sertoli cell of the rat testis, to analyze the intracellular endocytic pathway and to determine the endocytic behaviour of the Sertoli cell in relation to the stages of the cycle of the seminiferous epithelium.

(2) Markers to test fluid-phase endocytosis and doses used in the present study

To test fluid-phase endocytosis, the following tracers were used: Native ferritin (NF, Miles Laboratories), 0.3 mg in 0.1 ml of physiological saline pH 6.8; 0.3 mg of Concanavalin A conjugated with ferritin (Con A-F, Miles Laboratories) in 0.1 ml of sodium phosphate buffer (pH 7.2) containing 0.1M alpha-methyl-D-mannoside; horseradish peroxidase-colloidal gold complex (HRP-G) prepared according to the procedure of Ackerman and Freeman (1979) (Type II HRP, Sigma Chemical Company) at a dose of 0.8 mg in 0.1 ml phosphate buffer at pH 7.4 (see preparation below); bovine serum albumin or lactoalbumin-colloidal gold complex (albumin-G and lacto-albumin-G) prepared according to the method of Bendayan (1981) at a dose of 0.13 mg of albumin-G or lactoalbumin-G in 0.1 ml phosphate buffer at pH 7.4.

(3) Preparation of HRP-colloidal gold complex

A colloidal gold suspension was prepared according to the method of Ackerman and Freeman (1979) by adding 0.1 g of chlorauric acid to 1 litre of boiled distilled water. The suspension was stirred vigorously and 25 ml of 1% aqueous trisodium citrate, a reducing agent, was rapidly added. After cooling, the pH of the solution was adjusted to pH 7.2. Then the HRP-colloidal gold complex was prepared by the method of Geoghegan and Ackerman (1977) dissolving 8 mg of HRP (Type II, Sigma Chemical Company) in 5 ml of triple distilled water. This solution was added slowly to 200 ml of the colloidal gold suspension. After mixing for 1 minute, 2 ml of 1% aqueous polyethylene glycol was added to prevent aggregation of the forming HRP-colloidal gold complexes. The solution was centrifuged at 1,500 rpm for 20 minutes to remove large aggregates of HRP-colloidal gold complexes. The supernatant was then centrifuged at 11,500 rpm for 1 hour at 4°C. After discarding the supernatant, the pellet of HRP-colloidal gold was resuspended in phosphate buffer (pH 7.4) with 4% polyvinylpyrrolidone containing 0.2 mg/ml polyethylene glycol and recentrifuged at 11,500 rpm to separate any unlabelled HRP from the HRP-colloidal gold complexes. Following this final centrifugation the supernatant was discarded and the pellet of the colloidal gold labelled protein was suspended in 10 ml of the same buffer and stored.

(4) Preparation of albumin and lactoalbumin-colloidal gold complex

The albumin and lactoalbumin-colloidal gold complex were prepared following the procedure of Bendayan (1981): 0.5 mg of albumin or lactoalbumin (Sigma Chemical Company) dissolved in 0.1 ml of distilled water, was added to 10 ml of the gold suspension at pH 7.3. After centrifugation (25,000 rpm during 30 minutes), the sediment was resuspended in 0.3 ml of PBS (pH 7.4) containing 0.2 mg/ml of polyethylene glycol.

(5) Markers to test adsorptive endocytosis and doses used in the present study

The following markers were used to test adsorptive endocytosis: Cationic ferritin (CF, Miles Laboratories) at a dose of 0.3 mg in 0.1 ml of physiological saline (pI 8.4, pH 6.8) and Concanavalin A conjugated with ferritin at a dose of 0.3 mg in 0.1 ml of sodium phosphate buffer, pH 6.8.

(6) Administration of the markers

The doses and concentration of the different markers have already been described above. For the administration of any given tracer, the rats were anesthetized with sodium pentobarbital and the testis exposed through an abdominal incision. A given marker (0.1 ml) containing 0.01% Nile blue was injected into the lumen of the rete testis using a 30 gauge - 1/2 inch needle (Clegg and McMillan, 1965; Carr et al., 1968; Dym, 1976). The seminiferous tubules instantly turned blue as the tracers were introduced into the rete testis. At various time intervals after a single intraluminal injection, i.e. 1, 5, 15 and 30 minutes, and 1, 2, 4, 6 and 24 hours, the testes were fixed by perfusion and processed as described above.

(7) In vitro studies

In order to test specific versus nonspecific adsorption of the tracers to the apical plasma membrane of the Sertoli cells, some testes were fixed by perfusion in 2.5% glutaraldehyde, post-fixed for 1 hour in the same solution and then sectioned (75 µm) with a Sorvall TC-2 tissue chopper. The sections were placed in six different vials and rinsed for 1 hour in the corresponding buffers in which the different markers were suspended. The tissue was then incubated in media containing the different markers for 1 hour at 37°C. The tissue was then processed for electron microscopy in the routine manner.

(8) Non-treated tissues

For the study of the normal morphology of the rat seminiferous epithelium, particularly the Sertoli cell, and control of the quantitative analysis, non injected testes were fixed by perfusion with 5% glutaraldehyde and then processed for electron microscopy in the routine manner (see above).

SECTION 3: EFFECT OF CYTOCHALASIN D AND COLCHICINE ON ENDOCYTOSIS IN SERTOLI CELL

(1) Choice of inhibitors

As it was already discussed in the review of the literature, the involvement of microtubules and microfilaments in pinocytosis and phagocytosis is rather controversial (Geiger, 1983) and it could be subject to variations in different cell types and distinct mechanisms of endocytosis.

Microtubules are composed of dimeric tubulin subunits which exist in a dynamic equilibrium between the free and the polymerized state, the latter forming characteristic 25 nm-diameter, cylindrical microtubules (Starling et al., 1983). Colchicine binds to tubulin and thus interferes with polymerization/depolymerization of microtubules, causing a disturbance in the microtubule status of the cell (Orci et al., 1973; Stein and Stein, 1973; Patton 1974; Reaven and Reaven, 1975; Morales et al., 1982; Starling et al., 1983). Colchicine has shown to severely retard or to inhibit endocytosis in different cell types (Posner et al., 1982; Bergeron et al., 1983; Starling et al., 1983).

Certain compounds which interfere with the microfilamentous system such as the alkaloids cytochalasin B and D, have also been reported to affect the endocytic process in various cell types (Blok et al., 1982; Geiger et al., 1983). Cytochalasin D has been proved to effectively inhibit endocytosis in the rat intestinal epithelium.

(2) Influence of colchicine and cytochalasin D on fluid-phase endocytosis

To test the involvement of the microtubules and microfilaments in fluid-phase endocytosis, 0.2 mg of colchicine (Sigma Chemical Company) suspended in 0.1 ml of physiological saline was injected into the interstitial space of the testis of four albino rats. Interstitial injections of luminocolchicine at the same dosage and concentrations were used in four other rats. Luminocolchicine was prepared from colchine by ultraviolet irradiation (Wilson and Friedkin, 1966; Posner et al., 1982). Similarly, the four other albino rats were injected with 4.8 µg of cytochasin D (Sigma Chemical Company) dissolved in 0.1 ml of physiological saline containing 0.4% of dimethylsulfoxide (DMSO, Sigma Chemical Company). In each case after 1 hour of the injection of the inhibitors, 0.3 mg of native ferritin suspended in 0.1 ml of physiological saline (pH 6.8) was intraluminally administered through the rete testis. Two rats for each experiment were sacrificed one or two hours later. The material was processed in the same manner as described in Section 1.

(3) Influence of colchicine and cytochalasin D on the phagocytosis of the spermatids cytoplasmic residual bodies

Since phagocytosis of cytoplasmic residual bodies starts at stage VIII and last until the beginning of stage IX of the cycle (30 hours), two rats were intratesticularly injected 4 times every 8 hours per testis with 0.2 mg of colchicine or luminocolchicine in 0.1 ml of physiological saline, and two other rats received 4.8 µg of cytochalasin D in 0.1 ml of physiological saline containing 0.4% of DMSO per testis also every 8 hours. Thus the animals were sacrificed 32 hours after the first injection. As in other experiments, the tissues were processed for electron microscopy as described above.

SECTION 4: ANALYSIS OF THE DISTRIBUTION OF MICROFILAMENTS WITH SPECIAL REFERENCE TO THE PHAGOCYTOSIS OF THE RESIDUAL BODIES

In order to study the distribution of microfilaments during the phagocytosis of the cytoplasmic residual body (stage VIII of the cycle), the following technique with tannic acid was used to protect these structures from the disruption produced by OsO_4.

Two male albino rats (350-450 g) were anesthetized with sodium pentobarbital and their testes fixed by perfusion through the abdominal aorta with a mixture of 100 mM glutaraldehyde, 2 mg/ml tannic acid and 0.5 mg/ml saponin (Sigma Chemical Company) in "buffer A" containing 50 mM KCl, 5 mM MgCl at pH 7.0 (Maupin and Pollard, 1983). Fixed testes were then excised and cut into 1 mm^3 cubes which were stored in the same fixative for two additional hours at 4°C. The tissue was then rinsed with "buffer A" pH 6.0 and post-fixed with 40 mM (1%) of OsO_4 in buffer A, pH 6.0 at 4°C.

SECTION 5: CYTOCHEMISTRY

The testes of two albino rats were fixed by perfusion with 2% glutaraldehyde buffered in sodium cacodylate (0.1M) containing 0.5% $CaCl_2$ (pH 7.2). Following perfusion the testes were removed and placed in the same fixative for 1 hour at 4°C. The tissue after being washed in cacodylate buffer containing 4% sucrose was sectioned (75μm) with a Sorvall TC-2 tissue chopper. The sections were then rinsed several times in 0.1M sodium acetate buffer containing 5% sucrose at pH 5. For the demonstration of cytidine monophosphate (CMPase) activity, the sections were incubated for two hours at 37°C in a medium containing cytidine monophosphate (Sigma Chemical Company) at pH 5.0 (Novikoff, 1963). Trimetaphosphatase (TMPase) activity was demonstrated by incubation of the tissue in a medium containing trimetaphosphate (Sigma Chemical Company) a substrate at pH 5.0 per 1 hour at 37°C

(Doty et al, 1977). The tissue was processed for electron microscopy in the routine manner (see Section 1).

SECTION 6: MORPHOMETRIC AND STEREOLOGICAL METHODS

(1) Terminology

Morphometry can be defined as a method that deals with the measurements of organelles, cells and spaces whereas stereology is the three-dimensional interpretation of two-dimensional images of light or electron microscopy by the criteria of geometric probability (Weibel and Elias, 1965; Elias and Hyde, 1980).

(2) Determination of volume ratios

The determination of the fraction that one cell organelle or cell type occupies in the total volume of a cell or a tissue respectively is the easiest of all stereologic operations (Elias and Hyde, 1970). It is based on the principle of Delesse (1848, quoted by Elias and Hyde, 1970), which states that the areas of profiles of several tissue components are related as the volumes occupied in space by these components, always assuming random distribution and random orientation of components. There are many parameters which can be studied in tissue or cells such as number, volume, surface area and length of the linear feature of structures (Weibel and Elias, 1965). In the present work only volume densities of structures have been measured and therefore, no other parameters will be described here.

The estimation of the "volume ratios" can be done in several ways: "Planimetry" which uses a polar or electronic planimeter to trace out the area of all profiles contained in a section, add the areas and divide by the section area; the "cut and weight" method which consists of using electron micrographs of known weight, cutting all profiles and weighing them.

The weight ratio between the profiles and the sheet is the direct estimate of volume density; the "linear integration principle" proposed by Rosiwal in 1898 (quoted by Weibel and Bolender, 1973) consists of projecting a test line of known length and measuring the total length of the line segments included in the profiles. The volume density is then obtained directly from the ratio of profile area over the section area. Finally, the method which is widely used to determine volumetric data is "differential point counting", and as the name implies, it consists of counting the number of points of square lattice contained over the profiles of any structure and relating it to the total number of points on the section (Weibel and Bolender, 1973). In the present study, instead of using the "differential point counting" method, the absolute areas of the seminiferous epithelium, Sertoli cells, and secondary lysosomes contained in the cytoplasm of Sertoli cells were estimated by using a Carl Zeiss MOP-3. Thus, applying the principle of Delesse, the volume of the various components studied could be determed by measuring the absolute areas of their profiles (see below).

(3) Sampling procedures

Approximately 25-30 blocks of the testicular tissue were obtained from each of the four rats sacrificed after 6 hours injection with NF (see Section 2). Three or four semithin sections (0.5 μm thick) per block were cut and stained with toluidine blue. The semithin sections were examined under the light microscope to determine the stages of the cycle of the various present tubular cross sections. For each block, two perfect transversally cut tubules were selected and the blocks were trimmed appropriately. The selection procedure of the tubules ensured a fairly equal sampling of all the stages of the cycle.

Thin sections, with a silver interference colour using a diamond knife, were mounted on special copper grids having a simple aperture of 0.5 x 2.0 mm covered with celloidin. The sections were routinely stained for electron microscopy with 4% alcoholic uranyl acetate for 5 minutes, followed by lead citrate for 2 minutes, and then examined with a Philips 300 electron microscope.

Each cross section of the different stages of the cycle provided four series of micrographs composed of four to six negatives taken at the same magnification of 4,386 which were enlarged by a factor 2.6 to yield a final magnification of 11,403 times. These individual series of four to six micrographs corresponded to adjacent non superimposed areas from the base to the lumen of the seminiferous epithelium. A total number of 1,500 micrographs (approximately 375 per animal) were taken. Since the ferritin molecules could not be clearly identified at a magnification of 11,403, the same areas were reexamined under the electron microscope at a magnification of 25,000 and the number of labelled versus unlabelled dense secondary lysosomes and multivesicular bodies was estimated quantitatively.

(4) Measurements

In this study, the absolute areas of sections of Sertoli cells and lysosomes were estimated directly on electron micrographs. The Sertoli cell cytoplasm was identified and delineated using a coloured lumocolour pen, excluding all germ cells and late spermatids deeply inserted in apical recesses of Sertoli cells. The secondary lysosomes present in the cytoplasm of Sertoli cells were delineated using a different coloured lumocolour pen. Morphometric measurements of the absolute areas corresponding to the cytoplasm and secondary lysosomes of the Sertoli cells were obtained using a MOP-3

instrument and a magnetized tablet. The active measuring area of the tablet contains magnetized steel wires spaced at regular intervals in X and Y axes. The wire grid forms a magnetic field. The wires only provide pulse directions in X and Y and do not influence accuracy or resolution of the tablet. Pulses originating alternately at 2 sides of the table and travelling with a constant speed are superimposed. The speed of these pulses remains constant regardless of environmental conditions. When the magneto-strictive pulses are intercepted by the stylus, an accurate pulse count is established. This count is transformed into a distance or coordinate point by the micro-processor within a few microseconds. Thus, X and Y coordinates, length, area and other geometric magnitudes can be quickly and accurately established. The system is calibrated at the factory to display values in absolute mm and mm^2 (for detail, see Instruction Manual MOP-3, Carl Zeiss, 1979). The values obtained from each stage of the four animals studied were recorded separately. A similar approach was used to estimate the volume of Sertoli cells per unit volume of seminiferous epithelium measuring the absolute area occupied by sections of Sertoli cells and the absolute area of sections of the seminiferous epithelium in the same micrographs.

(5) Quantitative analysis

(a) Determination of the number of labelled secondary lysosomes per Sertoli cell

Since one of the goals of this study was to obtain quantitative information about the endocytic activity of the Sertoli cell at different stages of the cycle of the seminiferous epithelium, the following formula was applied to find out the number of labelled secondary lysosomes per Sertoli cell after 6 hours of intraluminal injection with 0.1 ml of physiological saline containing 0.2 mg of native ferritin:

$$\frac{\text{Number of labelled lysosomes}}{\text{Number of Sertoli cells}} =$$

$$\frac{\text{True nr of labelled lysosomes/given area of section}}{\text{True volume of epithelium/given area of section}} \times$$

$$\frac{\text{True volume of epithelium/length of tubule (*)}}{\text{True nr of Sertoli cells/length of tubule (*)}}$$

(b) True number of labelled lysosomes

Assuming that the lysosomes had larger diameters than the thickness of the section, then the number of counted lysosomes did not represent the "true absolute number" of secondary lysosomes. Thus, in order to establish the true number of labelled lysosomes the following correcting factor was derived from the Abercrombie equation (Chalkly, 1943):

$$\text{True nr of lysosomes} = \text{Counted lysosomes} \times \frac{t}{t + 2R}$$

where R represented the lysosomal radius and t the thickness of the section.

To know the value of R the following derivations were applied:

$$R^2 = \frac{3}{2\pi} A$$

$$R = \sqrt{\frac{3}{2\pi} A}$$ (See below "Average volume of secondary lysosomes in Sertoli cells")

where A represented the mean area obtained by dividing the cumulative area occupied by sections of secondary lysosomes (MOP measurements) by the total number of secondary lysosomes representing this cumulative area.

(c) True volume of seminiferous epithelium in section

Since the volume of the seminiferous epithelium represented the absolute value of the tissue in a given area expressed in MOP units (mm^2), the following formula was applied in order to obtain the true volume of this epithelium in μm^3:

$$\text{True volume of epithelium (in section)} = \frac{\text{MOP area} \times 10^6}{(\text{Mag})^2} \times t$$

where t was equal to the thickness of the section and Mag was equal to the corrected magnification used in this study (11.403).

(d) Formula used in the computer program

$$\text{If } \frac{\text{Nr of labelled lysosomes}}{\text{Nr of Sertoli cells}} =$$

$$\frac{\text{True nr of labelled lysosomes/given area of section}}{\text{True volume of epithelium/given area of section}} \times$$

$$\frac{\text{True volume of epithelium/length of tubule (*)}}{\text{True nr of Sertoli cells/length of tubule (*)}}$$

$$\text{then, } \frac{\text{Nr of labelled lysosomes}}{\text{Nr of Sertoli cells}} =$$

$$\frac{\text{Labelled counted lysosomes} \times t \times (\text{Mag})^2}{(t + 2R) \times \text{MOP area of epithelium} \times 10^6 \times t} \times$$

$$\frac{\text{True volume of epithelium (*)}}{\text{True nr of Sertoli cells (*)}}$$

The present formula was used to program a computer Hewlett Packard 86. The data and calculations were stored and carried out respectively by the same equipment.

Thus, the differences in the total number of labelled lysosomes per Sertoli cell at different stages of the cycle would reflect cyclical variations in the endocytic activity of this cell.

The asterisks (*) indicate the information obtained from an elegant and reliable morphometric study, published by Wing and Christensen (1982). It is important to point out that Wing and Christensen (1982) found that the numbers of Sertoli cells and major germ-cell types per unit length of seminiferous tubules remain essentially constant throughout all stages of

the seminiferous epithelium of the rat. This was consistent with the finding of Bustos-Obregon (1970) and Hermo (1972), from Sertoli cell counts in whole mounts of seminiferous tubules at stages II, IV, V and VII, and extended to all stages of the cycle.

(e) Determination of the total number of secondary lysosomes per Sertoli cells

In order to determine this ratio the same rationale employed for the determination of labelled secondary lysosomes per Sertoli cells was applied:

$$\text{Thus, } \frac{\text{True nr of lysosomes}}{\text{Nr of Sertoli cells}} =$$

$$\frac{\text{Total nr of counted lysosomes x t x (Mag)}^2}{(t + 2R) \text{ x MOP area of epithelium x } 10^6 \text{ x t}} \text{ x}$$

$$\frac{\text{True volume of epithelium (*)}}{\text{True nr of Sertoli cells (*)}}$$

The computer was also programmed according to the present formula, and the obtained data were stored in the computer files in order to obtain the corresponding calculations.

However, in this case the stages IX and XIII of a non treated animal were also studied with the purpose of analyzing whether or not the treatment affected the normal values.

(*) Wing and Christenson (1982).

(6) Corollaries

In order to take full advantage of the quantitative data obtained in this study with the purpose of knowing other ratios of the lysosomal population in the Sertoli cell at different stages of the cycle of the seminiferous epithelium, several other derivations were applied which are described in detail below.

(a) Average volume of secondary lysosomes in Sertoli cells

Since the secondary lysosomes were usually spherical in shape, a section through such spherical particles resulted in circles of different sizes. Hence, assuming that the lysosomes were spheres, the radius R would be equal to the distance from the centre to the peripheral limit of the sphere. In Figure 3 a graphic-visual approach to this problem has been devised to explain the principles applied in this research in order to obtain the average volume of lysosomes in Sertoli cells at different stages of the cycle of the seminiferous epithelium of the rat.

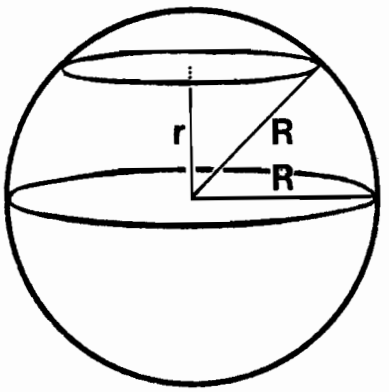

Fig. 3. The drawing shows that the resulting circles in a section are at a distance r from the centre, and hence the section area would be equal to $\pi (R^2 - r^2)$.

Consequently, the mean area of all sections could be integrated in the following manner:

$$\frac{\int_0^R \pi (R^2 - r^2)\ dr}{\int_0^R dr} = \frac{\pi R^2 [R-0] - \frac{\pi}{3} [R^3 - 0]}{R} = \frac{2\pi}{3} R^2$$

This value was measured experimentally from photographs (in mm^2) using the MOP-3 instrument. To convert the values in μm^2, the experimental measurements were multiplied by

$$\frac{10^6}{(\text{magnification})^2}$$

Now, if $A = \frac{2\pi}{3} R^2$

then, $R = \sqrt{\frac{3}{2\pi}}\ A^{1/2}$

Considering that the true average volume of secondary lysosomes would be

$$= \frac{4}{3} \pi R^3$$

$$= \frac{4\pi}{3} \frac{3}{2\pi} \sqrt{\frac{3}{2\pi}}\ A^{3/2}$$

$$= \sqrt{\frac{6}{\pi}}\ A^{3/2}$$

Then, by replacing the value of A measured with the MOP-3, the calculation of the average volume of secondary lysosomes could be obtained.

(b) Total volume of secondary lysosomes and total volume of labelled secondary lysosomes per Sertoli cell at different stages of the cycle

In order to obtain the present ratios the following formula was applied:

Total volume of secondary lysosomes/Sertoli cell =

True nr of lysosomes x Average volume of lysosomes

The same rationale was used to obtain the total volume of labelled secondary lysosomes, i.e., True nr of labelled lysosomes x Average volume of lysosomes.

(c) Percentage of labelled secondary lysosomes

Finally, the percentage of labelled secondary lysosomes in Sertoli cells at different stages of the cycle was obtained from the present derivation:

$$\text{Percentage of labelled secondary lysosomes} = \frac{\text{Number of labelled secondary lysosomes} \times 100}{\text{Total number of secondary lysosomes}}$$

(7) Correcting Factors

(a) Thickness of the section

The corrected thickness of the section (t) used in the depicted equations was derived from the measurements of cross sections of 9 re-embedded thin sections (silver interference colour). The thickness was found to be 48.37 nm ± 0.63 nm (SEM).

(b) Compression of the section

It was estimated that compression of the tissue by the sectioning causes a reduction of section length by about 10%. However, this effect is partially compensated by optical distortion of electron micrographs (Weibel et al., 1969; Assaf, 1980). Since it can be assumed that all cells and organelles are equally affected (Weibel et al., 1969), such a correction was judged irrelevant for the determination of absolute areas of the seminiferous epithelium Sertoli cells and secondary lysosomes.

(c) Magnification of the electron microscope and electron micrographs

The fields for quantitative analysis were all taken with a Philips 300 electron microscope at constant magnification. The electron microscope was calibrated using a carbon grating replica (Blouin et al., 1977) and the final magnification was calculated to be at 4,386. This value was chosen because it covered large sampling fields and at the same time permitted the identification of the clusters of secondary lysosomes. The enlargement of the picture was calibrated using a ruler to yield a multiplying factor of 2.6, consequently the final magnification of the electron micrographs was approximately 11,403.

Chapter IV

RESULTS

For the convenience of the reader this chapter will be divided into two parts:

The first part will deal with the electron microscope observations on the structure and cytochemistry of the lysosomal system, marker studies and experiments with disrupting drugs of microtubules and microfilaments with special reference to endocytosis, whereas part two will be dealing with the quantitative analysis of the lysosomal population.

PART ONE

(1) Description of the apical processes of Sertoli cells

The Sertoli cell was seen as a columnar element resting on a basal lamina and extending to the lumen of the seminiferous tubule (Figs. 9, 17, 30). When viewed with the electron microscope, the cytoplasm appeared highly indented by neighbouring germ cells and its apical region presented deep recesses containing the heads of the maturing spermatids (Fig. 7), resulting in the formation of long and thin processes that surrounded the cytoplasmic lobules of the elongated spermatids. The plasma membrane of the cytoplasmic processes facing the lumen of the seminiferous tubules often presented deep invaginations (Figs 4, 24). The cytoplasmic processes contained smooth empty-looking vesicles ranging in diameter between 0.1 to 0.2 μm which were irregular in shape. Frequently, these vesicles were "C" shaped in appearance (Figs. 4, 5, 17) and when viewed in cross section they appeared as double walled vesicles (Figs. 4, 5). These vesicles were always observed within the apical cytoplasmic processes of Sertoli cells at all stages of the cycle of the rat seminiferous epithelium. In addition

to the vesicles, some profiles of smooth endoplasmic reticulum containing granulo-filamentous material, small vesicular profiles and bundles of microtubules were observed within the cytoplasmic processes (Fig. 5). It has also been observed that the subsurface specializations made up by a) flattened cisternae of endoplasmic reticulum (ER) running parallel and next to the Sertoli cell plasma membrane facing the head of the spermatids; and b) bundles of actin filaments lodged between these ER cisternae and the plasma membrane were sometimes present within the cytoplasmic processes along the plasma membrane of the Sertoli cell facing the cytoplasmic lobule of the spermatids (Fig. 21).

(2) Description of the lysosomal population and associated elements in Sertoli cells

The lysosomal apparatus of the Sertoli cell consisted primarily of clusters of electron dense membrane-bound bodies presenting remarkable variations in their distribution in the cytoplasm during the cycle of the seminiferous epithelium. These membrane-bound bodies were also variable in number, size and electron density according to the different stages of the cycle. During stage IX to I (early) the membrane-bound bodies ranging in diameter from 0.2 to 0.4 μm and described as secondary lysosomes by Fawcett (1975) and Hermo et al. (1978) usually had a spherical shape and a homogenous granular content (Figs. 6, 7, 13). Frequently, small spherical lipid droplets and small electron-dense bodies were seen within some of the membrane bound granules (Figs. 6-8). Between stages II to VIII the content of the membrane-bound granules were more heterogeneous and presented a more ostensible electron density (Fig. 9). Small spherical lipid droplets, small electron-dense bodies and myelin figures were frequently observed in the content of these granules (Figs, 9, 30). Within

the cluster of secondary lysosomes were also observed the presence of large irregular shaped vacuoles with an electron lucent matrix containing small vesicles which were considered as multivesicular bodies. These structures sometimes presented a characteristic straight, fuzzy, filamentous edge on part of the cytoplasmic surface of the membrane (Figs, 6, 10, 15, 25, 26, 33). More spherical and smaller multivesicular bodies showing an electron denser matrix were also found among the clusters of lysosomal elements (Figs. 6, 11, 26, 34). In addition to these structures, a multitude of small vesicles of different types and electron densities were seen within the clusters of lysosomal elements. Thus, "pale vesicles" with a diameter ranging between 100 and 120 nm were numerous and usually seemed to pinch off from the large irregular multivesicular bodies. The pale vesicles were frequently observed around the large irregular multivesicular bodies or near the neighbouring plasma membrane of the recesses (Figs. 6, 10, 13, 25-27, 36). Vesicles containing an electron dense core separated by a halo from the membrane and having a diameter of approximately 100-170 nm were usually associated with the pale vesicles just described within the lysosomal clusters and sometimes appeared to be budding off from the dense secondary lysosomes and from the smaller and spherical multivesicular bodies (Figs. 11-13, 26, 27, 36). Microvesicles ranging between 25 and 35 nm were also observed among the lysosomal elements, sometimes forming clusters and sometimes neighbouring the two types of multivesicular bodies and the dense membrane-bound secondary lysosomes (Figs. 10, 12, 33). The cytoplasmic residual bodies were also associated to the clusters of secondary lysosomes. Cytoplasmic residual bodies were present at stages VIII and IX and they were easily identified by their size and content usually including lipids, membranous profiles, degenerating mitochondria and a mass of ribo-

Table A: *Description of the vesicular elements found in the cytoplasm of the sertoli cell*

Structure	Size	Schematic representation
Endocytic vesicles	0.1 - 0.2 µm	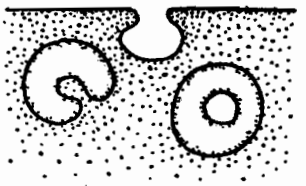
Endosomes (pale MVB)	0.4 - 0.6 µm	
Dense MVB	0.2 - 0.4 µm	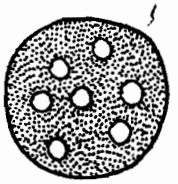
Dense core vesicles	100 - 170 nm	
Pale vesicles	100 - 120 nm	
Microvesicles	25 - 35 nm	
Secondary lysosomes	0.2 - 0.4 µm	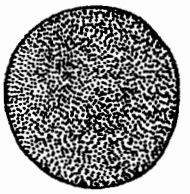

nucleoprotein (Figs. 19-21). The internalization and intracellular degradation of the cytoplasmic residual bodies are described in detail below (see "Formation and phagocytosis of the cytoplasmic residual bodies").

(3) Distribution of the lysosomal elements in Sertoli cells during the stages of the cycle of the seminiferous epithelium

The analysis of cross sections of seminiferous tubules with the electron microscope revealed that there was a marked variation in the distribution of the clusters of lysosomal elements within the Sertoli cells at different stages of the cycle of the seminiferous epithelium. However, the lysosomal elements, mainly the dense membrane-bound granules, were always present in large numbers within the Sertoli cell cytoplasm throughout the cycle and they were generally arranged in distinct clusters (Figs. 6, 7, 9, 13, 30). As was previously described, these clusters consisted of large, often heterogeneous, granular membrane-bound bodies, multivesicular bodies of different sizes, shapes and densities and of smaller vesicles of different types (Figs. 13, 26, 27). From stage IX to I (early) of the cycle the clusters of lysosomal elements were located in the supranuclear region of the Sertoli cells next to the apex of the elongated nuclei of the late spermatids (Fig. 7). Similarly, multivesicular bodies with a pale or dense matrix, as well as clusters of the small type of vesicles, also seemed to be more abundant in stages IX to I of the cycle than at other stages. During stages XII, XIII and XIV, the number of secondary lysosomes appeared to be more numerous than at any other stage of the cycle.

At stage I (late), the lysosomes accumulated at the base of the Sertoli cell cytoplasm next to the basement membrane remaining in that region during stages II to VIII of the cycle. The presence of structures showing

FIGURE 4

Apical cytoplasmic process of a Sertoli cell at stage XIII of the cycle. (X35300)
Numerous "c" shaped vesicles (v) with an electron lucent content are seen within the cytoplasmic process. Some vesicular profiles can be observed inside these vesicles (arrows) due to a different plane of section. The plasma membrane of the process exhibits a deep invagination (iv).
Cytoplasm and axoneme (A) of an adjacent spermatid (Sp) are also seen in this micrograph.

FIGURE 5

Apical region of a Sertoli cell at stage VIII of the cycle. (X37100)
Several vesicles showing an electron lucent content (v) are present within the apical cytoplasm of this cell. Smaller vesicles exhibiting a similar content are also seen in this region (arrowheads).
Some profiles of endoplasmic reticulum (ER) showing a granulofilamentous content are also present in the apical region of the Sertoli cell. Note the presence of a cytoplasmic residual body (RB) and the axoneme of a flagellum (A).

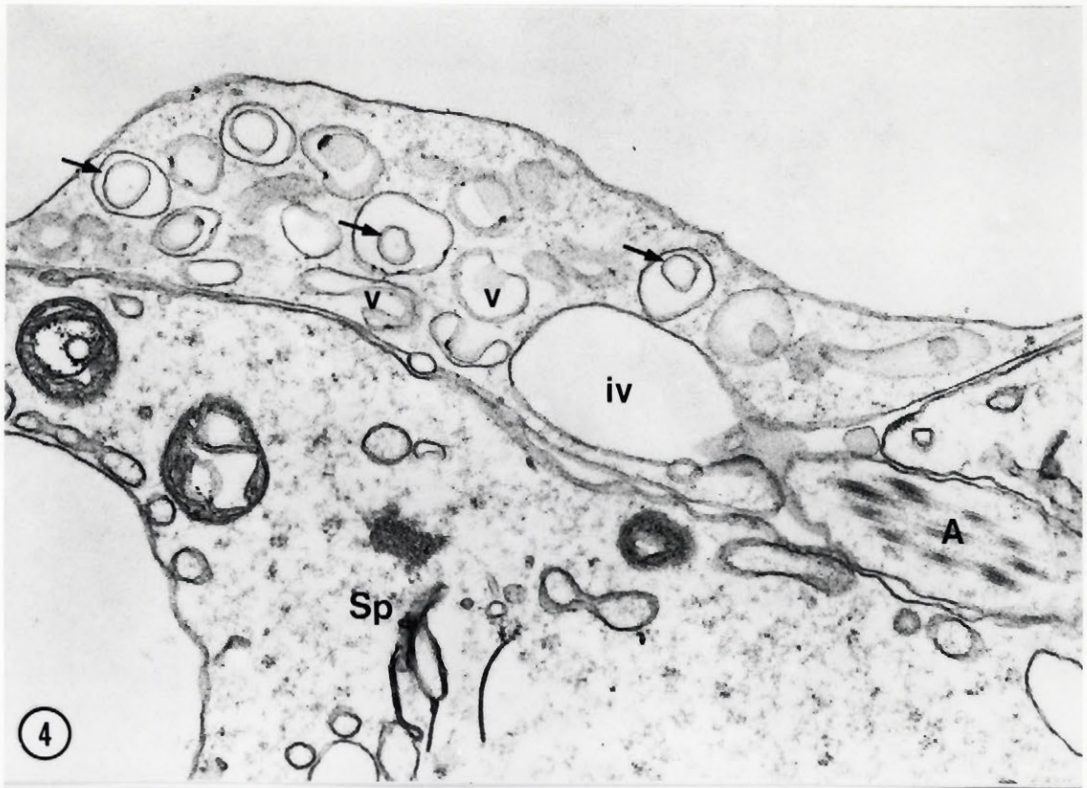
v
v
iv
A
Sp
4

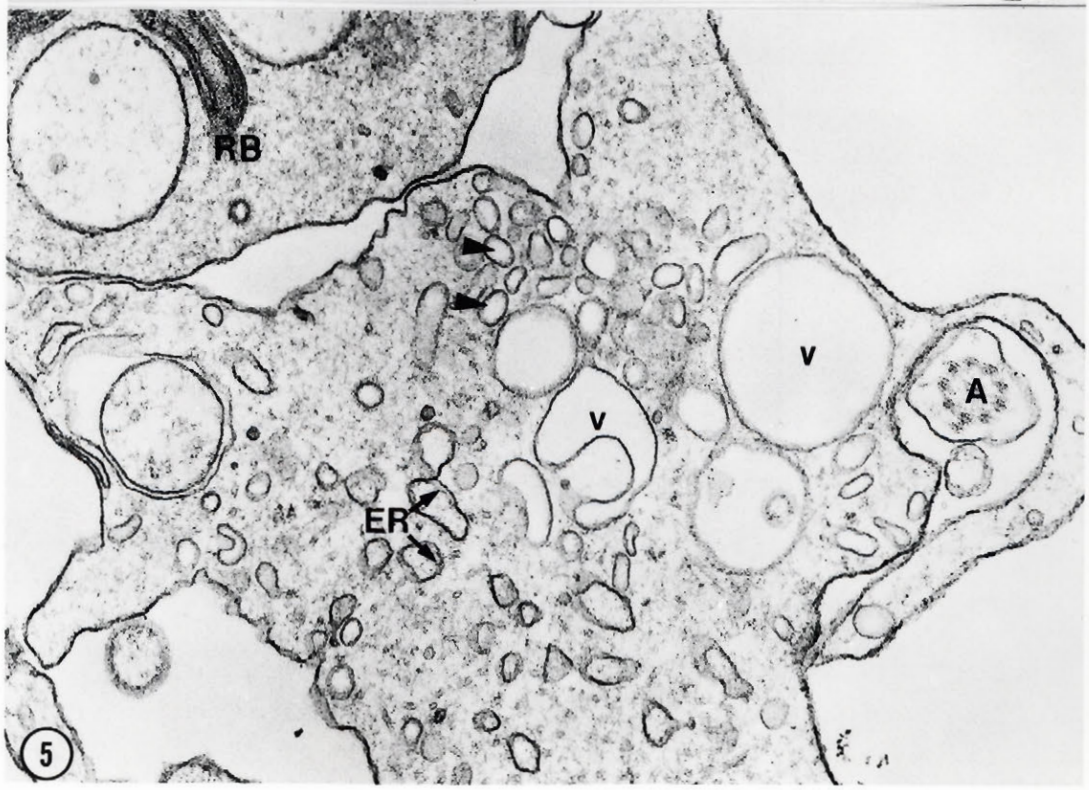
RB
v
v
A
ER
5

FIGURE 6

Supranuclear region of a Sertoli cell at stage XII of the cycle showing a typical cluster of vesicular elements and secondary lysosomes. (X37500)

The large irregular multivesicular body (E) contains an electron lucent matrix and a bristled patch on the outer side of the membrane (arrow head) characteristic of some endosomes. This element usually appears surrounded by pale vesicles (pv) of pale matrix. The cluster is also composed by more spherical and denser multi vesicular bodies (MVB) and by dense secondary lysosomes (SL) showing a granular content and sometimes small electron dense bodies (arrows). ER, endoplasmic reticulum; mit, mitochondria.

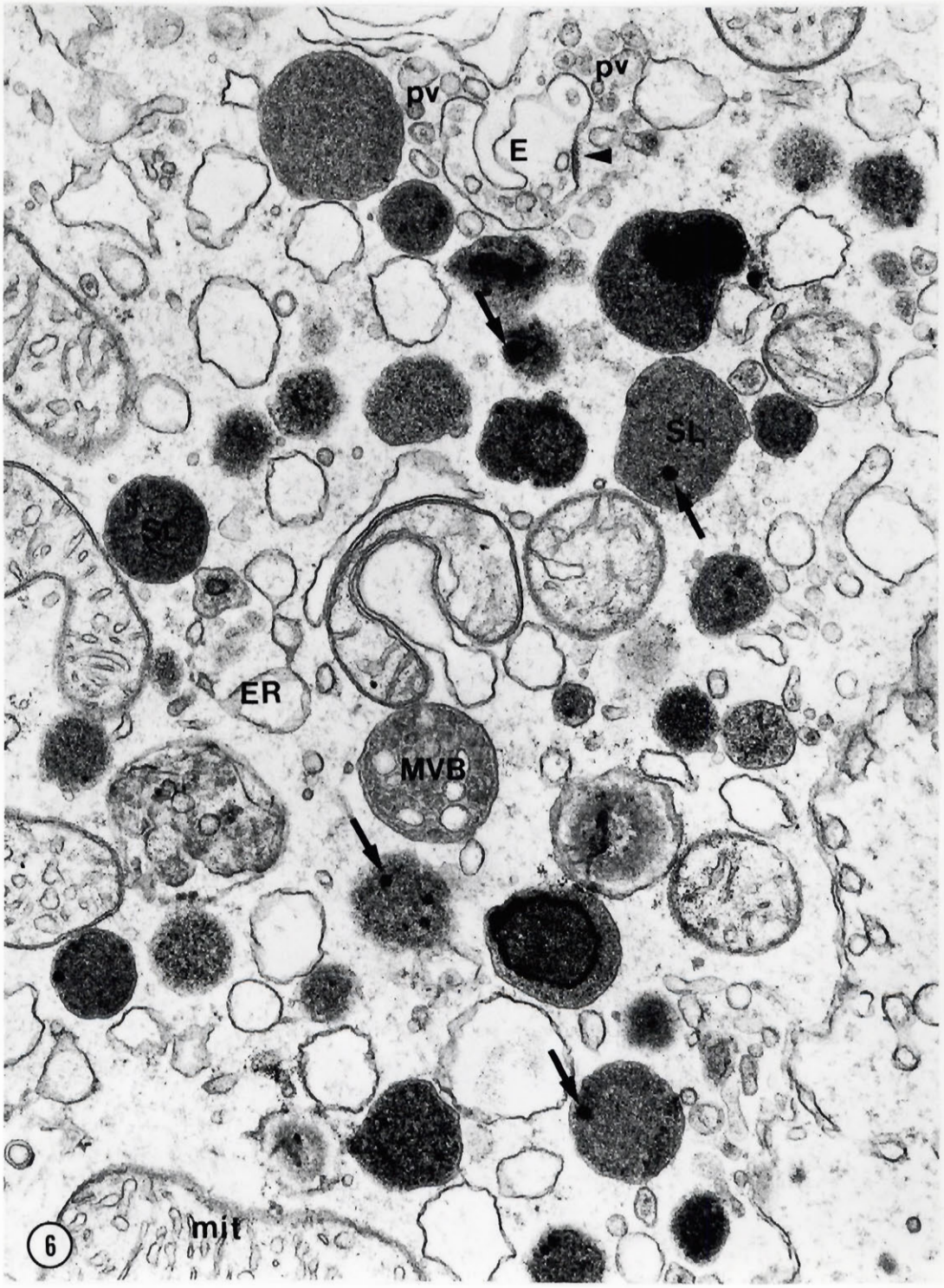
pv
pv
E
SL
SL
ER
MVB
mit
6

FIGURE 7

Apical region of a Sertoli cell at stage XIII of the cycle. (X29200)
A portion of a head of spermatid (hp) and a spermatid's cytoplasmic lobule (Sp) are seen in deep recesses of the Sertoli cell.
This region of the Sertoli cell presents numerous secondary lysosomes (SL) of spherical shape and a homogenous granular content. The secondary lysosomes usually contain electron dense particles of small size (arrows).

FIGURE 8

Image suggesting fusion (arrow) between a dense secondary lysosome (above) and a spherical multi vesicular body (below). (X28000)
An electron dense body characteristic of the secondary lysosomes (arrowhead) can be observed in the matrix of this element.

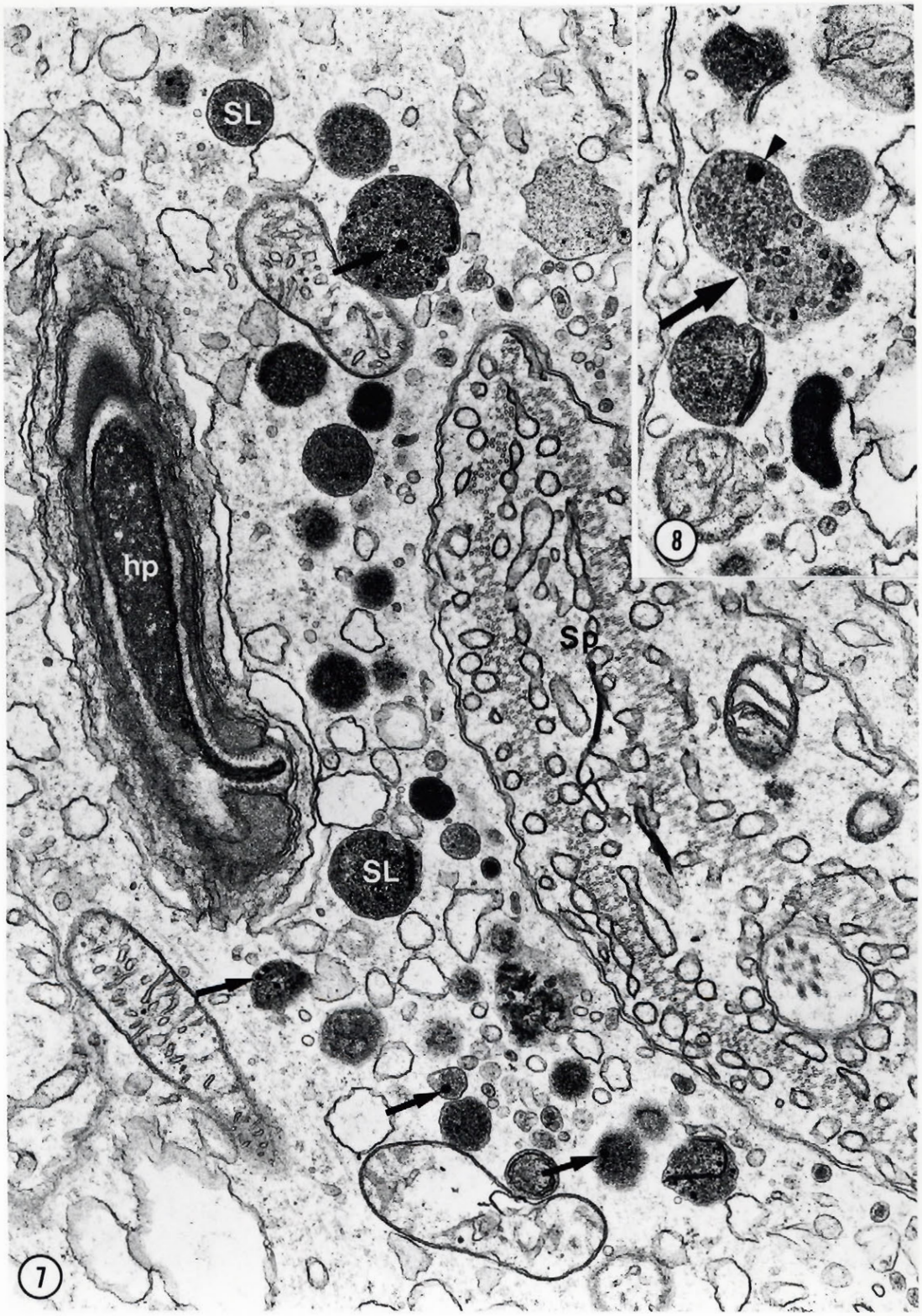
SL
hp
SP
SL
7
8

FIGURE 9

Basal region of a Sertoli cell at stage VII of the cycle. (X21000)
Numerous membrane-bound bodies representing secondary lysosomes (SL) are seen forming clusters next to the basement membrane (BM). The secondary lysosomes present an electron dense granular content and sometimes membranous profiles (arrows).

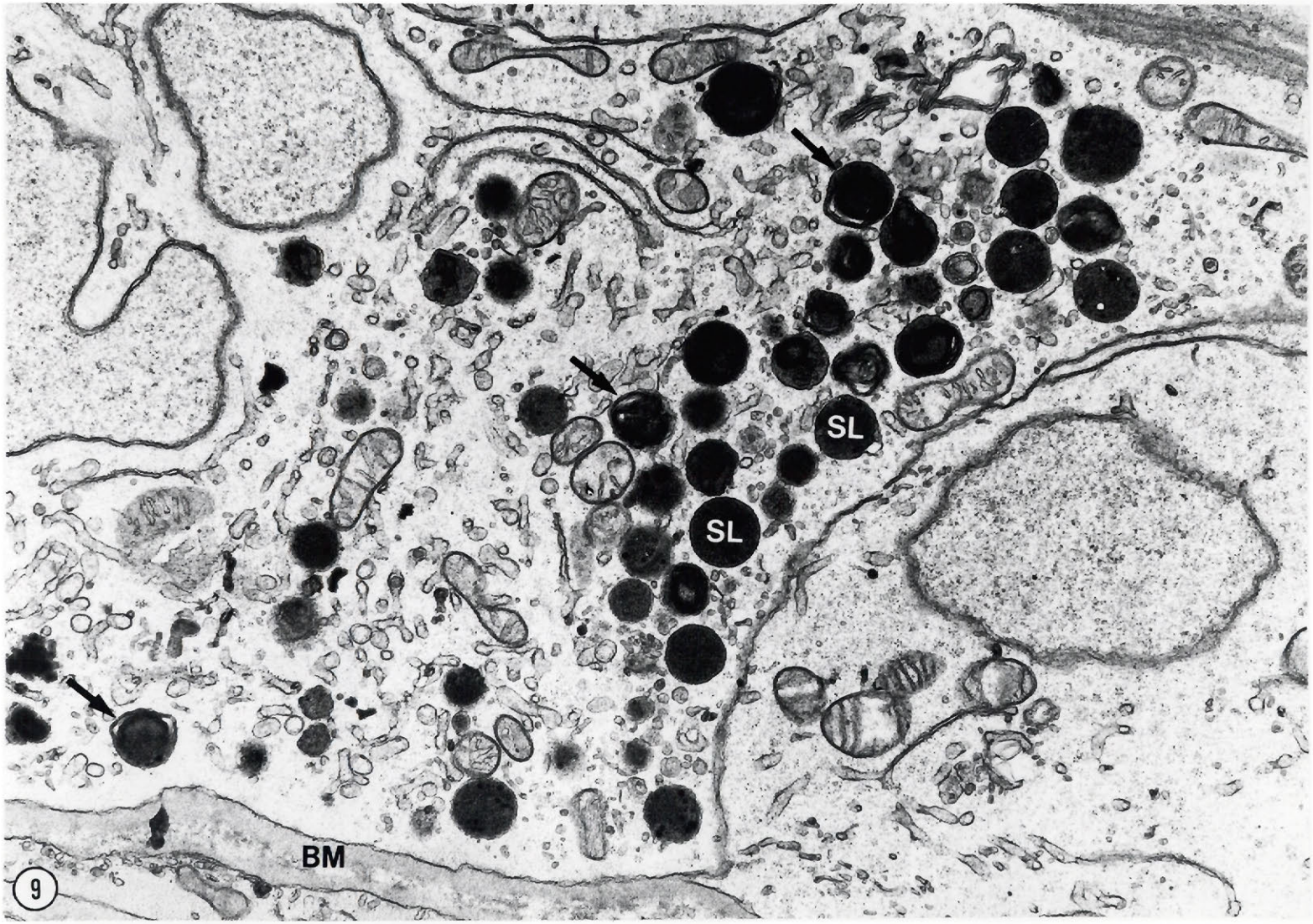
SL
SL
BM
9

FIGURE 10-12

Supranuclear region of three Sertoli cells.

Fig. 10: Endosome (E) showing a tubulo-vesicular profile (arrow) apparently pinching off from this structure and a bristled patch on the outer side of the membrane. Nearby a cluster of micro-vesicles (mv). (X47300)

Fig. 11: Dense spherical multivesicular body showing two dense core vesicles budding off from this element (arrows). (48700)

Fig. 12: Group of dense secondary lysosomes (SL). A dense core vesicle seems to be pinching off from one of these elements (arrow). A cluster of microvesicles (mv) can be seen in this field. (X63000)

FIGURE 13

Apical cytoplasmic region of a Sertoli cell showing a cluster of vesicular elements and secondary lysosomes. (X48700)

The cluster is composed by an endosome (E) showing a pale matrix and a bristled patch on the outer side of the membrane (arrowhead), several secondary lysosomes (SL) and numerous pale vesicles (pv) and dense core vesicles (dv).

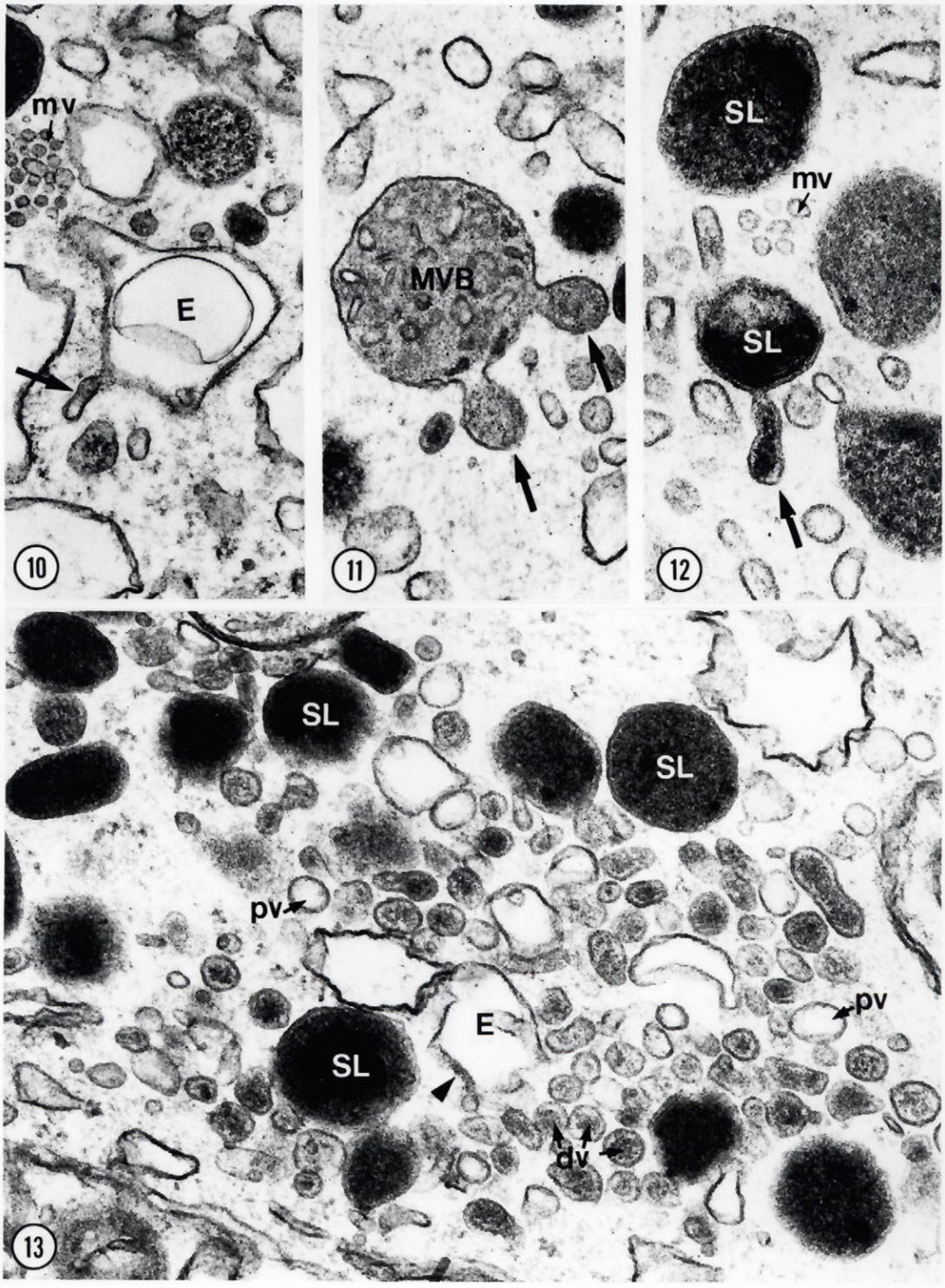
mv
E
10
MVB
11
SL
mv
SL
12
SL
SL
pv
E
SL
pv
dv
13

signs of fusion, as judged by their shape and content, between membrane-bound bodies of homogenous granular matrix and membrane-bound bodies showing a darker content were observed throughout all stages of the cycle but they were particularly frequent between stages I to VII (Figs. 28-29). Lysosomal granules showing signs of fusion between membrane-bound bodies of different electron densities and spherical multivesicular bodies of dense matrix were sometimes seen among the clusters of lysosomal elements (Fig. 8). Multivesicular bodies and associated vesicles such as "pale vesicles", "dense core vesicles", and "microvesicles" (described above) were rarely identified among the clusters from stages II to VII of the cycle. At stage IX the secondary lysosomes were observed in the supranuclear region of the Sertoli cell merging with the cytoplasmic residual bodies released by the late spermatids and phagocytosed by the Sertoli cell (Fig. 20).

(4) Formation and phagocytosis of the cytoplasmic residual bodies

During the "acrosome and maturation phase", the bulk of the spermatid cytoplasm moved back resulting in a marked elongation of these cells. The heads of spermatids were located in deep recesses of the adluminal compartment of Sertoli cells about midway between the base and the free surface of the seminiferous epithelium. Toward the end of the "maturation phase" the heads of late spermatids appeared next to the lumen. By the end of stage VII of the cycle the Sertoli cells maintained the spermatids in a juxtaluminal position by means of large apical drop-like processes, each of which encapsulated a single sickle-shaped spermatid head. Concurrently with this displacement toward the free surface of the epithelium, the formation of the subsurface specialization was identified. This structure consisted of a single layer of flattened cisternae of the endoplasmic

reticulum, which laid parallel to the Sertoli cell surface facing the acrosome of the spermatids, and bundles of filaments which occupied the layer of cytoplasm between the subsurface ER cisternae and the Sertoli cell plasma membrane. In addition to the subsurface specialization, the formation of the tubulo-bulbar complexes and the complex evolution of the endoplasmic reticulum of the encapsulating cytoplasm of the Sertoli cell were observed. However, since these various structures have already been described in detail by Russell and Clermont (1976) and by Clermont et al. (1980), they will not be described in the present thesis. At the end of the maturation phase the heads of the spermatids approached the lumen and the cisternae and filaments disappeared from the adjacent Sertoli cell cytoplasm. Thus, the junctional specialization was no longer present at the moment of the spermiation. By the end of stage VIII of the seminiferous epithelium, the apical Sertoli cell cytoplasm was highly irregular presenting shallow pits in which the rostral portions of the sperm heads were lodged and deeper crypts containing the cytoplasmic residual bodies still connected to the neck of the spermatids by a cytoplasmic stalk. During spermiation, the sperm heads were progressively extruded towards the lumen from the apical drop-like processes of Sertoli cells, the connecting stalk broke and the cytoplasmic residual bodies remained adsorved in shallow depressions of the Sertoli cell cytoplasm (Fig. 17). By the end of stage VIII and at the beginning of stage IX, thin cytoplasmic processes of the Sertoli cell progressively surrounded the cytoplasmic droplets followed by fusion of Sertoli cell plasma membrane above the cytoplasmic residual bodies, obliterating the opening of the invagination (Fig. 18). The thin cytoplasmic processes of Sertoli cells were pseudopod - like extensions

of the apical cytoplasm which presented numerous bundles of microtubules oriented along the axis of these structures and from which membrane-bound organelles were largely excluded (Figs. 17-18). Therefore, the fusion of the plasma membrane of the Sertoli cell above the cytoplasmic residual bodies resulted in the formation of phagosomes. Thus, the phagosomes were double walled bodies located in the apical cytoplasm of Sertoli cells formed by the inner plasma membrane of the cytoplasmic residual bodies enclosed by the plasma membrane of the Sertoli cell. Both membranes appeared separated by a space of approximately 100-150 Å (Figs. 18-19).

At the beginning of stage IX of the cycle, the phagosomes were located deep within the Sertoli cell cytoplasm and were still delimited by two membranes. Frequently, the inner membrane seemed to break down and occasionally secondary lysosomes appeared to fuse with the outer membrane of the phagosomes (Figs. 20-21). Concomitantly, the content of the phagosomes was made up of some lipidic inclusions, membranous profiles, degenerating mitochondria and a mass of ribonucleoprotein (Figs. 20-21). Intermediate figures of cytoplasmic residual bodies showing an increasing amount of lipids were often observed (Fig. 23). By the end of stage IX the dissolution of the residual bodies coincided with the appearance of large lipid droplets at the base of the Sertoli cell.

(5) Cytochemical Studies

Several structures present within the clusters of different vesicular elements showed acid phosphatase activity. While most of the large irregular pale multivesicular bodies did not show positive reaction (Fig. 16), the more spherical, smaller and denser multivesicular bodies did show TMPase and CMPase activity. The membrane-bound granules already considered by several authors as secondary lysosomes presented strong acid phosphatase activity (Fig. 16).

FIGURES 14-16

Areas of Sertoli cells after the tissue has been incubated with cytidine monophosphate for 2 hours. (X37000)

The reaction product is seen within dense secondary lysosomes (SL) (Figs. 14 and 16) and within dense core vesicles (arrowheads) (Figs. 14, 15 and 16). A pale matrix multivesicular body (E) presenting a bristled patch on the outer side of the membrane (arrow) characteristic of some endosomes is devoid of reaction product (Fig. 16).

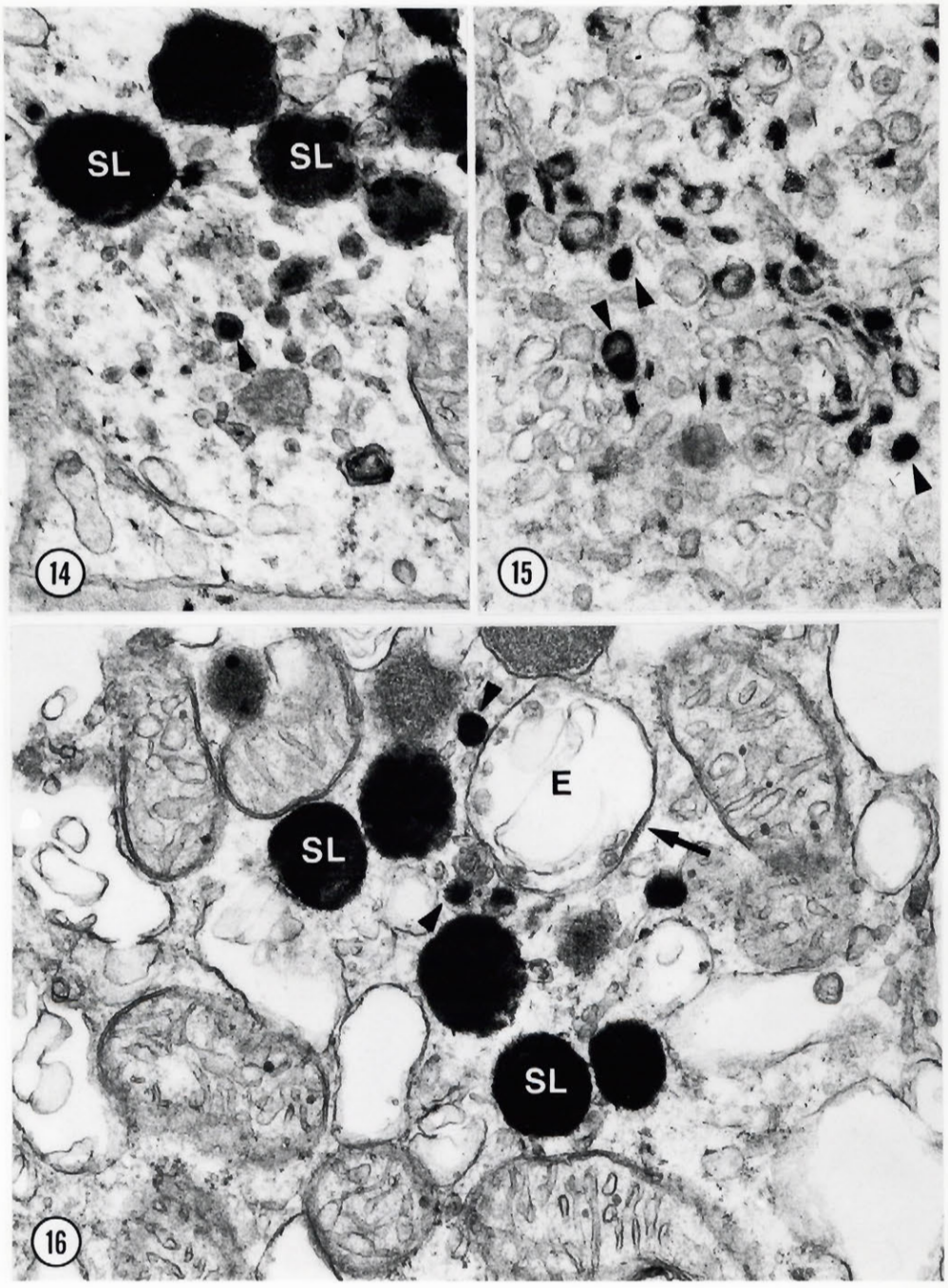
SL
SL
14
15
E
SL
SL
16

FIGURE 17

Spermatid's cytoplasmic residual bodies (RB) attached to certain segments of the apical plasma membrane of Sertoli cell at early stage IX.(X9600)

Note the presence of thin cytoplasmic processes (arrows) spreading around the cytoplasmic residual bodies. Numerous "c" shaped vesicles (v) cut in different planes of section can be observed within the apical cytoplasm of the Sertoli cell.

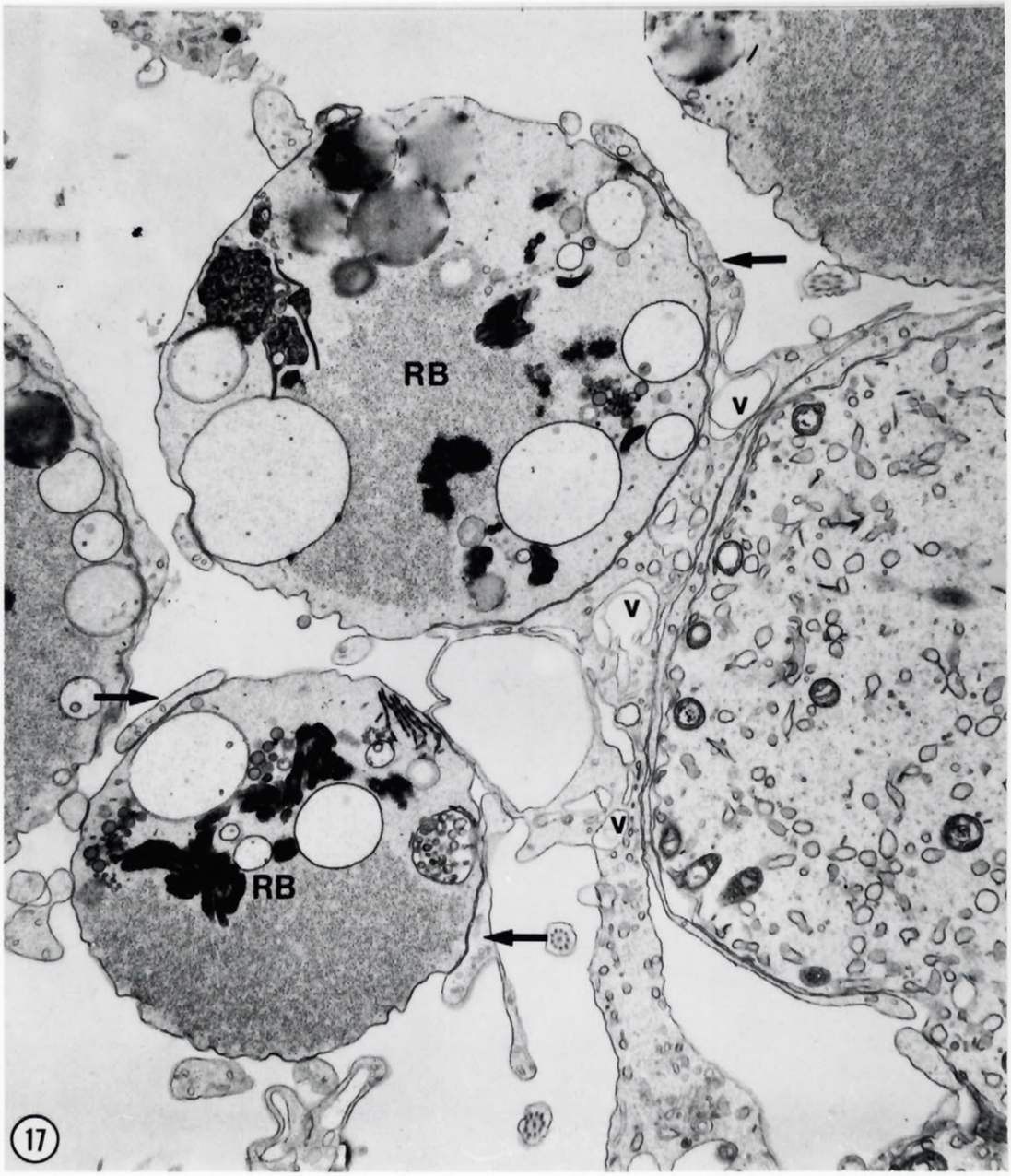
RB
V
V
V
RB
17

FIGURE 18

Phagosome (PH) surrounded by apical cytoplasmic processes of a Sertoli cell at stage IX of the cycle. (X25000)

The phagosome contains a spermatid's cytoplasmic residual body. The outer membrane is formed by an internalized fragment of the apical plasma membrane of the Sertoli cell, whereas the inner one corresponds to the plasma membrane of the cytoplasmic residual body.

The cytoplasmic residual body contains numerous mitochondrias (mit), vacuoles of different sizes (va) and some lipid droplets (lip).

Bundles of microtubules (m) can be seen within the apical cytoplasmic processes of the Sertoli cell.

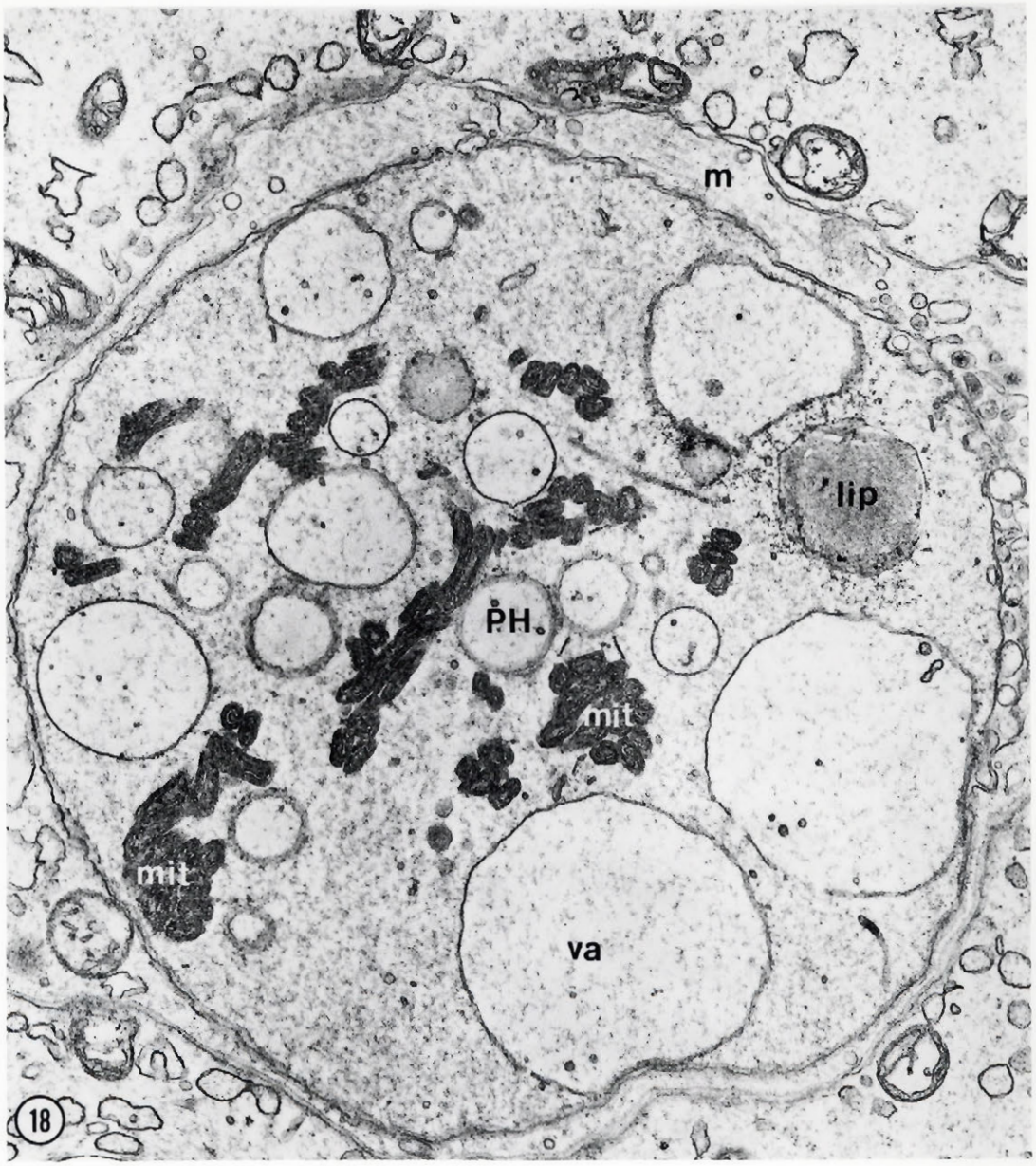
m
lip
PH.
mit
mit
va
18

FIGURE 19

Supranuclear region of a Sertoli cell at stage IX of the cycle.(X27000)
Double walled phagosome (PH) containing a spermatid's cytoplasmic residual body. The residual body presents vacuoles (va), lipid droplets (lip) and masses of ribonucleoprotein (rp).
Around the phagosome, several lysosomes (SL) and bundles of microtubules (m) can be seen in the cytoplasm of the Sertoli cell.

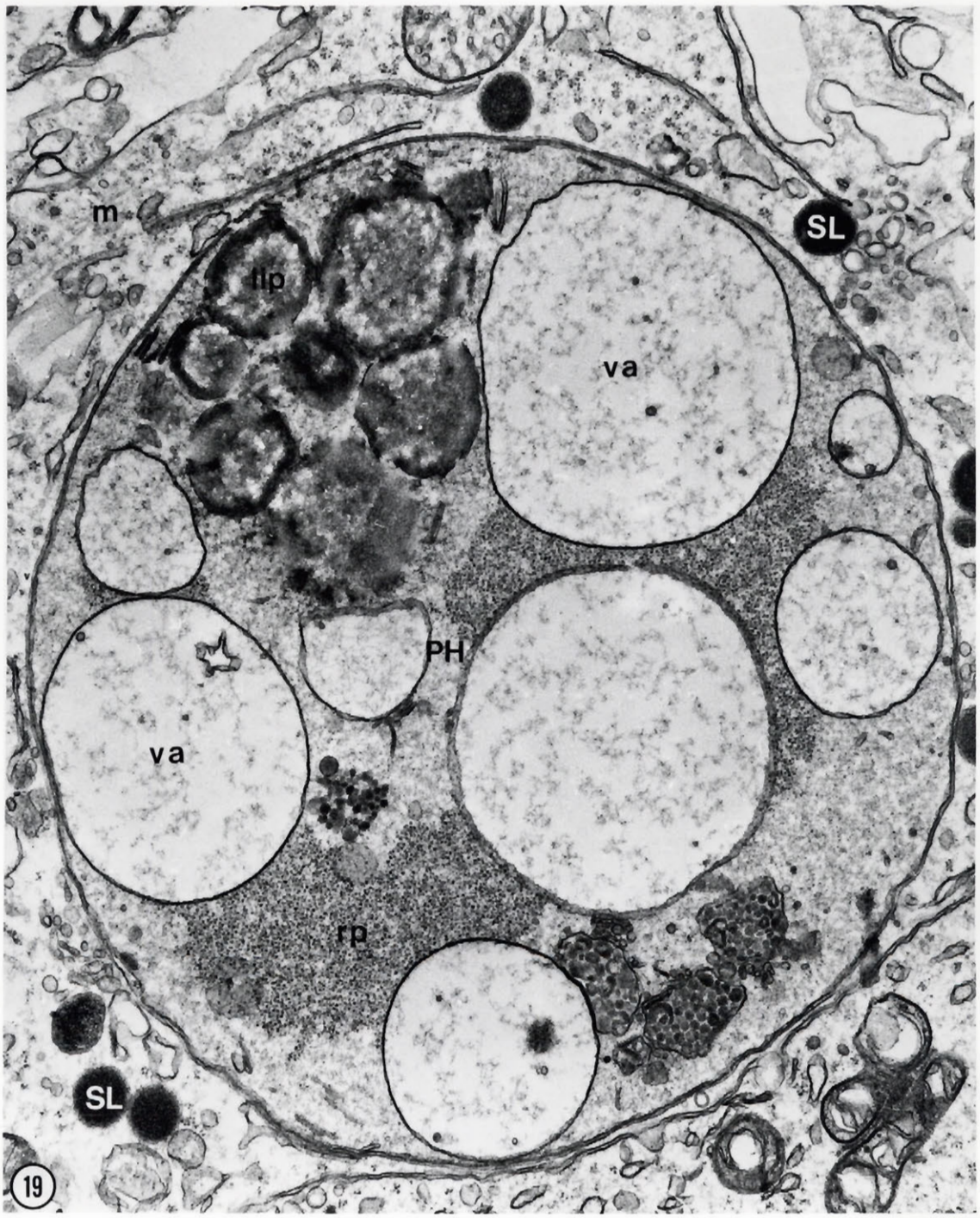
m
lip
SL
va
PH
va
rp
SL
19

FIGURE 20

Phagolysosome (PL) containing a spermatid's cytoplasmic residual body. (X57800)

The plasma membrane of the cytoplasmic residual body is not longer intact on one side of the phagolysosome.

Several secondary lysosomes (SL) can be seen around the phagolysosome and one of then has fused with this element (arrowhead).

The presence of electron dense bodies (arrows) can be seen within some secondary lysosomes.

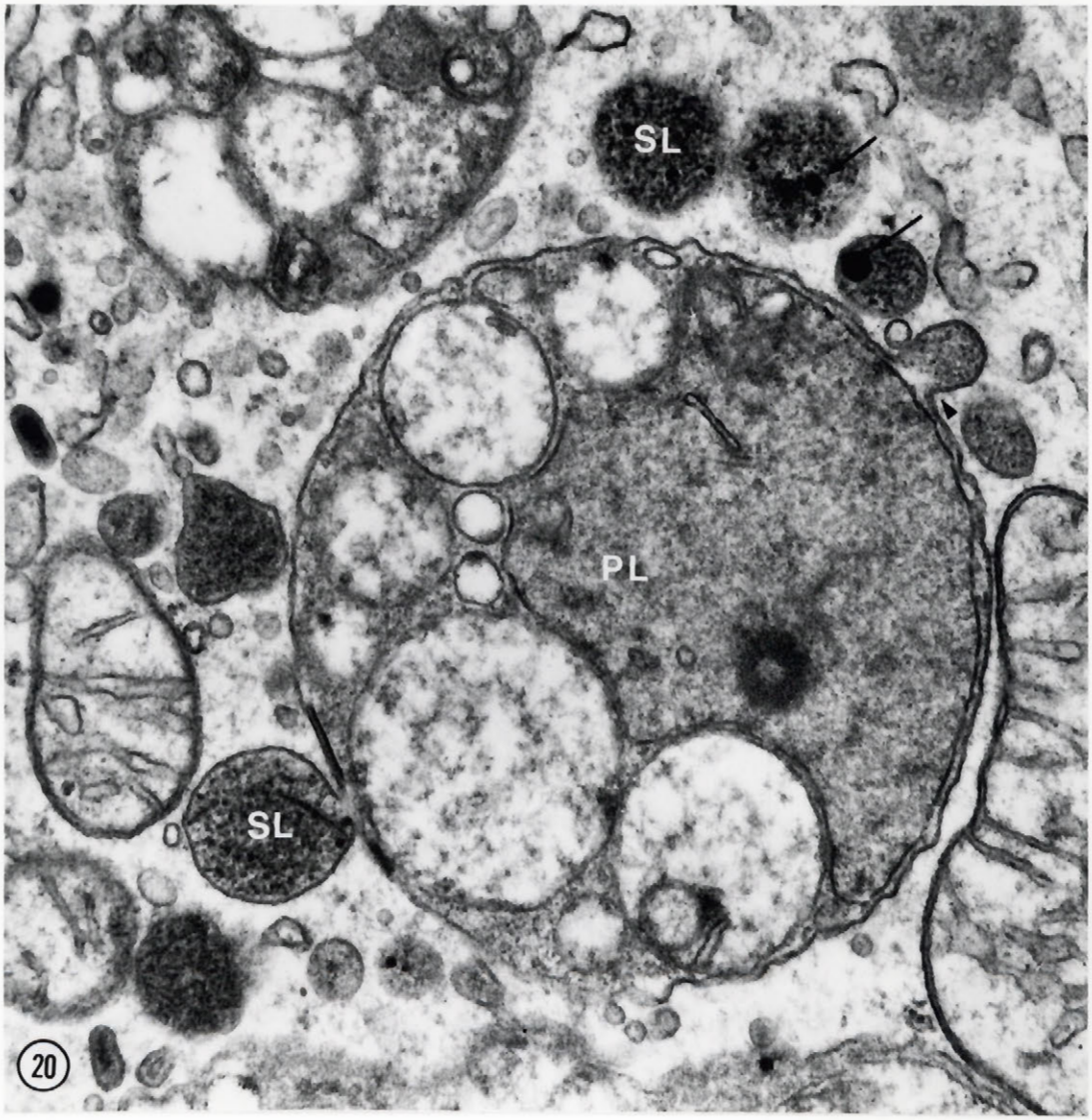
SL
PL
SL
20

FIGURE 21

Supranuclear region of a Sertoli cell at stage IX of the cycle showing the presence of a phagolysosome (PL) containing a cytoplasmic residual body.(X20000) Note the breakdown of the inner membrane and lysis of the cytoplasmic components of the residual body. Several lysosomes (SL) are seen close to this structure.

This micrograph also shows some profiles of Golgi saccules (G) and subsurface specializations parallel to the head and cytoplasmic lobule of the spermatids (SP).

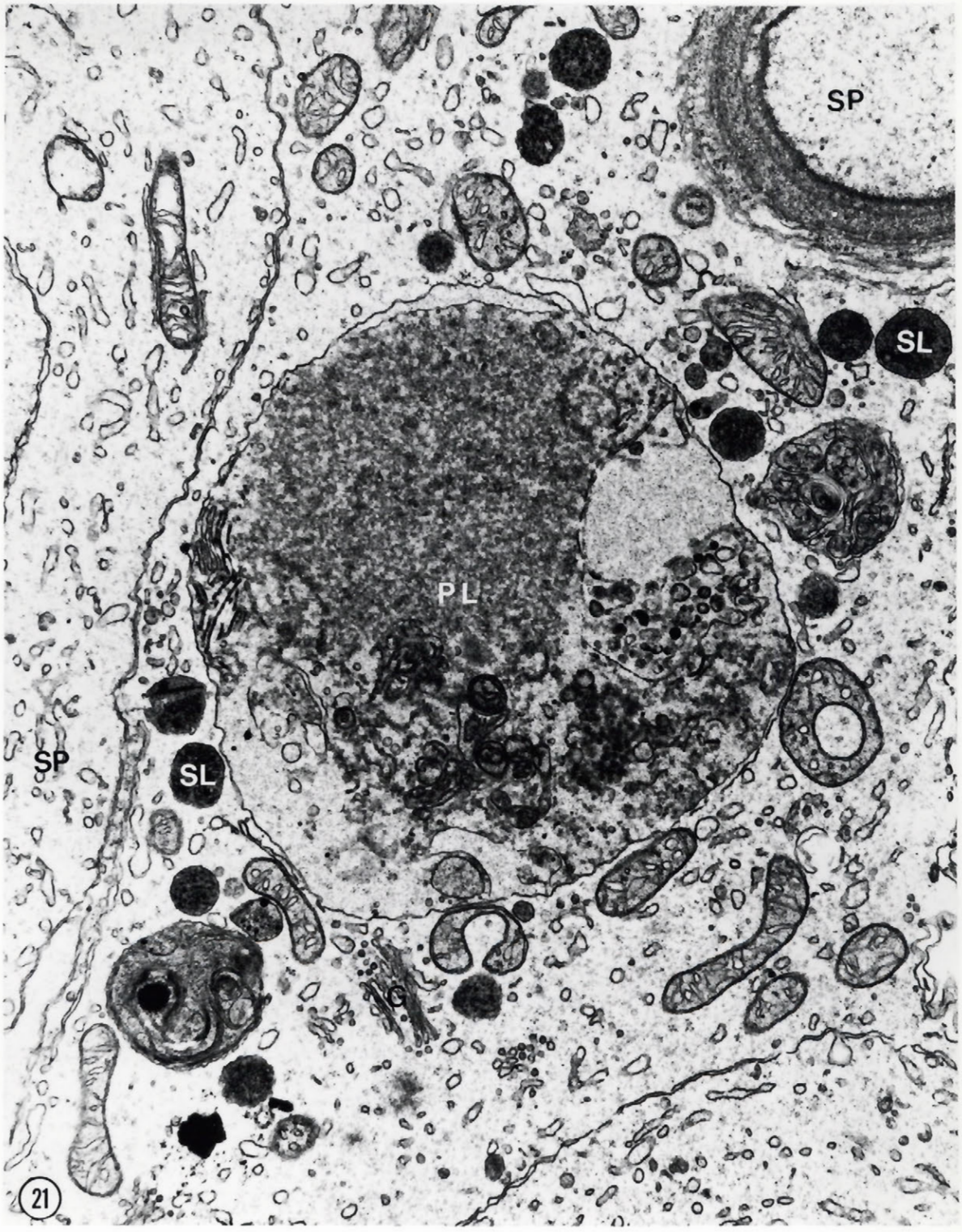
SP
SL
PL
SP
SL
G
21

FIGURES 22-23

Phagolysosomes containing the spermatid's cytoplasmic residual bodies (PL). (X20500)

CMPase (Fig. 22) and TMPase (Fig.23) activity can be detected within these elements and within several secondary lysosomes (SL) as well.

Note the presence of some lipidic droplets (lip) within a phagolysosome located in the basal region of a Sertoli cell (Fig. 23).

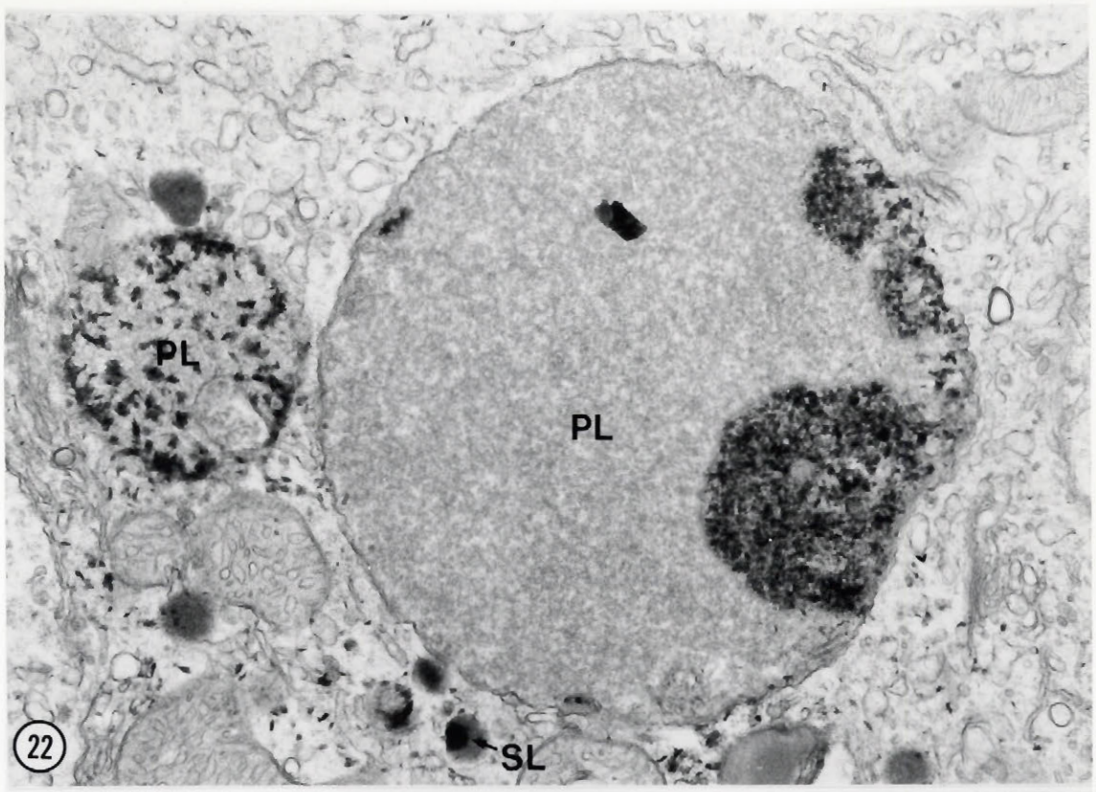

22

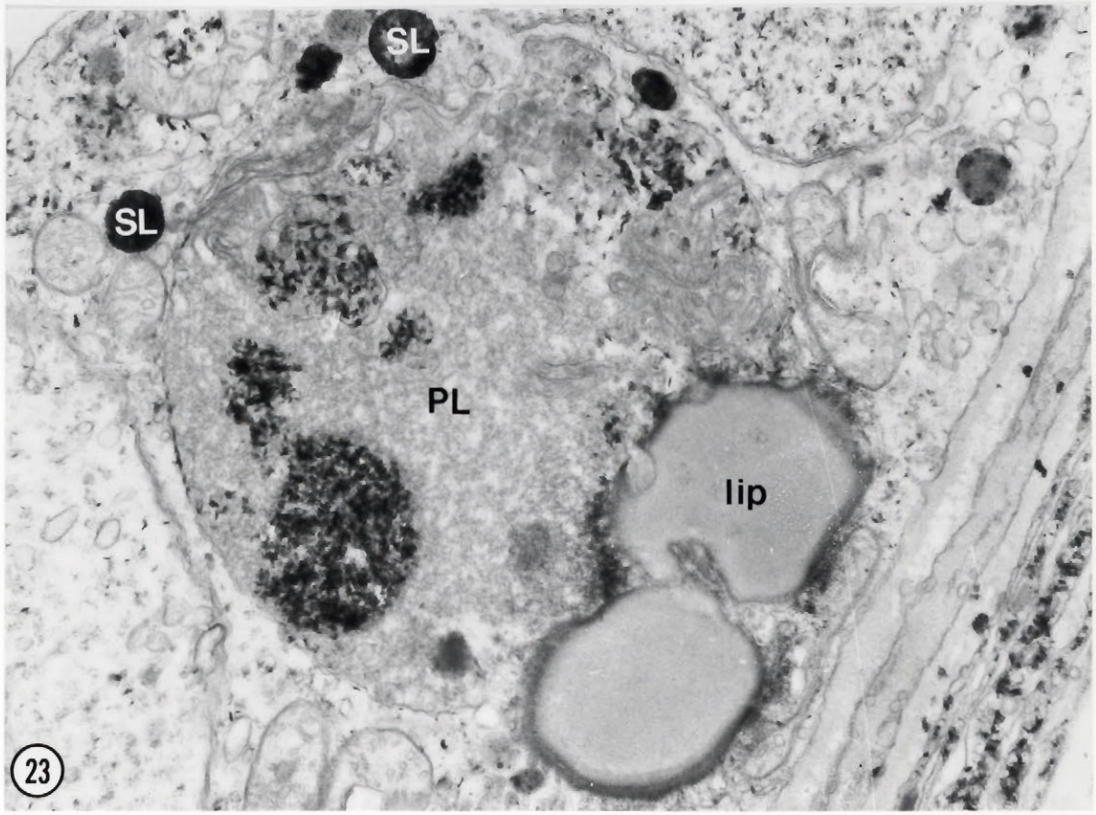

23

Some of the various membranous elements present within the clusters, i.e. "dense core vesicles" (120-170 nm in diameter), often showed positive reaction to both TMPase and CMPase (Figs. 14, 15). On the other hand, the "pale vesicles" (100-120 nm in diameter) did not exhibit reaction product to any of the cytochemical procedures. During stage VIII of the cycle, the early double membrane-bound phagosomes containing the cytoplasmic residual bodies of the late spermatids located in the apical region of the Sertoli cell did not present acid phosphatase activity, whereas at early stage IX, the phagosomes surrounded by a single membrane and found in the middle or basal cytoplasm of the Sertoli cell showed phosphatase activity (Figs. 22, 23).

(6) HRP-colloidal gold complex (HRP-G), Native Ferritin (NF), Albumin and Lactoalbumin-colloidal gold complex (Albumin-G and Lactoalbumin-G), and Concanavalin A-F in the presence of alpha-methyl-D-mannoside

Within 1 to 15 minutes after injection, NF was localized exclusively within large and irregular vesicles in the apical cytoplasm of the Sertoli cells (Fig. 24). This marker was found freely suspended in the electron lucent matrix of these vesicles (Fig. 24). At 30 min after injection the tracer was found within the large irregular multivesicular bodies (Figs. 25, 26). Since endosomes are defined as vacuoles involved in fluid-phase endocytosis or receptor mediated endocytosis, and considered to be "pre-lysosomal" in nature, the large irregular multivesicular bodies of pale matrix will be referred in this work as endosomes. Furthermore, they showed the plaques of coated fuzz characteristic of some types of endosomes (Willingham et al, 1981; Beguinot et al., 1983) (Figs. 6, 10, 17, 26, 27, 34). Some "pale vesicles" pinching off from or around the pale irregular multivesicular bodies were also labelled (Figs. 25-27). At one hour, the native

ferritin was in the denser matrix of more compact, spherical multivesicular bodies (Fig. 26). Some dense core vesicles were also seen labelled (Fig. 27). At 2, 4, 6 and 24 hours, the ferritin was found within the dark matrix of secondary lysosomes (Figs. 27, 31). Images suggesting fusion between labelled and unlabelled secondary lysosomes, as judged by the shape and content of the lysosomes, were frequently seen at all stages of the cycle, particularly in stages I to VII of the cycle (Figs. 28 - 29).

During late stage VIII of the cycle of the seminiferous epithelium, the double membrane-bound phagosomes containing the spermatid's cytoplasmic residual bodies and located at the apex of Sertoli cells were unlabelled with tracers at any interval after injection. At stage IX of the cycle the single membrane-bound phagosomes present in the middle and basal cytoplasm of the Sertoli cells remained unlabelled 2 hours after injection, although several labelled lysosomes were often observed around these structures. Between 4 and 6 hours the phagosomes showed distinct degrees of labelling, and the tracers were usually located at the periphery of these bodies (Fig. 31).

In contrast, the microvesicles (25-35 nm in diameter) either appearing in groups or forming a crown around the multivesicular bodies and dense secondary lysosomes remained unlabelled at any time interval. HRP-G, Albumin-G, Lactoalbumin-G and Concanavalin A-F in the presence of alpha-methyl-D-mannoside presented a distribution identical to the one just described for NF (Figs. 33-38).

In vitro experiments performed on material previously fixed and incubated for 1 hour at 37°C with the different tracers utilized to demonstrate fluid-phase pinocytosis showed that neither NF, HRP-G, Albumin-G, Lactoalbumin-G nor Con A-F in the presence of alpha-methyl-D-mannoside bound to the apical plasma membrane of the cell or to the membrane of the large endocytic vesicles.

FIGURE 24

Intraluminal injection of Native Ferritin

(15 min.)

Apical cytoplasmic process of a Sertoli cell

at stage XII.(X62000)

NF molecules are seen free in the luminal content

of three endocytic vesicles (EV).

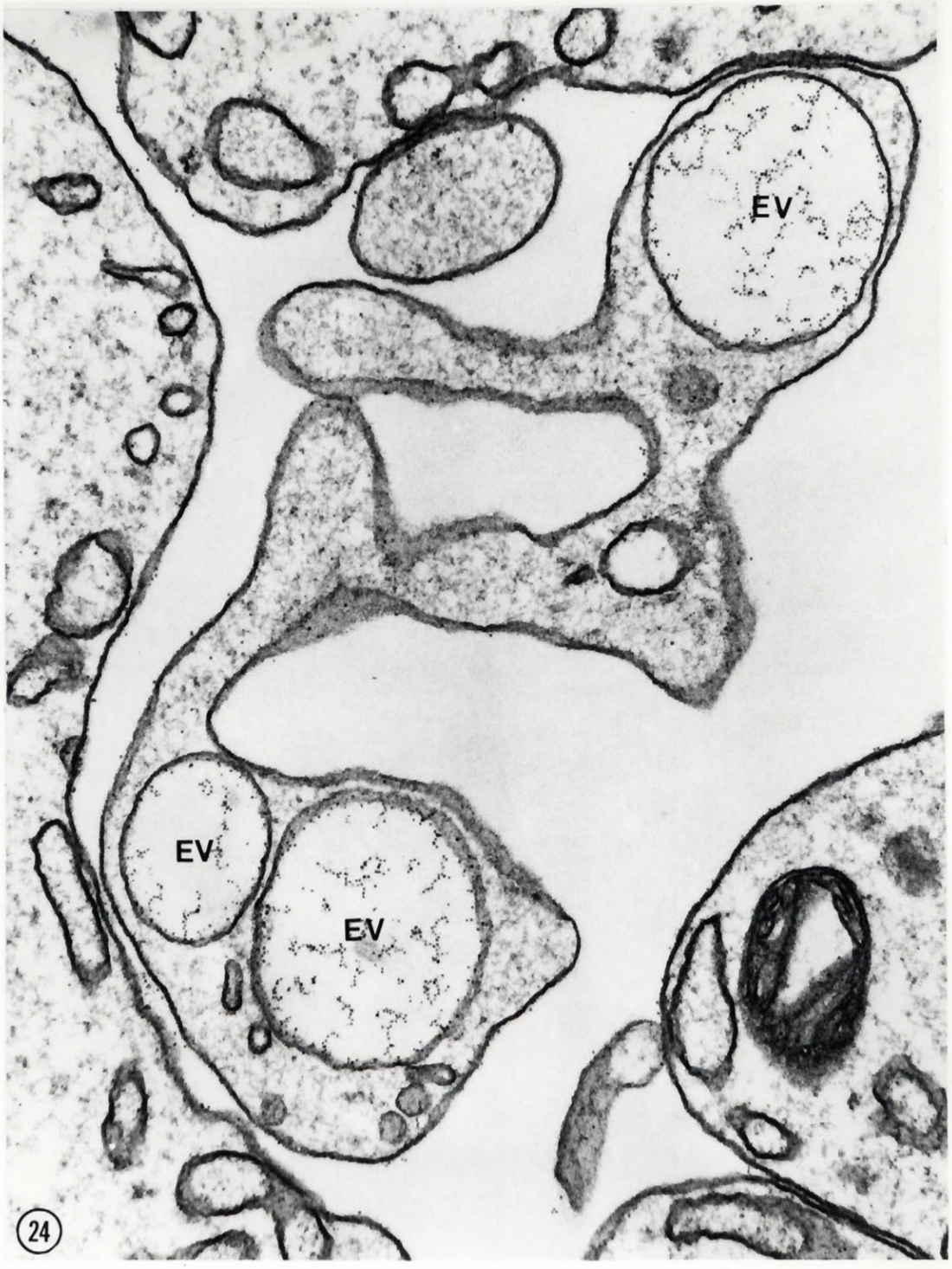
EV
EV
EV
24

FIGURE 25

Supranuclear region of a Sertoli cell, 30 min. after injection of native ferritin into the lumen of the seminiferous tubules. Multivesicular body of pale matrix (E) containing tracer. This element also presents a bristled patch on the outer side of the membrane characteristic of some endosomes. A tubulo vesicular structure with a content showing a similar electron density seems to be pinching off from this body (arrow). Note that while some pale vesicles (pv) are labelled, the dense core vesicles (dv) remain unlabelled at this time interval. In this micrograph, dense secondary lysosomes can be observed devoid of tracer. (X47800)

FIGURE 26

Endosome (E) and spherical multivesicular body of dense matrix (MVB) labelled with native ferritin 1 hour after injection into the lumen of the seminiferous tubule. Pale vesicles (pv), some of them labelled (arrow head), and dense core vesicles (dv) can be seen in this field. Several microvesicles (mv) are observed near the spherical multivesicular body. (X48100)

FIGURE 27

Apical cytoplasmic region of a Sertoli cell, 2 hours after injection of native ferritin. Tracer can be seen within dense secondary lysosomes (SL), pale vesicles (pv) and dense core vesicles (dv). (X53100)

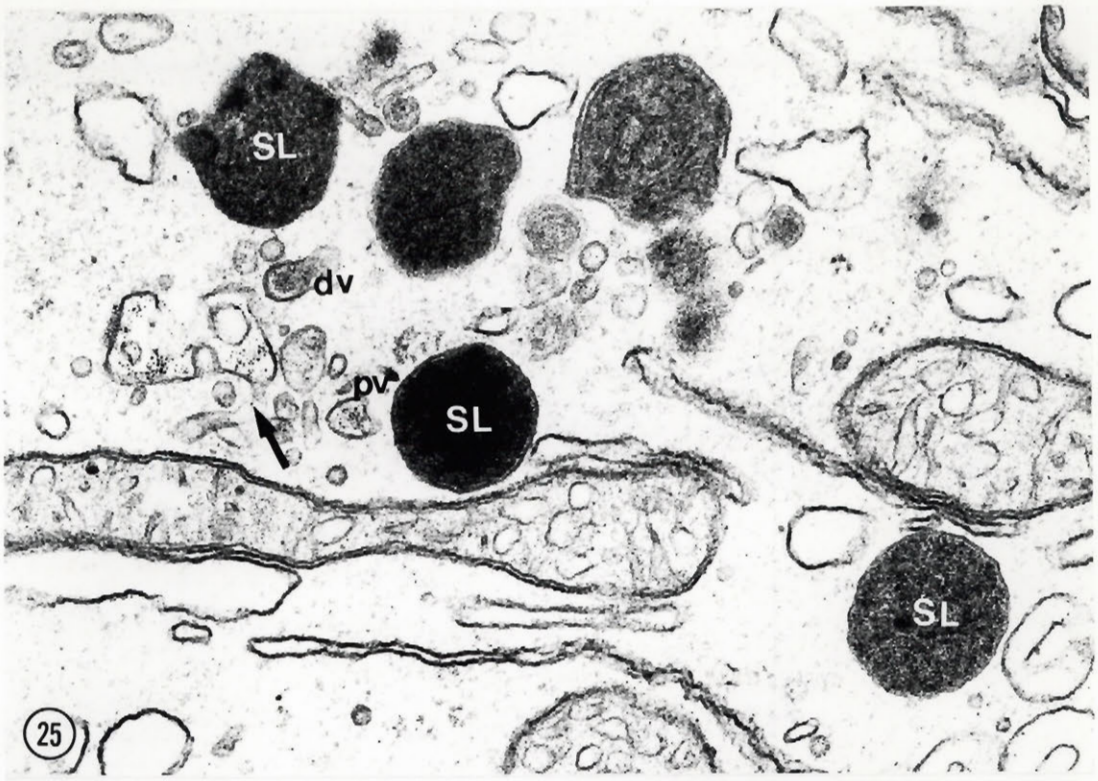
SL
dv
pv
SL
SL
25

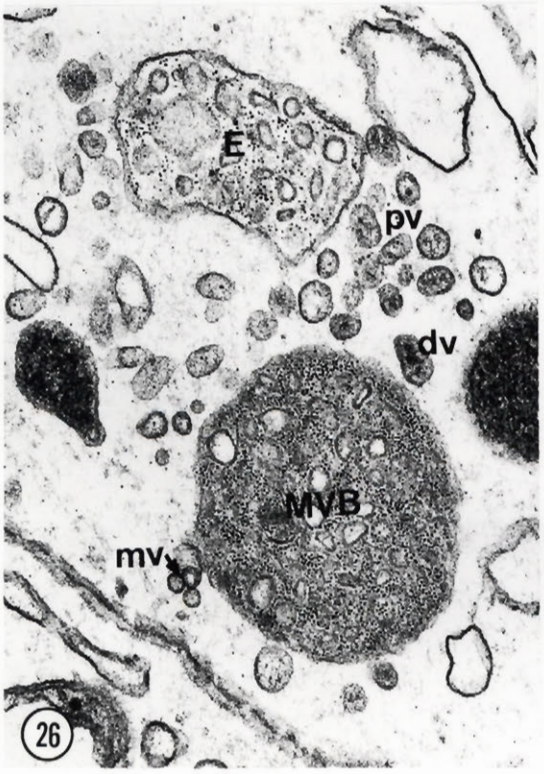
E
pv
dv
MVB
mv
26

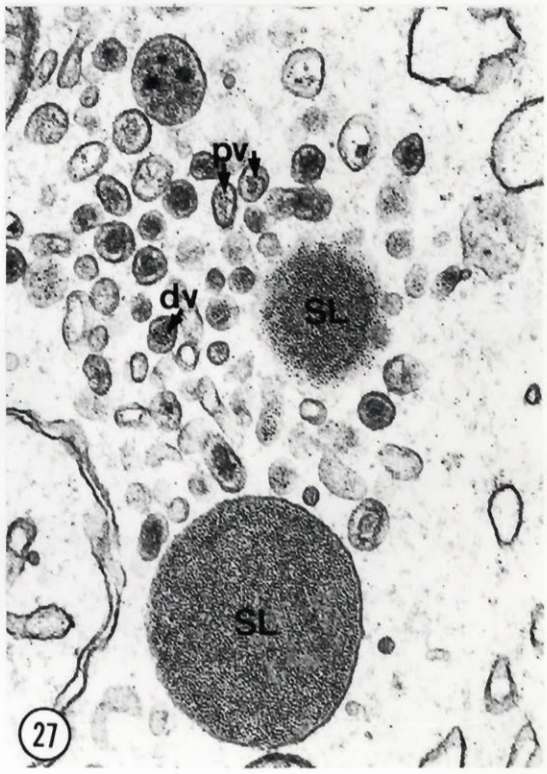
pv
dv
SL
SL
27

FIGURES 28-29

Basal aspect of a Sertoli cell at stage II of the cycle, 4 hours after injection of native ferritin.

Fig. 28: the unlabelled secondary lysosomes (SLu) present usually a darker content than the labelled ones (SLa). (X60700)

Fig. 29: figure suggesting fusion between a labelled secondary lysosome and an unlabelled secondary lysosome of darker matrix. (X58000)

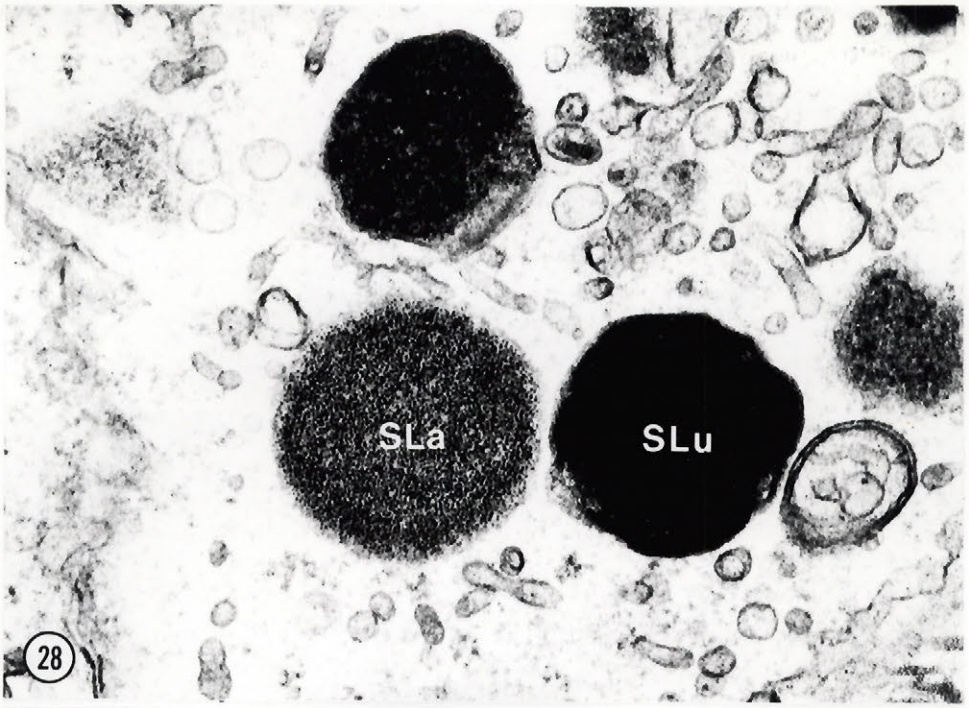
SLa
SLu
28

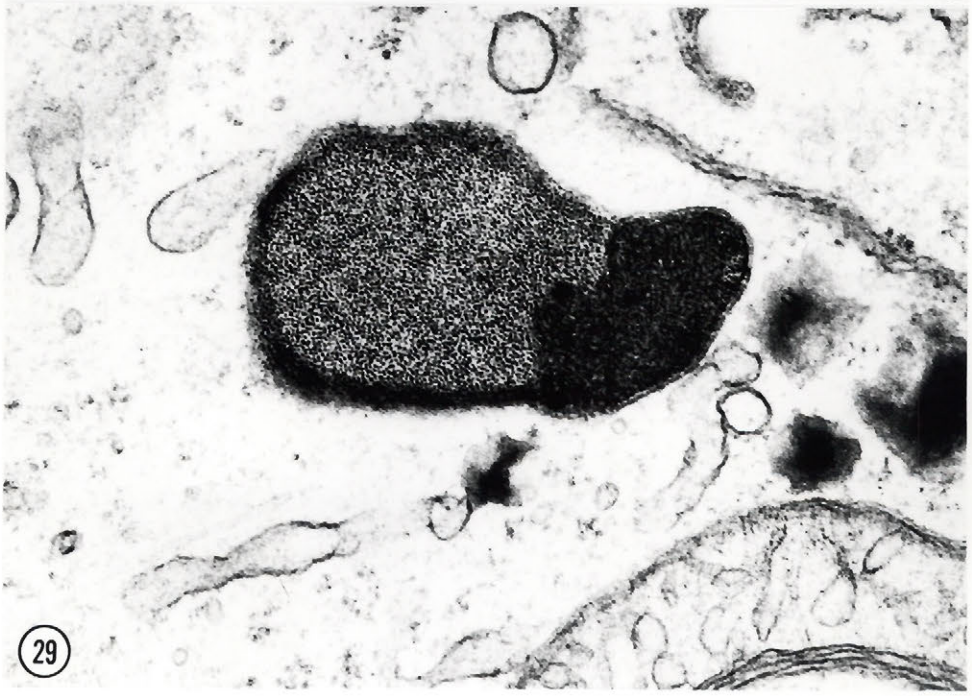
29

FIGURE 30

Basal aspect of a Sertoli cell at stage VI of the cycle 2 hours after injection of native ferritin into the lumen of the seminiferous tubules. Several secondary lysosomes (SL), pale vesicles (pv) and dense core vesicles (dv) contain the tracer. Note the presence of figures suggesting fusion between labelled and unlabelled secondary lysosomes of different electron densities (arrows). Some secondary lysosomes contain figures of myelin (my), small lipidic droplets (lip) and electron dense bodies (arrowheads). (X38000)

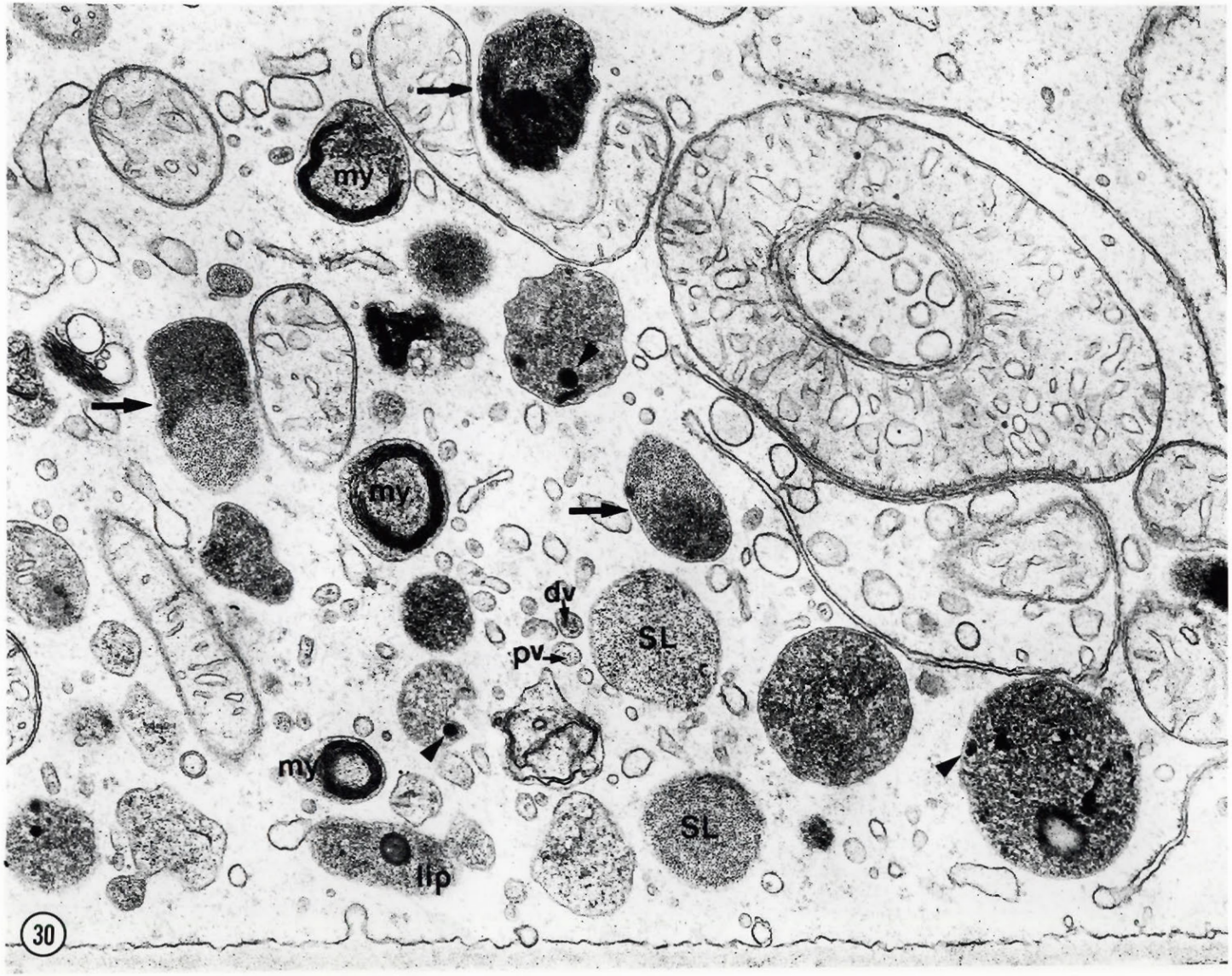
my
my
my
dv
pv
SL
SL
lip
30

FIGURE 31

Supranuclear region of a Sertoli cell at stage I (early) after 6 hours of native ferritin infused into the lumen of the seminiferous tubules. Several secondary lysosomes (SL) are seen loaded with the tracer. A few small dense core vesicles (dv) are also labelled. (X42000)

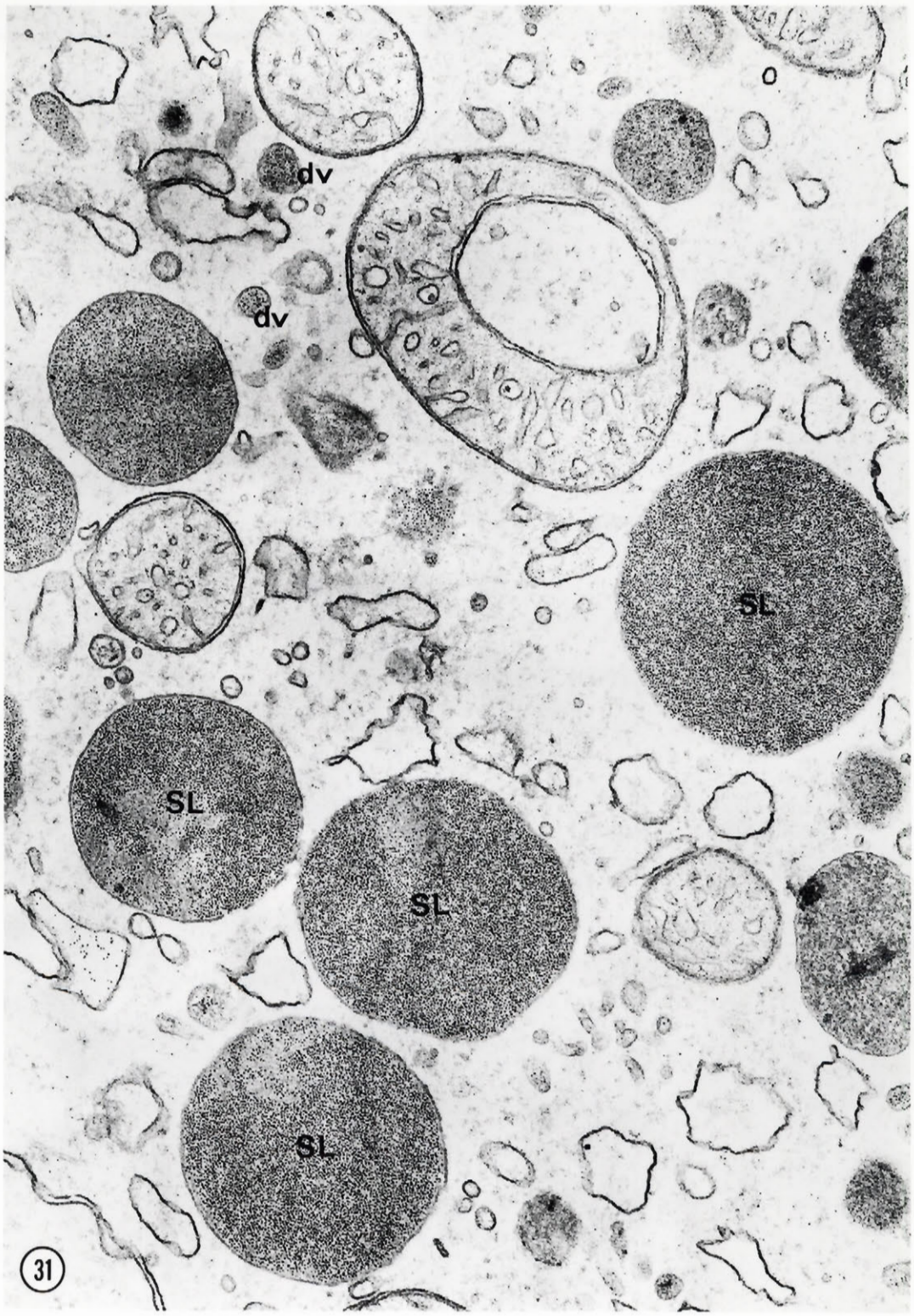
dv
dv
SL
SL
SL
SL
31

FIGURE 32

Intraluminal injection of Native Ferritin (6hours). Phagolysosome (PL) containing some membranous profiles and degenerating mitochondria of a spermatid's cytoplasmic residual body.(X39800)
NF molecules can be seen within this element preferentially located at the periphery. Some labelled secondary lysosomes (SL), as well as, labelled vesicles (arrowheads) can be seen around this body.

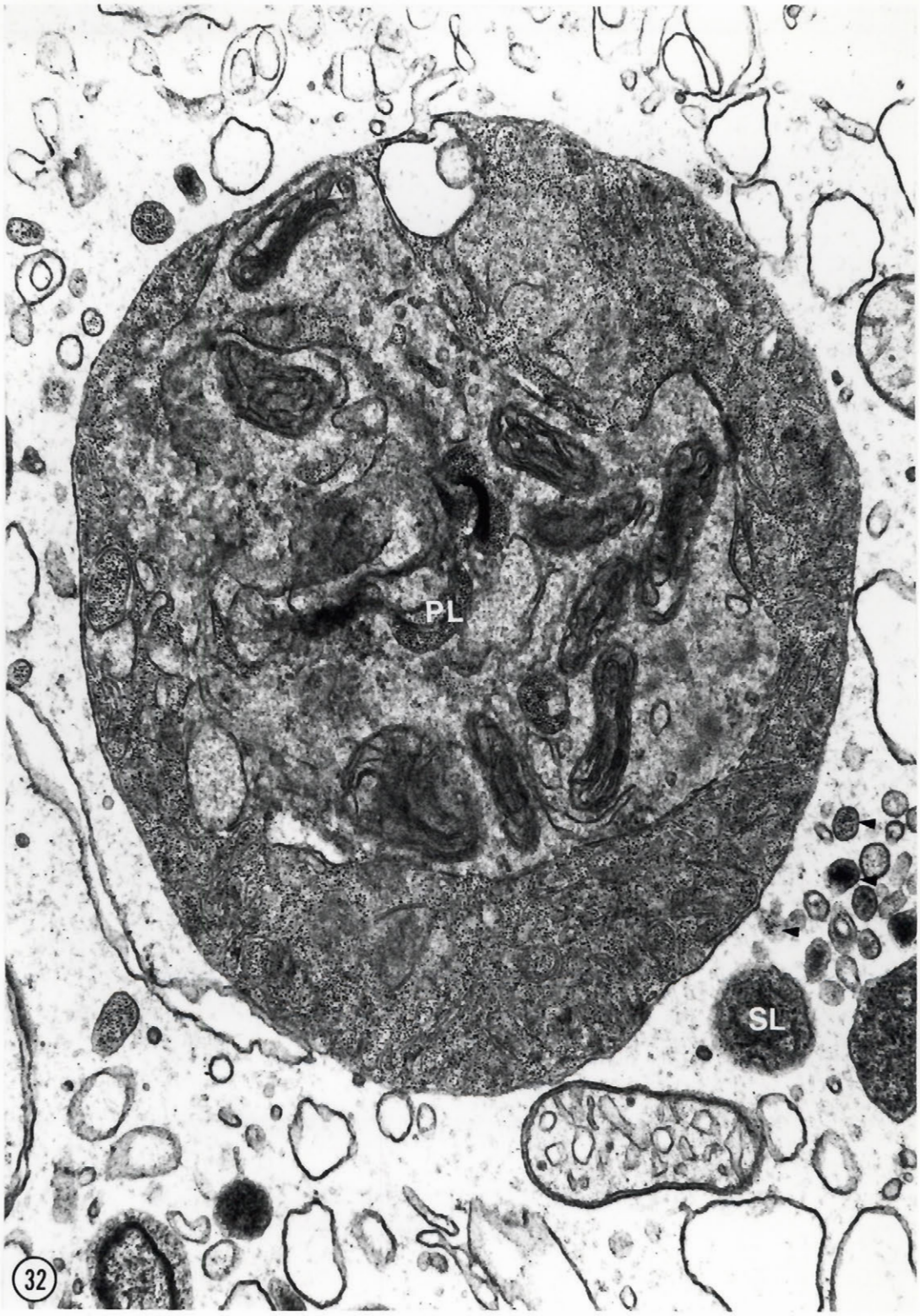
PL
SL
32

FIGURE 33

Supranuclear region of Sertoli cell 15 min. after injection of HRP-G into the lumen of the seminiferous tubules. Large irregular multivesicular body of pale matrix (E) contains the tracer. Note the presence of a straight, fuzzy, lamellar edge on the outer side of the membrane, characteristic of some types of endosomes (arrowhead). Several microvesicles (arrows) and one unlabelled secondary lysosome (SL) are seen close to this structure.(X48000)

FIGURE 34

Spherical multivesicular body (MVB) contains gold particles at one hour after injection of HRP-G. (X52000)

FIGURE 35

Supranuclear region of a Sertoli cell 2 hours after injection of HRP-G into the lumen of the seminiferous tubules. Gold particles are seen in a dense secondary lysosome (SL). Sp portion of head spermatid. (X47000)

FIGURE 36

Apical cytoplasmic region of a Sertoli cell 30 min. after injection of HRP-G into the lumen of seminiferous tubules. The tracer can be seen within some pale vesicles (pv) but it is absent from dense core vesicles (dv). (X49000)

FIGURE 37

Supranuclear region of a Sertoli cell 2 hours after injection of albumin-G. Gold particles are seen within dense secondary lysosomes (SL). (X47000)

FIGURE 38

Basal aspect of a Sertoli cell 2 hours after injection of lactoalbumin-G. Secondary lysosome (SL) contains the tracer. A dense core vesicle (arrow) seems to be budding off from this element. (X49800)

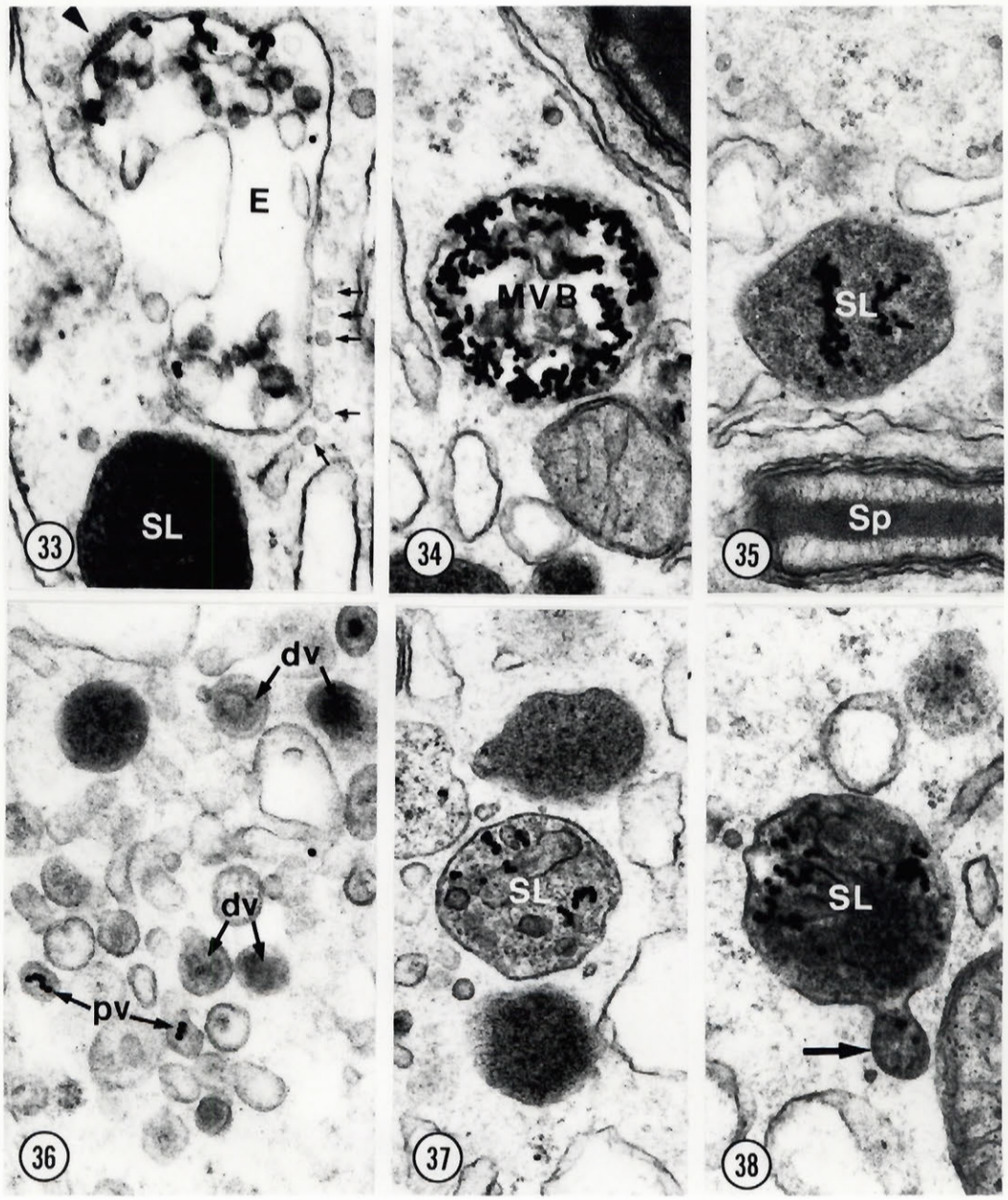
E
SL
33
MVB
34
SL
Sp
35
dv
dv
pv
36
SL
37
SL
38

FIGURE 39

Apical cytoplasmic process of a Sertoli cell (AP) at stage XIII, 15 min. after injection of cationic ferritin into the lumen of the seminiferous tubule. Although this tracer binds to the plasma membrane of the Sertoli cell, the ferritin is not internalized in the endocytic vesicles (EV). (X45000)

FIGURE 40

Apical cytoplasmic process of a Sertoli cell at stage I, 15 min. after injection of Con A-F. Concanavalin A-F binds to the apical processes of Sertoli cell (AP) at all stages of the cycle and like CF, it is not incorporated into the endocytic vesicles (EV) by an adsorptive mechanism. Occasionally a few molecules of Con A-F can be found free in the luminal content of some vesicles (arrow) which seemingly represent unbound Con A-F. (X45000)

FIGURE 41

Apical region of a Sertoli cell at stage VIII of the cycle, 1 hour after intraluminal injection of cationic ferritin. Multivesicular body (mvb) associated to the tubulo-bulbar complexes (TBC) containing ferritin molecules. Sp portion of a head of late spermatid. (X38000)

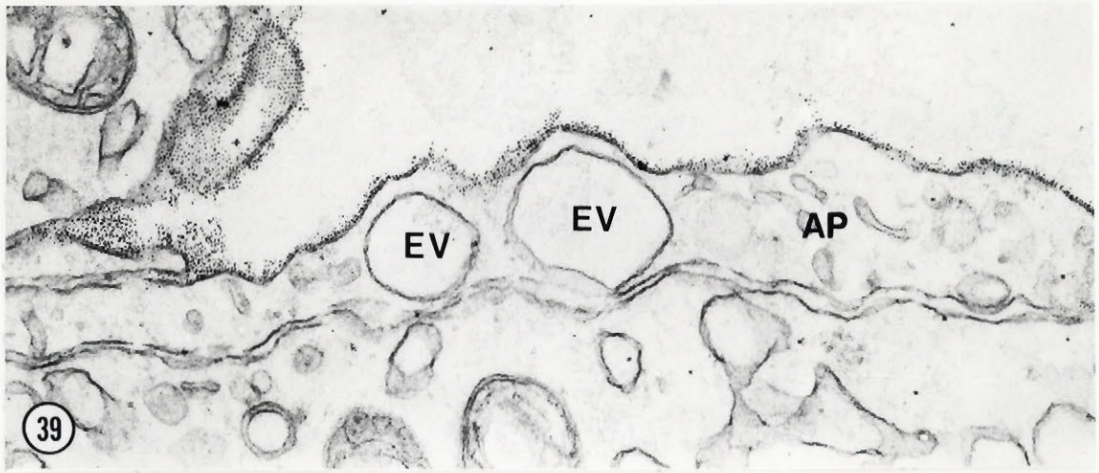
EV
EV
AP
39

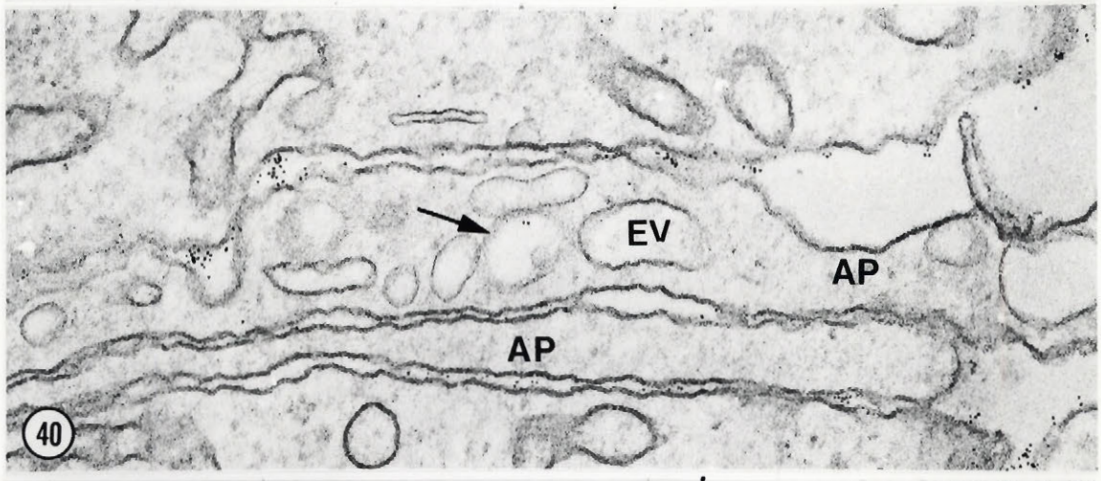
EV
AP
AP
40

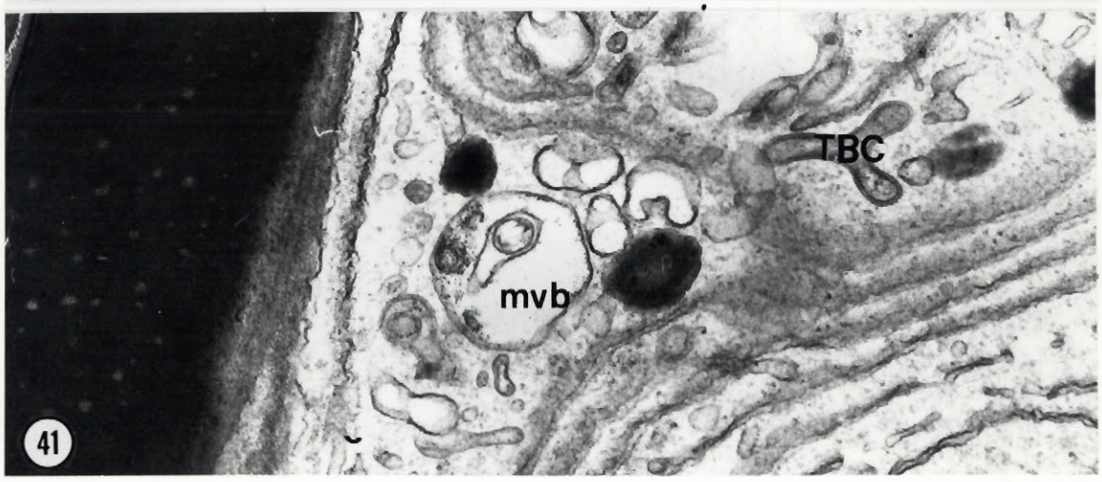
TBC
mvb
41

(7) Cationic Ferritin (CF) and Concanavalin A-Ferritin (Con A-F)

Cationic Ferritin and Con A-F bound to the plasma membrane of the apical processes of the Sertoli cell. However, in most of the stages of the cycle of the seminiferous epithelium the apical endocytic vesicles were unlabelled with either CF or Con A-F (Figs. 39, 40). Occasionally, some endocytic vesicles seemed to be carrying few molecules of unbound Con A-F after 15 minutes injection (Fig. 40) and exceptionally some lysosomes were labelled with this tracer. At stage VIII of the cycle several endocytic vesicles and multivesicular bodies associated with the tubulobulbar complexes were relatively well labelled with both Con A-F or CF. In addition, the tracer seemed to be adsorved to the membrane of the endocytic vesicles and multivesicular bodies (Fig. 41). It was also noted that Con A-F and CF were bound to the plasma membrane of early and late spermatids along their flagellum and to the membrane of the cytoplasmic residual bodies (Figs. 42-44). Thus, the internalization of membrane-bound tracers was limited to structures found in the apical Sertoli cell processes in stages VII to VIII and associated with the tubulobulbar complex.

(8) Influence of colchicine on fluid-phase pinocytosis

The fine structure of the seminiferous epithelium after two or three hours of intratesticular injection with 0.2 mg of colchicine was similar to that of the normal seminiferous epithelium and to the seminiferous epithelium treated with luminocholchicine. However, sloughing of fragments of Sertoli cell cytoplasm and associated germ cells into the lumen of several seminiferous tubules was also noted, as already described by Russell et al (1981). Thus, only those cross sections of seminiferous tubules showing cellular integrity of the Sertoli cells were chosen for this study.

The animals previously treated with colchicine and sacrificed one hour after intraluminal injection with NF showed active incorporation of the

FIGURE 42

Cross section of a group of flagellae of step 18 spermatids 15 min. after intraluminal injection of Con A-F. Concanavalin A-F binds to the plasma membrane of these cells (arrowheads). (X43800)

FIGURE 43

Longitudinal section of two flagellae of step 18 spermatids 15 min. after injection of CF into the lumen of the seminiferous tubules.
CF molecules bind to the plasma membrane (arrowheads). (X44000)

FIGURE 44

Spermatid's cytoplasmic residual body (RB) at stage VIII of the cycle labelled with cationic ferritin 15 minutes after injection.
Note the presence of the tracer in the intercellular space (arrowhead). (X43500)

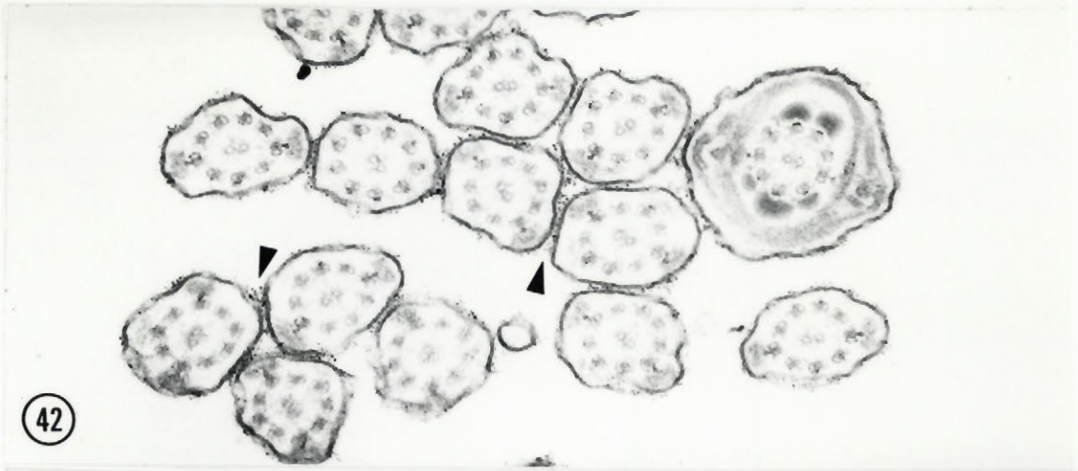

42

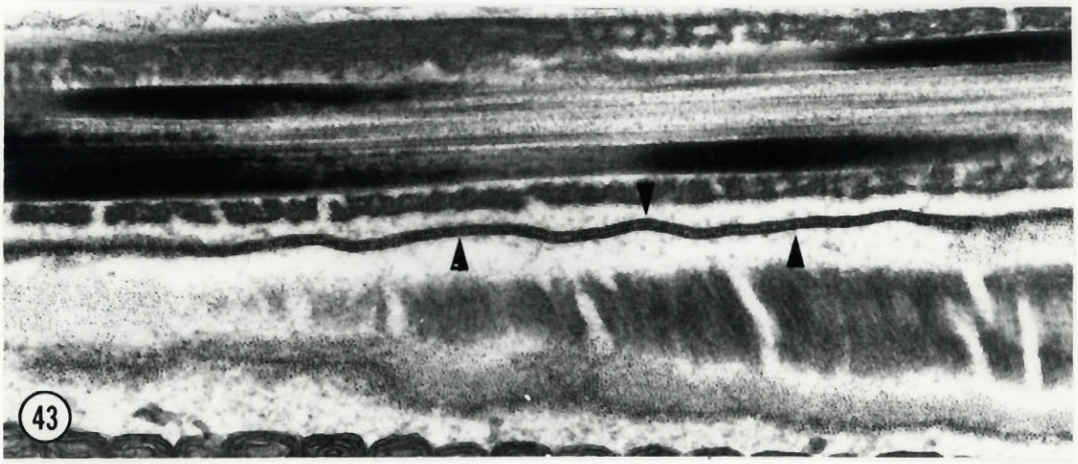

43

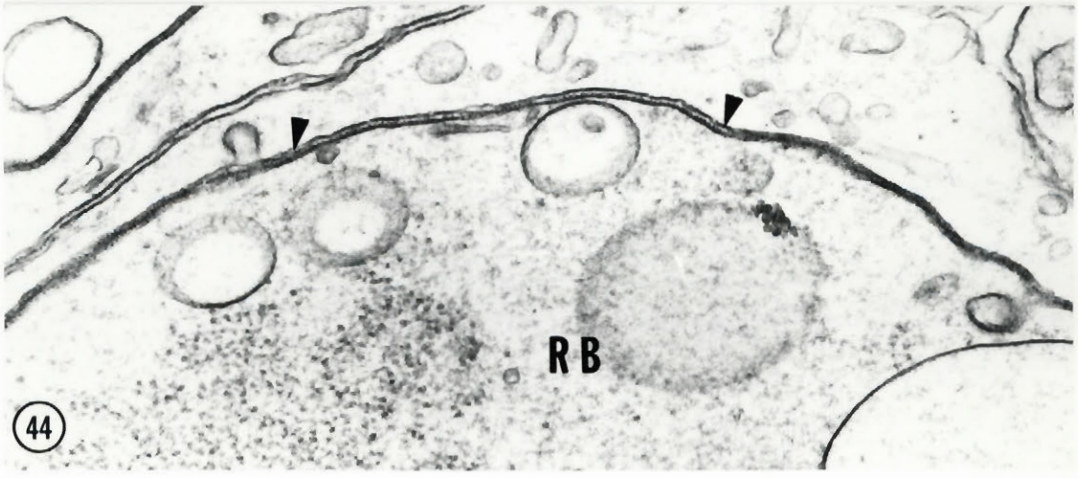

44

marker into the apical endocytic vesicles and multivesicular bodies of different densities (Fig. 45). Two hours later the ferritin was present within the dense secondary lysosomes (Fig. 45). It was also noted that colchicine produced a complete depletion of the microtubules that normally were found in the Sertoli cell cytoplasm and induced the arrest of germ cell mitosis and meiosis. Luminocolchicine, a colchicine analogue, did not produce a disruption of microtubules and did not show any effect on fluid-phase uptake of tracers and on the subsequent labelling of the lysosomal elements.

(9) Influence of cytochalasin D on fluid-phase pinocytosis

The ultrastructure of Sertoli cells did not show noticeable modifications after either two or three hours of intratesticular injection of 4.8 µg of cytochalasin D when compared with the normal Sertoli cells from testis that did not receive any injection.

One hour after intratesticular injection with cytochalasin D, the rats received a single injection of 0.2 mg of NF through the rete testis and the animals were sacrificed one or two hours later. Despite the previous injection with the inhibitor, NF was actively incorporated by Sertoli cells in apical endocytic vesicles and in both the pale irregular and dense spherical multivesicular bodies (Fig. 46). Two hours after injection, NF was found in the dense membrane-bound secondary lysosomes (Fig. 46).

(10) Influence of colchicine on the phagocytosis of the cytoplasmic residual bodies

The formation of the cytoplasmic residual bodies occurred at late stage VII and early stage VIII of the cycle and represented a considerable amount of cytoplasm lost from the maturing spermatid. By the end of stage

FIGURE 45

Supranuclear region of a Sertoli cell (Stage I early) treated with colchicine, two hours after injection with NF (X75000)
Colchicine does not prevent the uptake of ferritin molecules which can be seen within endocytic vesicles (EV), endosomes (E), dense spherical multivesicular bodies (MVB), secondary lysosomes (SL) and both, pale vesicles (pv) and dense core vesicles (dv).

FIGURE 46

Supranuclear region of a Sertoli cell (Stage I early) treated with cytochalasin D, two hours after injection with NF. (X72100)
Cytochalasin D does not suppress the incorporation of the tracer which can be observed within a secondary lysosome (SL), a spherical multivesicular body (MVB), a pale vesicle (pv) and a dense core vesicle (dv). Cytochalasin D does not affect the microtubule integrity (m).

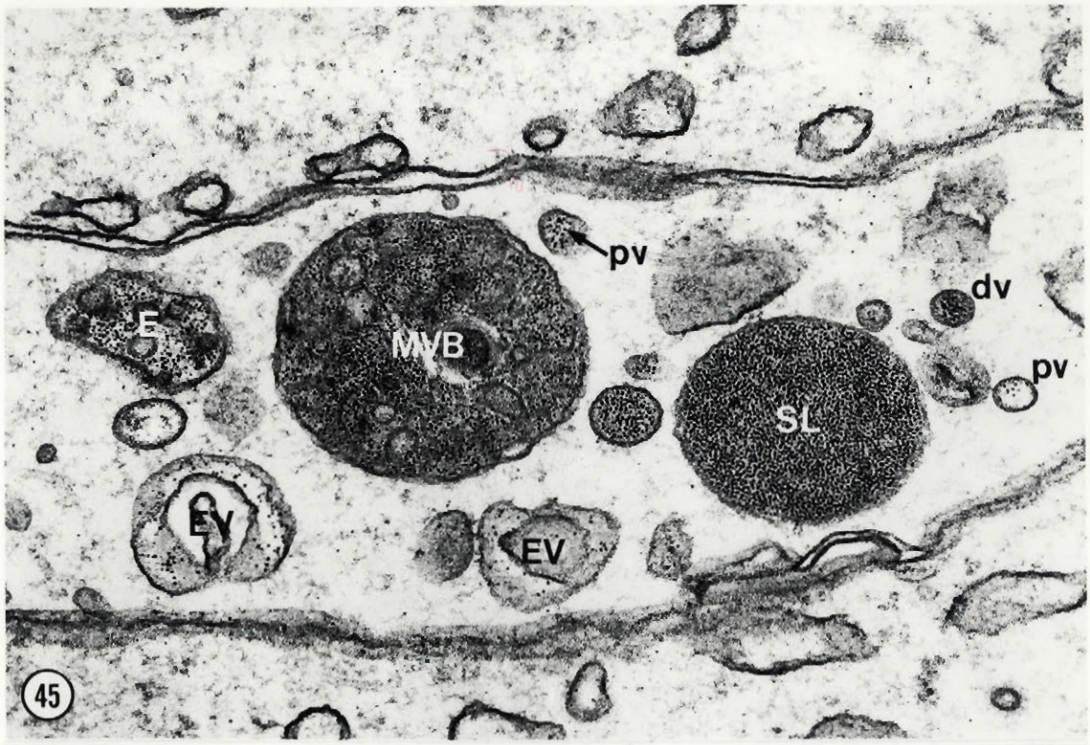
pv
dv
E
MVB
pv
SL
EV
EV
45

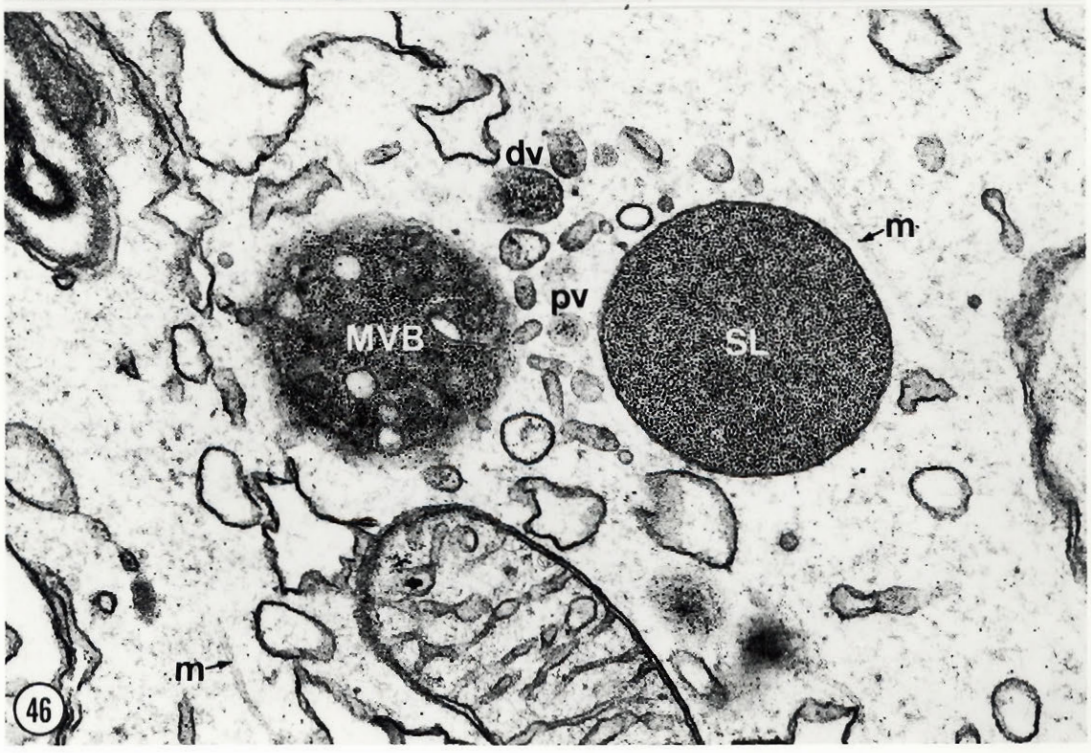
dv
m
pv
MVB
SL
m
46

VIII, thin cytoplasmic processes of the Sertoli cell containing numerous microtubules surrounded the cytoplasmic residual bodies resulting in their phagocytosis by the Sertoli cells.

The sloughing of fragments of Sertoli cell cytoplasm and associated germ cells was more evident after 32 hours of intratesticular administration of colchicine. However, numerous cross sections of seminiferous tubules remained intact. Thus, only the cross sections of tubules at stages VIII and IX of the cycle in which the seminiferous epithelium exhibited structural integrity were selected for the present study.

Colchicine suppressed phagocytosis of the cytoplasmic residual bodies but did not inhibit the process of spermiation. Thus, all the cytoplasmic residual bodies were retained at the apical surface of the Sertoli cell at early and late stage IX of the cycle, that corresponded to the stage VIII at the moment of initiation of the treatment (Figs. 47, 48). In addition, colchicine disrupted completely the microtubules present in the Sertoli cell, including those found in the thin cytoplasmic processes involved in the phagocytosis of the cytoplasmic residual bodies. Colchicine also produced an arrest of germ cell mitosis and meiosis. On the other hand, luminocolchicine did not deplete the microtubules found in the cytoplasm of the Sertoli cell and did not interfere with the phagocytosis of the cytoplasmic residual bodies (Figs. 49, 50).

(11) Influence of Cytochalasin D on the phagocytosis of the cytoplasmic residual bodies

After 32 hours of treatment of the testis with cytochalasin D, the fine structure of the seminiferous epithelium remained similar to that of the normal tissue. Cytochalasin D did not interfere with the phagocytosis and breakdown of the cytoplasmic residual bodies (Figs. 51, 52). These

FIGURES 47-48

Testis injected 4 times every 8 hours with 0.2 mg of colchicine. Fig. 47: Section of seminiferous epithelium at stage VIII (before spermiation) characterized by the presence of cytoplasmic residual bodies and late spermatids on the luminal side (L) of the epithelium. (X400) Fig.48: Section of seminiferous epithelium at stage IX (after spermiation) characterized by the absence of late spermatids attached to the epithelium. (X400) Note that colchicine treatment does not inhibit spermiation but suppresses the internalization of the cytoplasmic residual bodies (arrow head).

FIGURES 49-50

Testis control injected with luminocolchicine. Fig. 49: Light micrograph showing a portion of seminiferous epithelium at stage VIII of the cycle. (X400) Fig. 50: Light micrograph of a portion of seminiferous epithelium at stage IX. (X400) Luminocolchicine does not interfere with the internalization of the cytoplasmic residual bodies by Sertoli cells, which can be seen within phagosomes in the cytoplasm of these cells (arrowheads).

FIGURES 51-52

Testis injected 4 times every 8 hours with 4.8 μg of cytochalasin D. Fig. 51: Section of seminiferous epithelium at stage VIII. (X400) Fig. 52: Section of seminiferous epithelium at stage IX. (X400) The presence of phagosomes in the cytoplasm of the Sertoli cells containing the cytoplasmic residual bodies (Fig. 52, arrowheads) indicates that cytochalasin D does not affect the phagocytosis of these elements.

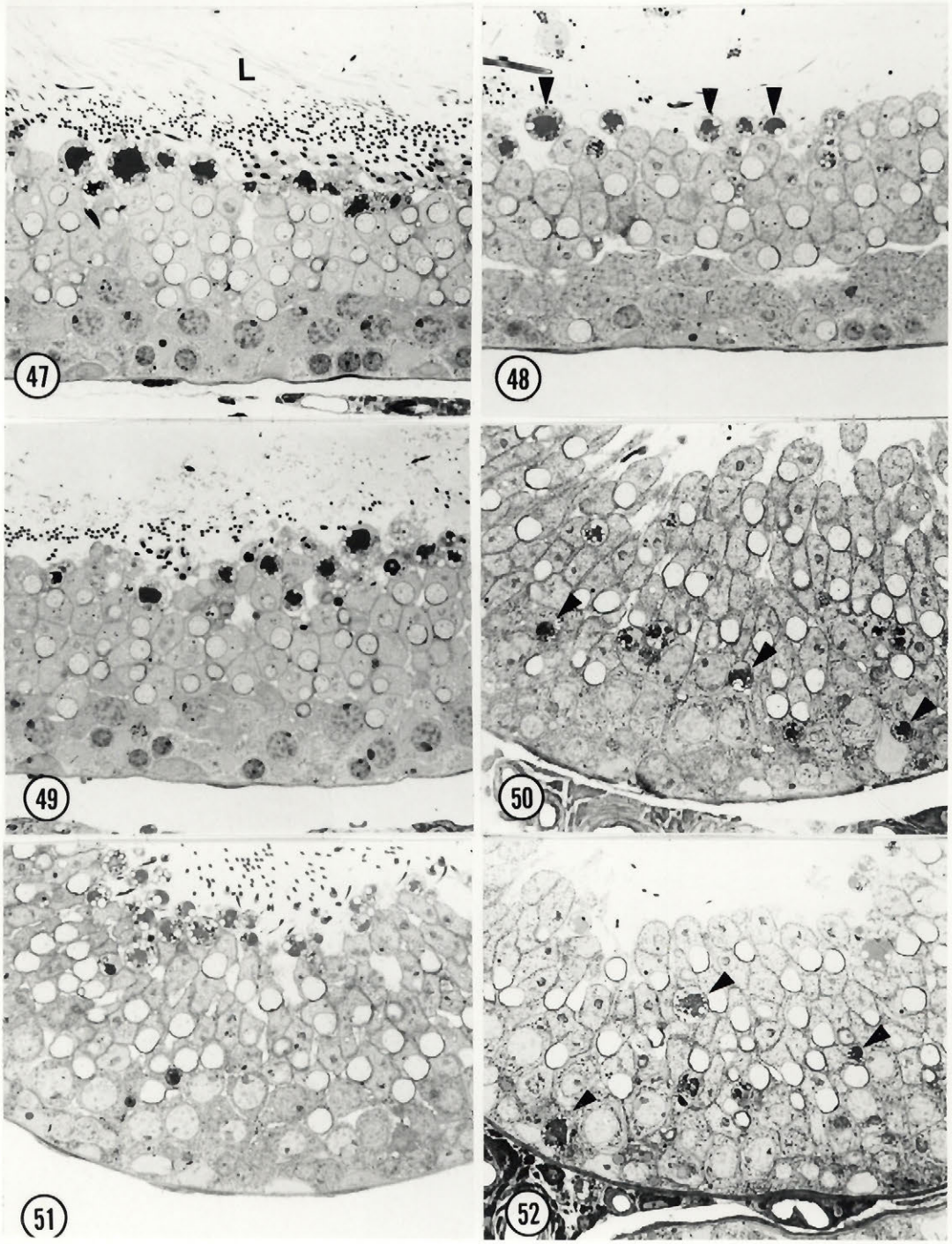
L
47
48
49
50
51
52

results were consistent with the absence of microfilaments in the submembranal region of the Sertoli cell facing the cytoplasmic residual bodies after treatment with tannic acid, which is an agent that protects the microfilaments from the disruption by OsO_4 making possible its visualization.

PART TWO

An exhaustive quantitative analysis was carried out at the electron microscope level in order to estimate the total number and the total volume of the labelled secondary lysosomes per Sertoli cell at different stages of the cycle after 6 hours of intraluminal injection with NF as well as to determine the true number and total volume of secondary lysosomes per Sertoli cell at different stages of the cycle. In addition, the average volume of secondary lysosomes and the percentage of labelled secondary lysosomes per Sertoli cell at different stages of the cycle were included. All the values in Tables I, II, III and VI are accompanied by their standard deviations of the means (SEM).

(1) Number of secondary lysosomes per Sertoli cell

A systematic and quantitative study was performed on 1500 microphotographs with the purpose of determining the total number of secondary lysosomes per individual Sertoli cell at different stages of the cycle.

Secondary lysosomes have been defined as an acid hydrolase membrane-bound body that has already acquired substrates by endocytosis or by autophagy (Posner et al., 1982; Steinman et al., 1983). The spherical multivesicular bodies showing a denser matrix and the dense membrane-bound bodies ranging in diameter from 0.2 to 0.4 μm were considered as secondary lysosomes. The pale large irregular multivesiculat bodies referred to in this thesis as endosomes, the dense core vesicles (100-170 nm)

and the pale vesicles (100-120 nm) were not taken into account in the present morphometric analysis.

The test of "two-way analysis of variance" revealed that there were significant differences in the total number of secondary lysosomes per Sertoli cell among the 14 stages of the cycle of the seminiferous epithelium ($p \leqslant 0.0005$). Moreover, the analysis of the variance showed that there were no statistical differences among the four experiments.

The total number of secondary lysosomes per Sertoli cell (Table I, Fig. 53) increased from stage X (278±23.0 SEM) reaching the highest number at stage XIV of the cycle of the seminiferous epithelium (556±8.0 SEM). The number decreased rapidly from stage I (333±7.5 SEM) up to stage III (232±7.0 SEM), remaining relatively constant throughout stages IV to VII. At stage IX of the cycle a dramatic decrease in the number of lysosomes was observed when the value reached 100±24.0 SEM per Sertoli cell. Statistical analysis by "t" test demonstrated statistical differences between stages XIV and I early ($p \leqslant 0.005$, VIII and IX ($p \leqslant 0.005$), IX and X ($P \leqslant 0.005$), and X and XIII ($p \leqslant 0.005$), whereas there were no statistical differences between stages II and VIII. The number of secondary lysosomes registered from the control (normal testis that did not receive any injection) was similar to the values of the experimental animals. This result suggested that the intraluminal injection did not influence the total number of secondary lysosomes present in the Sertoli cells (Fig. 53, Table I).

(2) Number of labelled secondary lysosomes per Sertoli cell

Statistical analysis by the two-way analysis of the variance showed that there were significant differences in the total number of labelled secondary lysosomes per Sertoli cell among the 14 stages of the cycle ($p \leqslant 0.0005$).

The quantitative analysis revealed an increase in the number of labelled secondary lysosomes per Sertoli cell from stage IX of the cycle of the seminiferous epithelium (54±13.0 SEM), reaching a peak at stage XIII (338±16.5 SEM). The absolute number of labelled secondary lysosomes decreased abruptly from stage I (143±9.5 SEM) to stage II of the cycle (33±2.0 SEM), remaining low until stage VIII (32±2.5 SEM) (See Table II, Fig. 54). The statistical analysis by "t" test demonstrated that there were statistical differences between stages XIII and I early ($p \leqslant 0.005$), I early and II ($p \leqslant 0.005$), and VIII and XIII ($p \leqslant 0.005$), while there were no statistical differences between stages II and VIII of the cycle. In addition, the analysis of the variance showed no statistical differences among the four experimental groups.

(3) Average volume of secondary lysosomes

The analysis of variance indicated that there were statistical differences between different stages of the cycle ($p \leqslant 0.001$).

The average volume of secondary lysosomes remained relatively constant between stages XIV and I and from stage I to stage XI. At stage XII of the cycle an increase of the average volume of secondary lysosomes was registered (0.143 μm^3±0.002 SEM) that remained high during stage XIII (See Table III, Fig. 55).

The "t" test confirmed significant differences between stages XI and XII ($p \leqslant 0.005$) and between stages XIII and XIV ($p \leqslant 0.001$). On the other hand, the "t" test showed no statistical differences between stages III and IV, IV and VI, and IX and XI. Therefore, the high values of the average volume of secondary lysosomes registered during stages XII and XIII were significantly higher than those obtained at other stages of the cycle.

(4) Total volume of secondary lysosomes

The total volume of secondary lysosomes per Sertoli cell was obtained by multiplying the total number of secondary lysosomes by the average volume of this structure (Table IV). Since the average volume of secondary lysosomes remained relatively constant throughout the cycle of the seminiferous epithelium except at stages XII and XIII in which the values were higher, the total volume of secondary lysosomes at different stages of the cycle was consistent with that of the total number of lysosomes per Sertoli cell (Compare Figs. 53 and 56). Thus, the lowest value was registered again at stage IX of the cycle with 11.4 μm^3 (Control = 10.27 μm^3), and the highest at stage XIII of the cycle with 76.85 μm^3 (Control = 76.75 μm^3).

(5) Total volume of labelled secondary lysosomes

The same rationale was applied to calculate the total volume of labelled secondary lysosomes per Sertoli cell. Since the average volume of secondary lysosomes was relatively constant throughout the cycle except at stages XII and XIII, the total volume of secondary lysosomes paralleled the values of the true number of labelled secondary lysosomes (Compare Figs. 54 and 57). Thus, the total volume of secondary lysosomes increased from stage IX of the cycle (6.156 μm^3) reaching a more prominent peak when compared with the peak of the true number of labelled secondary lysosomes at stage XIII (49.01 μm^3) (See Table V). However, this prominent peak was a consequence of the increase of the average volume of secondary lysosomes registered during stage XIII of the cycle of the seminiferous epithelium. Then the total volume of labelled lysosomes decreased abruptly from stage XIII to stage II of the cycle, remaining low until stage VIII.

(6) Percentage of labelled lysosomes per Sertoli cell

From the data on the absolute numbers of labelled and unlabelled lysosomes obtained at the various stages of the cycle (Tables I and II), the percent of labelled lysosomes per Sertoli cells at the 14 stages of the cycle were calculated (Table VI, Fig. 58).

The analysis of variance showed significant differences in the percentage of labelled secondary lysosomes throughout the cycle of the seminiferous epithelium.

Two distinct levels of labelling of the secondary lysosomes of the Sertoli cells were observed during the cycle (Table VI, Fig. 58). From stage II to stage VIII, the percentage of labelled lysosomes remained at relatively low level. On the other hand, the percentage of labelled lysosomes increased abruptly in stage IX and remained at high level until stage XIV of the cycle. The highest percentage of labelled secondary lysosomes was registered at stage XIII of the cycle of the seminiferous epithelium. During stage I of the succeeding cycle, the percentage of labelled lysosomes decreased to return to the low value of stage II.

The "t" test revealed no statistical differences among the stages II to VIII confirming the constant low level registered during these stages of the cycle. On the other hand, the "t" test showed statistical differences between stages VIII and IX ($p \leqslant 0.005$) and I early and I late ($p \leqslant 0.005$). These various results indicated that the values obtained in stages II to VIII (low values) were significantly different from the values obtained in stages IX to XIV (high values). Furthermore, the "t" test analysis indicated that amongst the high values, the one obtained in stage XIII was significantly higher than those obtained for stages IX, X, XI, XII and XIV.

TABLE I

Number of secondary lysosomes per Sertoli cell

Stages of the cycle	Experimental Groups				Mean (±SEM)	
	1	2	3	4		
I e	339	334	349	312	333 ± 7.5	
I l	337	328	285	243	298 ±21.5	
II	288	240	216	262	251 ±15.0	
III	250	216	226	234	232 ± 7.0	
IV	156	250	224	248	220 ±21.5	
V	259	290	212	214	244 ±18.5	
VI	330	281	205	225	260 ±28.0	
VII	204	215	236	249	226 ±10.0	
VIII	183	203	240	255	220 ±16.0	
IX	87	99	49	166	100 ±24.0	(79)*
X	244	272	250	345	278 ±23.0	
XI	242	239	316	244	260 ±18.5	
XII	329	327	387	344	347 ±13.5	
XIII	591	449	553	529	530 ±30.0	(533)*
XIV	549	560	538	576	556 ± 8.0	

* Values derived from the estimates of one control animal not injected with native ferritin.

TABLE II

Number of labelled secondary lysosomes per Sertoli cell

Stages of the cycle	Experimental groups				Mean (±SEM)
	1	2	3	4	
I e	140	134	171	127	143 ± 9.5
I l	106	86	74	66	83 ± 8.5
II	37	36	27	34	33 ± 2.0
III	42	29	23	35	32 ± 4.0
IV	36	38	32	32	35 ± 1.5
V	49	53	33	21	39 ± 7.0
VI	55	40	39	28	41 ± 5.5
VII	31	28	22	31	28 ± 2.0
VIII	34	30	38	26	32 ± 2.5
IX	48	54	24	89	54 ±13.0
X	145	157	133	172	152 ± 8.0
XI	136	130	175	139	145 ±10.0
XII	197	185	207	189	195 ± 4.5
XIII	350	305	380	317	338 ±16.5
XIV	326	275	274	307	296 ±12.5

TABLE III

Average volume of secondary lysosomes (μm^3)

Stages of the cycle	Experimental Groups				Mean (±SEM)	
	1	2	3	4		
I e	.097	.114	.129	.137	.119 ±.009	
I l	.102	.105	.114	.132	.114 ±.005	
II	.109	.119	.124	.127	.120 ±.003	
III	.131	.150	.100	.100	.120 ±.012	
IV	.133	.131	.131	.137	.133 ±.001	
V	.126	.116	.129	.135	.126 ±.003	
VI	.099	.112	.131	.138	.120 ±.008	
VII	.131	.126	.123	.110	.122 ±.006	
VIII	.103	.124	.118	.120	.116 ±.004	
IX	.110	.113	.103	.128	.114 ±.005	(.130)*
X	.118	.106	.116	.130	.117 ±.004	
XI	.114	.117	.123	.130	.121 ±.004	
XII	.134	.166	.157	.150	.152 ±.006	
XIII	.142	.152	.147	.141	.145 ±.002	(.144)*
XIV	.109	.116	.101	.135	.115 ±.007	

* Values derived from estimates of one testis (control) not injected with tracer .

TABLE IV Volume of secondary lysosomes per Sertoli cell

Stages of the Cycle	Volume in μm^3	
Ie	39.627	
Il	33.972	
II	30.12	
III	27.84	
IV	29.26	
V	30.744	
VI	31.2	
VII	27.572	
VIII	25.52	
IX	11.4	(10.27)*
X	32.526	
XI	31.46	
XII	52.744	
XIII	76.85	(76.75)*
XIV	63.94	

TABLE V Volume of labelled secondary lysosomes per Sertoli cell

Stages of the cycle	Volume in μm^3
Ie	17.017
Il	9.462
II	3.96
III	3.84
IV	4.655
V	4.914
VI	4.92
VII	3.416
VIII	3.712
IX	6.156
X	17.784
XI	17.545
XII	29.64
XIII	49.01
XIV	34.04

* Values derived from the estimates of one animal (control) not injected with tracer.

TABLE VI

Percentage of labelled lysosomes per Sertoli cell

Stages of the Cycle	Experimental groups 1	2	3	4	Mean (± SEM)
Ie	41.30	40.00	48.88	40.62	42.70 ± 2.08
Il	31.43	26.08	25.92	27.27	27.68 ± 1.29
II	12.90	14.81	12.50	13.04	13.31 ± 0.51
III	16.66	13.63	10.00	15.00	13.82 ± 1.42
IV	23.07	15.38	14.28	13.04	16.44 ± 2.26
V	19.05	18.18	15.78	10.00	15.75 ± 2.04
VI	16.66	14.28	19.04	12.50	15.62 ± 1.42
VII	15.00	13.04	9.52	12.50	12.52 ± 1.13
VIII	18.75	14.81	16.00	10.34	14.98 ± 1.75
IX	55.55	54.54	50.00	53.33	53.36 ± 1.21
X	59.52	57.57	53.12	50.00	55.05 ± 2.15
XI	56.41	54.28	55.55	56.66	55.73 ± 0.54
XII	60.00	56.52	53.57	55.00	56.27 ± 1.38
XIII	59.21	67.92	68.65	60.00	63.95 ± 2.52
XIV	59.25	49.15	51.02	53.33	53.19 ± 2.19

FIGURE 53

Number of secondary lysosomes per Sertoli cell at the 14 stages of the cycle of the seminiferous epithelium.

The total number of secondary lysosomes per Sertoli cell increases from stage IX to stage XIV of the cycle. The number of secondary lysosomes per Sertoli cell decreases abruptly from stage XIV to stage II remaining at the same level until stage VIII of the cycle. The lowest values occur at stage IX when a prominent drop in the number of secondary lysosomes is registered.

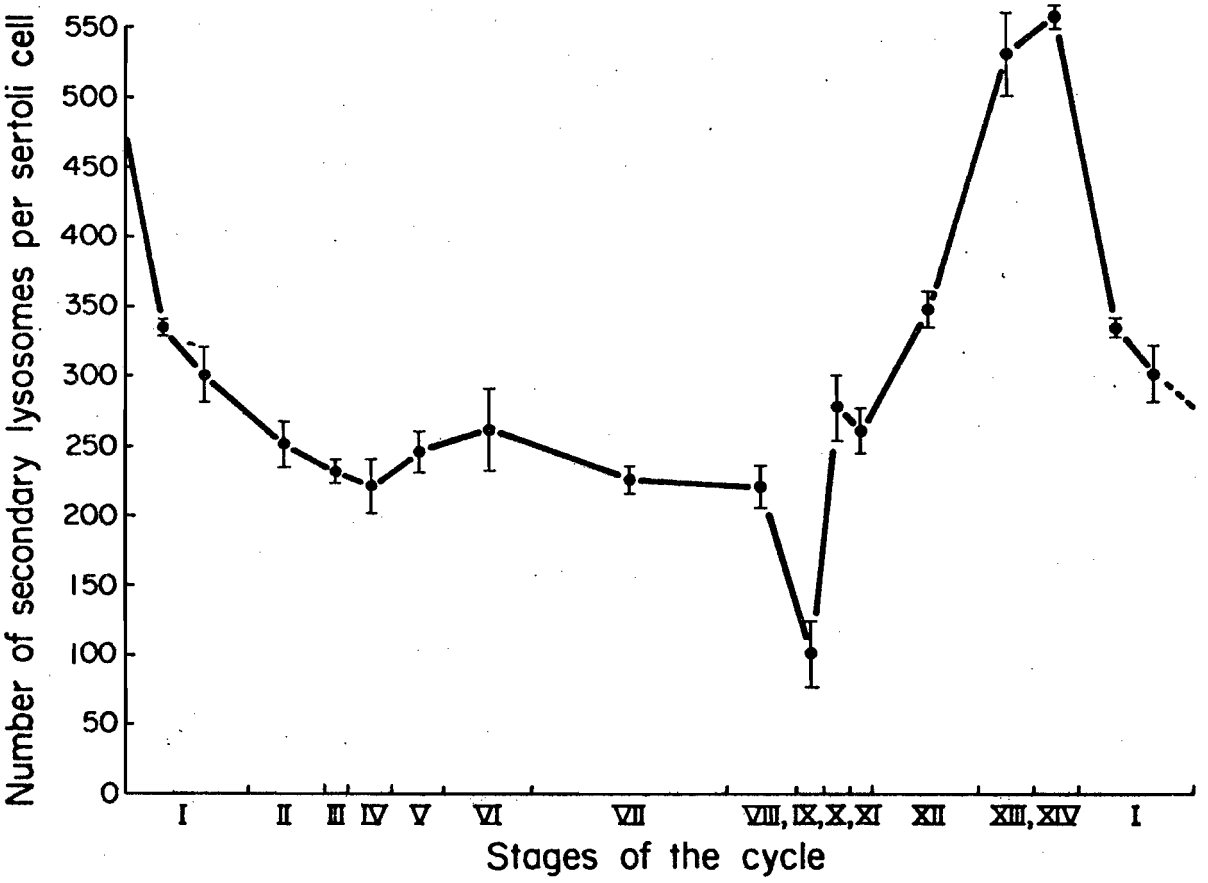
Number of secondary lysosomes per sertoli cell
550
500
450
400
350
300
250
200
150
100
50
0
I
II
III
IV
V
VI
VII
VIII, IX, X, XI
XII
XIII, XIV
I
Stages of the cycle

FIGURE 54

Number of labelled secondary lysosomes per Sertoli cell at the 14 stages of the cycle of the seminiferous epithelium.

The number of labelled secondary lysosomes, six hours after intraluminal injection with native ferritin increases from stage IX to stage XIII, during which the highest values are registered. The number of labelled secondary lysosomes per Sertoli cell decreases abruptly from stage XIV to stage II. The low value of stage II persists until stage VIII of the cycle.

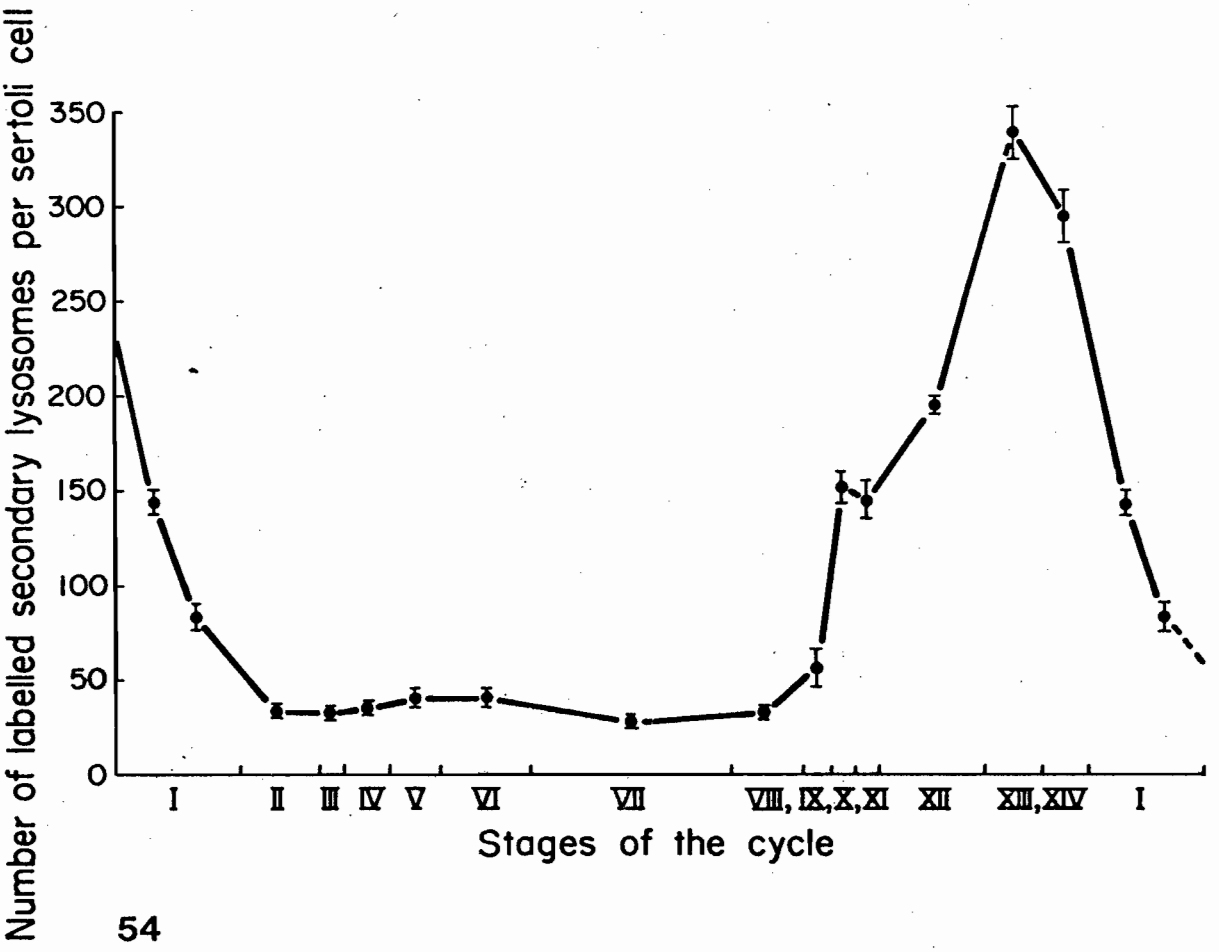
Number of labelled secondary lysosomes per sertoli cell
350
300
250
200
150
100
50
0
I
II
III
IV
V
VI
VII
VIII, IX, X, XI
XII
XIII, XIV
I
Stages of the cycle

FIGURE 55

Average volume of secondary lysosomes in Sertoli cells at the 14 stages of the cycle of the seminiferous epithelium.

The average volume of secondary lysosomes does not change signifincantly throughout all the stages of the cycle, except at stages XII-XIII during which these values are higher.

The analysis of the variance revealed that the increase in the average volume of secondary lysosomes registered at these stages of the cycle is statistically significant.

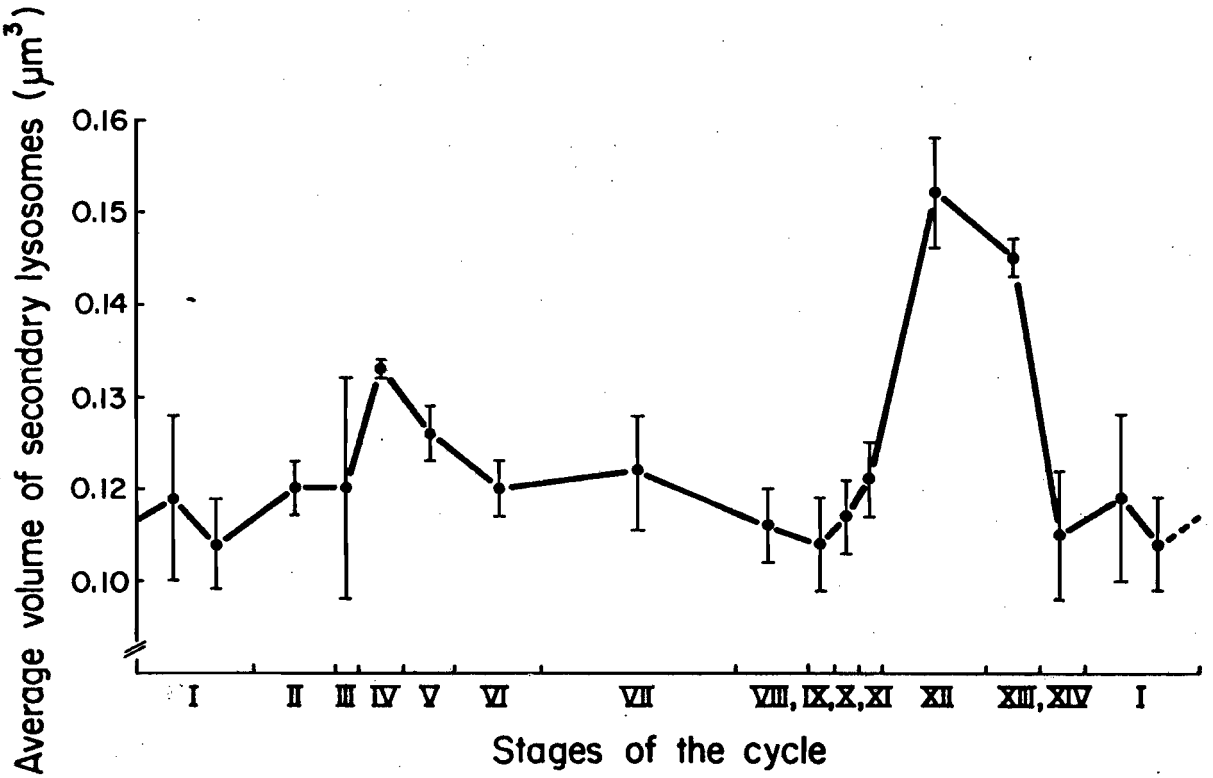
Average volume of secondary lysosomes (μm³)
0.16
0.15
0.14
0.13
0.12
0.10
I
II
III
IV
V
VI
VII
VIII, IX, X, XI
XII
XIII, XIV
I
Stages of the cycle

FIGURE 56

Total volume of secondary lysosomes per Sertoli cell at the 14 stages of the cycle of the seminiferous epithelium.

The volume of secondary lysosomes per Sertoli cell increases from stage IX to stage XIII of the cycle. This value decreases accutely from stage XIV to stage II. From stage II to stage VIII, the volume of secondary lysosomes does not show a significant change, decreasing abruptly to the lowest level at stage IX of the cycle.

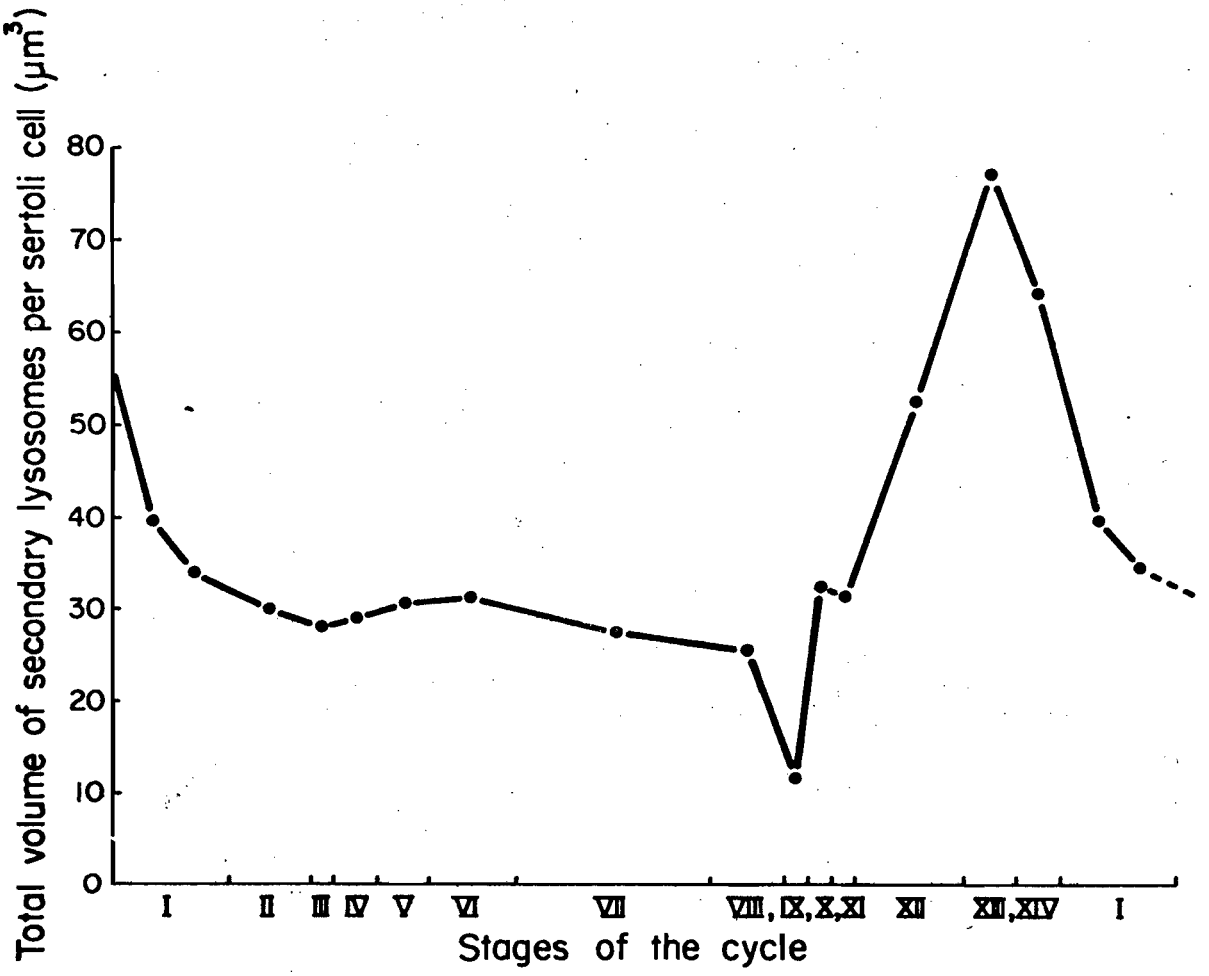
Total volume of secondary lysosomes per sertoli cell (μm³)
80
70
60
50
40
30
20
10
0
I
II
III
IV
V
VI
VII
VIII, IX, X, XI
XII
XIII, XIV
I
Stages of the cycle

FIGURE 57

Total volume of labelled secondary lysosomes per Sertoli cell at the 14 stages of the cycle of the seminiferous epithelium.

The total volume of NF-labelled secondary lysosomes per Sertoli cell after six hours of tracer injection increases from stage IX reaching the highest value at stage XIII of the cycle. The volume of labelled secondary lysosomes decreases sharply from stage XIV to stage II, remaining low until stage VIII.

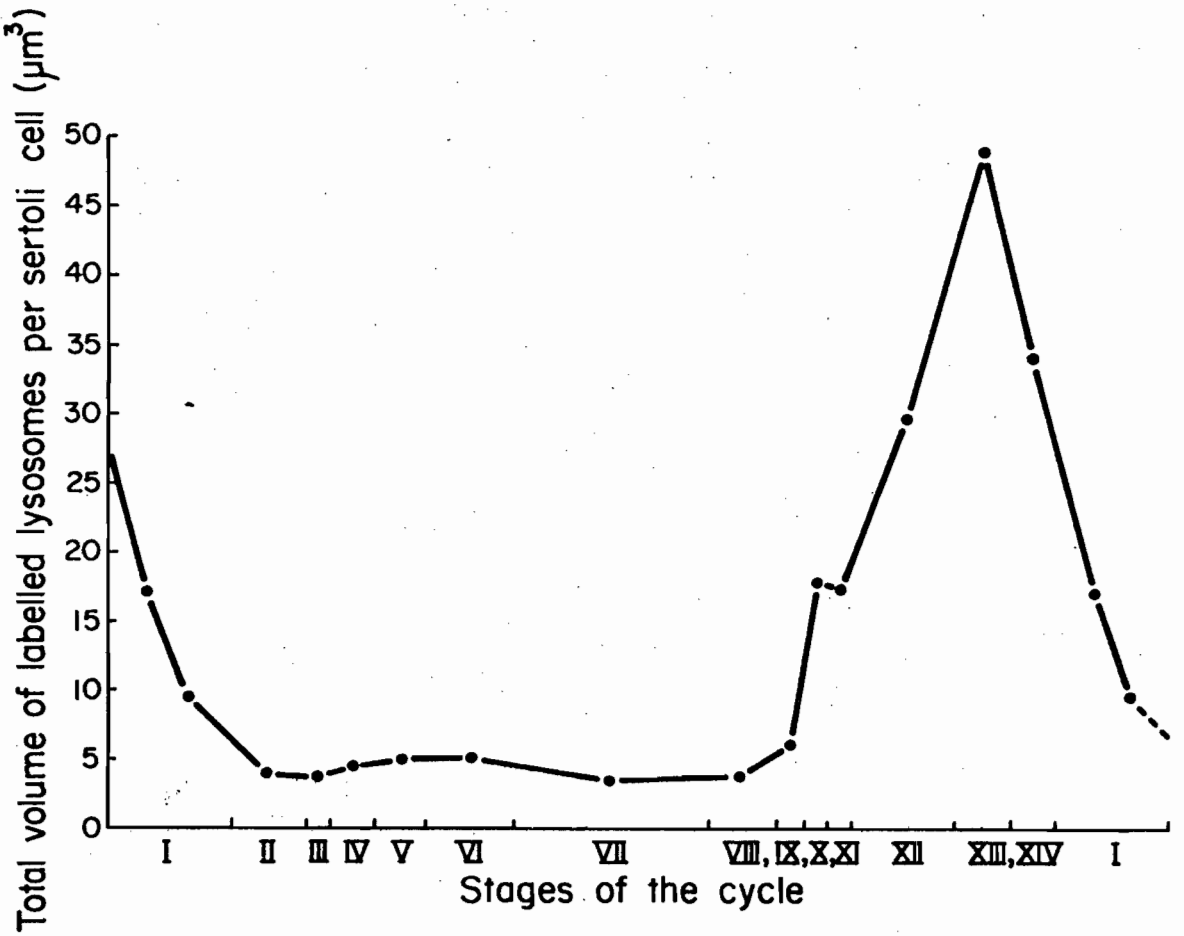
Total volume of labelled lysosomes per sertoli cell (μm³)
0
5
10
15
20
25
30
35
40
45
50
I
II
III
IV
V
VI
VII
VIII, IX, X, XI
XII
XIII, XIV
I
Stages of the cycle

FIGURE 58

Percentage of NF-labelled secondary lysosomes in Sertoli cells at the 14 stages of the cycle of the seminiferous epithelium.

Two distinct levels of endocytic activity are observed during the cycle. From stage II to stage VIII the percentage of labelled lysosomes remains at a relatively low level. During stage IX the percentage of labelled lysosomes increases abruptly and remains at a high level until stage XIV. At stage I the percentage of labelled lysosomes decreases significantly to return to the low level of stage II. Note that the highest value is registered at stage XIII of the cycle.

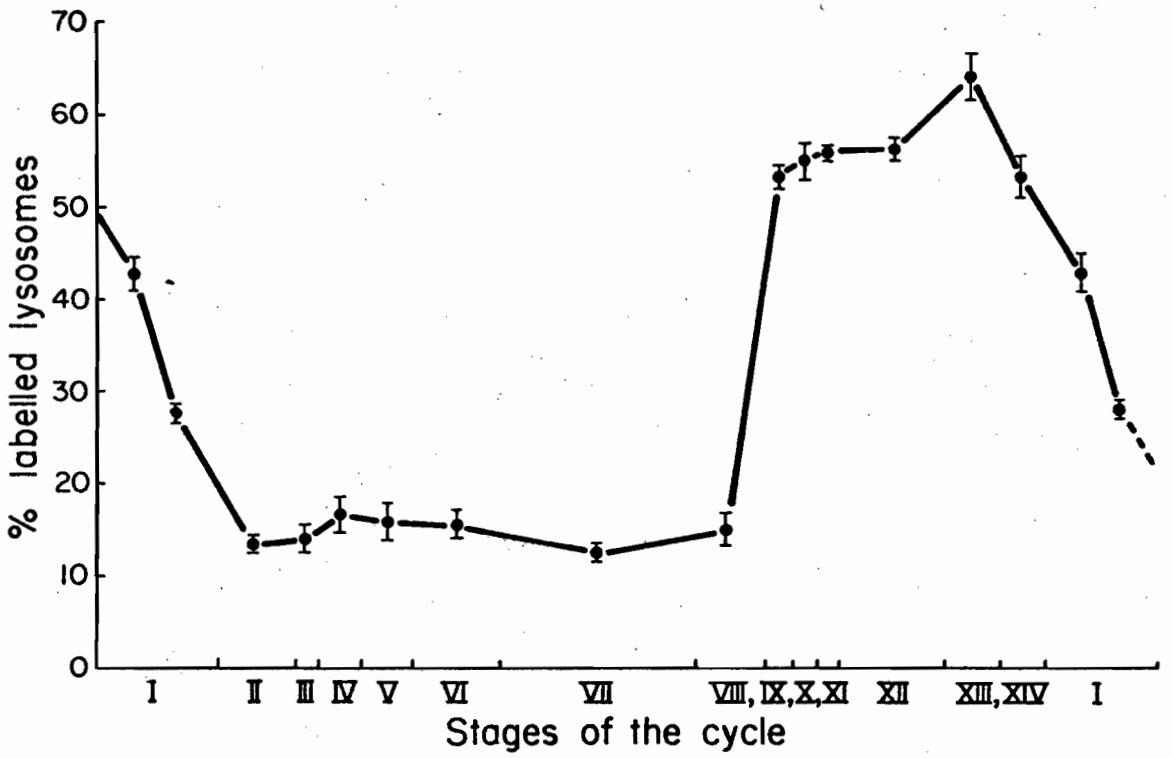
70
60
50
40
30
20
10
0
% labelled lysosomes
I
II
III
IV
V
VI
VII
VIII, IX, X, XI
XII
XIII, XIV
I
Stages of the cycle

Chapter V

DISCUSSION

Although phagocytosis is a well accepted function for the Sertoli cell, the detail of the internalization of the cytoplasmic residual bodies of the spermatids had yet to be analyzed as well as their intracellular degradation, and the involvement of the secondary lysosomes in this process. Our results have suggested that the initial interaction between the cytoplasmic residual bodies and the apical processes of the Sertoli cell is mediated by specific receptors present in the Sertoli cell plasma membrane. We have also shown that the secondary lysosomes play a very important role in the intracellular degradation of these elements.

In addition to phagocytosis we have clearly demonstrated the capacity of the Sertoli cell to remove fluids and solutes from the lumen of the seminiferous tubules mainly by a mechanism of fluid-phase pinocytosis. We have also presented quantitative evidence showing that the endocytic activity of Sertoli cell varies significantly during the cycle of the seminiferous epithelium of the rat.

The present discussion has been divided into the following chapters: (1) Phagocytosis and pinocytosis in Sertoli cells, (2) Intracellular pathway of the endocytosed materials, (3) Demonstration of cyclic endocytic activity in Sertoli cells, (4) General summary and conclusions.

(1) Phagocytosis and pinocytosis in Sertoli cells; mechanism of uptake

(a) Phagocytosis of the cytoplasmic residual bodies

The results obtained in the present investigation show that at stage VIII of the cycle, phagocytosis of the cytoplasmic residual bodies is a clear consequence of "phagocytic recognition" and membrane-to-membrane interaction between the plasma membrane (PM) of the cytoplasmic residual bodies of the spermatids and specialized areas of the apical plasma membrane of the Sertoli cell (Fig. 60). Phagocytic recognition has been defined as the process by which phagocytes select particles to be internalized (Silverstein et al., 1977). Thus phagocytosis in Sertoli cells, as in other phagocytes, requires that the particle, in this case the cytoplasmic residual bodies, has to be attached to the surface of this cell (Simon and Burke, 1970; Burton et al., 1976; Griffin et al., 1976; Silverstein et al., 1977; Burton et al., 1982; Aulenbacher et al., 1983; Steinman et al., 1983; Tsubakio et al., 1983). Silverstein et al. (1977) have pointed out that particle attachment is not an energy-dependent process, and that particle ingestion is blocked by low temperature or by metabolic inhibitors. The ingestion of the cytoplasmic residual bodies is accomplished by progressive spreading of the Sertoli cell processes over the surface of the attached cytoplasmic residual bodies. Similar findings have been reported in different phagocytes (Griffin et al., 1976; Silverstein et al., 1977; Fawcett and Doxey, 1982; Stein et al., 1983). In several types of phagocytic cells the plasma membrane motility required for particle ingestion presumably utilizes forces generated by submembranous actin rich bundles of microfilaments (Axiline and Reaven, 1974; Griffin et al., 1976; Southwick and Stossel, 1983). The Sertoli cell plasma membrane motility for the ingestion of the cytplasmic residual bodies does not require actin polymerization

since treatment with cytochalasin D, an agent that impairs actin gelation, does not suppress the first step of phagocytosis in this cell. On the other hand, the process seems to be mediated by microtubules since colchicine inhibits the uptake of the cytoplasmic residual bodies. Similar observations have been shown by Aoki (1980) who, in a study of the involvement of the microtubules in spermiation, reported shedding of the late spermatids and retention of the cytoplasmic residual bodies after microinjections of colchicine and nacodozol.

The interaction of the particles to be ingested with phagocytes may be due to nonspecific electrostatic or hydrophobic forces (nonspecific phagocytosis), or may be mediated by specific receptors (receptor mediated phagocytosis). The former process has been recognized during the ingestion of inert materials and is performed by both professional and facultative phagocytes (Silverstein et al., 1977). However, some particles as well as cells can attach to the surface of "professional phagocytes" without significant incorporation. Thus, binding is not necessarily followed by the ingestion step. In fact, the Sertoli cell shows some adhesiveness to all germ cells but only exerts phagocytosis to degenerating germ cells (Reddy and Svoboda, 1967; Black, 1971; Russell and Clermont, 1977) and to the cytoplasmic residual bodies (Fawcett et al, 1977). The treatment with colchicine does not suppress spermiation and release of the mature spermatids (stage VIII); however, all the residual cytoplasmic bodies remain attached to the apical plasma membrane of the Sertoli cell. Thus, the retention of the cytoplasmic residual bodies after the inhibition of their phagocytosis by microtubule disrupting agents may be due to a very specific membrane-to-membrane interaction between the plasma membrane of the cytoplasmic residual bodies of the spermatids and certain segments of

the apical plasma membrane of the Sertoli cell. Consequently, Sertoli cells behave as professional phagocytes since phagocytosis of the cytoplasmic residual bodies is a function inherent to these cells that takes place during and immediately after spermiation (stage VIII) in a very specific manner.

As it has already been mentioned earlier, Griffin and Silverstein (1974) have proposed a model in professional phagocytes to explain receptor mediated phagocytosis known as the "zipper model of phagocytosis". The model proposes a first step in which ligand-receptor interaction is required to initiate the aggregation of contractile proteins, presumptively of the actin type. The contractile proteins lead to the extensions of pseudopods around the attached particle which in turn leads to further receptor-ligand interaction and this in turn to further aggregation of contractile proteins. The process may be repeated several times until the plasma membrane fuses above the particle, resulting in the formation of a phagosome. The zipper model is apparently applicable to the Sertoli cell, although the evidence suggests that the contractile elements involved during phagocytosis in this cell are microtubules rather than microfilaments.

In conclusion, the Sertoli cell behaves as a professional phagocyte in which phagocytosis of the cytoplasmic residual bodies is due to a specific process of membrane-to-membrane interaction and mediated by microtubules.

(b) Pinocytosis in Sertoli cells

Since neither fluid-phase pinocytosis nor adsorptive pinocytosis has ever been satisfactorily demonstrated in the Sertoli cell with conventional markers and proper controls, it was decided to assess the exact nature of the mechanism of pinocytosis by this cell at different stages of the cycle

of the seminiferous epithelium using different markers, such as horseradish peroxidase-G, albumin-G, lactoalbumin-G, native ferritin, cationic ferritin and Con A-F in the presence or absence of alpha-methyl-D-mannoside.

The various tracers used in the present investigation have already been used extensively to test adsorptive or fluid-phase endocytosis in several cell types.[1]

---

[1] Cationized Ferritin (CF) binds electrostatically to anionic groups at the cell surface (Danon et al., 1972; Skutelky et al., 1977; Simionescu and Simionescu, 1978; Andrews, 1981; Jakoi et al., 1981; Peress and Topkins, 1981; Anderson and Batten, 1982; Brac, 1983; Johanson, 1983; Marikowsky et al., 1983) and is internalized via adsorptive endocytosis by several cell types (Farqhuar, 1978; Moller and Chang, 1978; Simionescu and Simionescu, 1978; Hewit et al., 1979; Denef and Ekholm, 1980; Blok et al., 1981; Van Deurs et al., 1981; Anderson and Batten, 1982; Gronblad et al., 1982; Jersild, 1982; Van Deurs and Nilausen, 1982; Brac, 1983; McLean and Sanders, 1983; Nilsson and Van Deurs, 1983; Morales et al., 1983; 1984). Con A-F has also been shown to be incorporated by adsorptive endocytosis in different cell types (Yokoyama et al., 1980; Imamura et al., 1981; Salisburry et al., 1981; Willingham et al., 1981; Gordon-Weeks and Jones, 1983; Leak and Sun, 1983; Morales et al., 1983; 1984), since it binds to alpha-D-mannose and alpha-D-glucose residues present in the glycocalyx (Nicolson, 1972; Nicolson, 1974; Gillouzo and Feldmann, 1977; Roth and Wagner, 1977; Brown and Hunt, 1978; Virtanen et al., 1978; Ichev and Ovtscharoff, 1981; Pinto da Silva et al., 1981; Chavez and Enders, 1982; Gordon-Weeks and Jones, 1983; Zinmeister and Ackerman, 1983). On the other hand, NF does not bind specifically to the plasma membrane and was shown in a wide variety of cells to be incorporated by fluid-phase endocytosis (Farqhuar, 1978; Peress and Tompkins, 1981; Gonella et al, 1982; Hermo et al., 1982; Morales et al., 1983; 1984; Van Deurs and Nilausen, 1983). Horseradish peroxidase (HRP) has also been used extensively as a standard marker to demonstrate fluid-phase endocytosis (Steinman and Cohn, 1972; Steinman et al., 1974; Silverstein et al., 1977; Simionescu and Simionescu, 1978; Blok et al., 1981; Goud et al., 1981; Pool et al., 1982; Raikhel and Lea, 1982; Van Deurs and Nilausen, 1983), and horseradish peroxidase bound to colloidal gold was recently used for the same purpose (Morales and Hermo, 1983; Morales et al., 1984). Similarly, albumin and lactoalbumin, two proteins normally found in the seminiferous tubular fluid and believed to be synthetized by the seminiferous epithelium (Kormano et al., 1971; Koskimies and Kormano, 1973; Turner et al., 1970; Byers et al., in press), and Con A-F in the presence of alpha-methyl-D-mannoside cannot bind to reactive sugars of the plasme membrane (Nicolson, 1972; 1974; Goldstein 1975; Gillouzo and Feldmann, 1977; Roth and Wagner, 1977; Brown and Hunt, 1978; Ichev and Otscharoff, 1981; Welsch and Shumacher, 1983; Morales et al., 1984) can be used to demonstrate fluid-phase endocytosis (Besterman et al., 1983; Daukas et al., 1983; Geuze et al., 1983; Hermo et al., 1983; Morales et al., 1984).

Within 1 to 15 minutes after injection, all the tracers for fluid-phase endocytosis were localized exclusively within large and irregular endocytic vesicles in the apical cytoplasm of the Sertoli cell. Nevertheless, the markers were freely suspended in the electronlucent matrix of those vesicles. Although some authors have reported mannose specific binding sites and internalization for horseradish peroxidase and albumin (Tietze et al., 1982; Ockner et al., 1983; Strauss, 1983; Sung et al., 1983), the in vitro experiments performed on material fixed and then incubated in the appropriate tracer for 1 hour at 37°C clearly showed that neither NF, HRP-G, albumin-G, lactoalbumin-G nor Con A-F in the presence of alpha-methyl-D mannoside bound to the apical plasma membrane or to the membrane of the endocytic invaginations present at the apical aspect of the Sertoli cell. Therefore, these markers were taken up by the process of fluid-phase pinocytosis.

In contrast, CF and Con A-F bound to the plasma membrane of the apical processes of the Sertoli cell and to the plasma membrane of early and late spermatids along their flagellum, as well as to the membrane of the residual bodies. However, CF and Con A-F are not internalized at most stages of the cycle, except at stage VIII where some endocytic vesicles and multivesicular bodies associated with the tubulobulbar complexes are moderately labelled. Occasionally, few molecules of unbound Con A-F were found free in the electronlucent content of some endocytic vesicles. This could be due to the possible interaction between luminal glycoproteins with Con A-F molecules inhibiting their active sites and being incorporated via fluid-phase endocytosis.

The present investigation clearly indicated that the Sertoli cell practices fluid-phase pinocytosis in all stages of the cycle of the semini-

ferous epithelium and that this cell shows a relative capacity to perform adsorptive endocytosis limited to stage VIII of the cycle. Steinman et al. (1983) have pointed out that one cannot assume that simple binding to the plasma membrane is necessarily followed by internalization, since the adsorbed material must be attached to a segment of plasma membrane that is internalized. Therefore, despite the binding of the tracers for adsorptive pinocytosis to the apical plasma membrane, the Sertoli cell does not incorporate either CF or Con A at different stages of the cycle except at stage VIII. One explanation for the limited capacity of the Sertoli cell to incorporate substances via adsorptive pinocytosis at stage VIII could be due to the presence of specific receptors amongst other glycoproteins of the apical cell coat surfaces for the phagocytosis of the cytoplasmic residual bodies which may interact electrostatically with CF or perhaps by means of their terminal sugars with Con A-F. Thus, the binding of these nonspecific markers may trigger their internalization by a process of adsorptive pinocytosis resembling the initial uptake of the cytoplasmic residual bodies in which attachment of these structures to the Sertoli cell plasma membrane is required for their internalization.

In addition, fluid-phase pinocytosis in Sertoli cells occurs in pinocytic vesicles of large sizes (ranging between 0.1 to 0.2 μm) showing a pale matrix which forms from non-coated regions of the apical plasma membrane. Moreover, pinocytosis in Sertoli cells is a process independent of microfilament gelation and microtubule polymerization and is observed in all stages of the cycle. Therefore, fluid-phase pinocytosis in Sertoli cells is interpreted as a process constitutive in nature.

Preliminary observations using tracers for both fluid-phase pinocytosis and adsorptive pinocytosis injected into the interstitial spaces of the

rat testis show that Sertoli cells do not take up the tracers at its base, even after long periods of time following the injection (unpublished data). These results confirm previous observations performed by Aoki and Fawcett (1975) who reported the incapacity of Sertoli cells to internalize horseradish peroxidase interstitially infused during long periods of time. However, it is noticeable to observe frequently coated pits and coated vesicles in the basal aspect of Sertoli cells. Furthermore, several authors have reported the specific binding of FSH to the basal plasma membrane of Sertoli cells (Orth and Christensen, 1977, 1978; Salhanick and Wiebe, 1980). Since peptide hormones have been shown to be internalized by receptor mediated endocytosis in several cell types (Posner et al, 1982), this specific mechanism of uptake may exist in Sertoli cells involving those areas of the basal plasma membrane below the tight junctions which are accessible for these hormones.

In conclusion, Sertoli cell practices fluid-phase pinocytosis in all stages of the cycle and under the present experimental conditions it shows a limited capacity to perform adsorptive pinocytosis at stage VIII of the cycle. Furthermore, fluid-phase pinocytosis in Sertoli cell is a constitutive mechanism independent of microtubular polymerization and microfilament gelation. Fluid-phase pinocytosis is a full-time occupation of this cell, therefore Sertoli cell must be considered as a "professional pinocytic cell".

(2) Intracellular pathway of the endocytosed materials

(a) Pinocytic pathway

The use of electron-dense markers and cytochemical procedures has permitted the analysis of the endocytic pathway and the involvement of the lysosomal apparatus of the Sertoli cell in this process. The evidence

obtained in this investigation showed that Sertoli cells are active endocytic cells which internalize by fluid-phase endocytosis different tracers that do not bind either to the apical plasma membrane or to the membrane of the endocytic vesicles of electron lucent matrix ranging between 0.1 to 0.2 μm. The endocytosed tracers (NF, HRP-G, albumin-G, lactoalbumin-G and Con A-F in the presence of alpha-methyl-D-mannoside) first reach large irregularly shaped multivesicular bodies (MVBs) showing a pale stained matrix (30 minutes after injection) which are possibly formed by fusion of the large pinocytic vesicles. Steinman et al.(1983) have pointed out that in many cases the formation of endocytic vacuoles (endosomes) is due to the fusion of the external membrane faces of pinocytic vesicles. The large irregular multivesicular bodies do not present acid phosphatase activity. The present findings suggest that the large irregular MVBs are "pre-lysosomal" structures since these elements do not present acid phosphatase activity. Steinman et al.(1976) and Wall et al.(1980) have demonstrated that endosomes labelled with markers either for fluid-phase endocytosis or for receptor mediated endocytosis acquire acid hydrolases presumptively coming from primary lysosomes. Willingham et al.(1981) have called receptosome a non-digestive structure involved in receptor mediated endocytosis. Recently Beguinot et al.(1983) have considered the term receptosome as equivalent to endosome. The receptosomes have been described as smooth-surfaced vacuoles presenting some vesicular profiles characteristic of MVBs and a peculiar straight, fuzzy lamellar edge on the outer side of the membrane. Thus, the large pale irregular MVBs of the Sertoli cell which present the same characteristics may be considered to be the equivalent of the endosomes described in several other cell types (Steinman et al, 1983). The endosomes and the equivalent

pre-lysosomal structures, i.e. CURL and receptosomes, have been shown to be involved in membrane and receptors recycling (Geuze et al., 1983; Harding et al., 1983; Steinman et al., 1983). Membrane recycling is presumed to be vesicular (Silverstein et al., 1977; Posner et al., 1982; Douglas et al., 1983; Farqhuar et al., 1983; Geuze et al., 1983; Smith and Jarett, 1983; Steinman et al., 1983), and one possible consequence of a vesicular mechanism of membrane retrieval from intracellular compartments is that the material in those compartments will be passively carried and released from the cell (Silverstein et al., 1977; Steinman et al., 1983). This process has been called reflux or regurgitation (Steinman et al., 1983), and it has been suggested to be mediated by exocytosis of recycling vesicles (Silverstein et al., 1977; Steinman et al., 1983). We have demonstrated that the "pale vesicles" ranging in diameter between 100 to 120 nm present among the clusters of lysosomes in Sertoli cells not only pinch off from the endosomes (large irregular MVBs of pre-lysosomal nature), but also carry endocytosed material present in these structures after their labelling. The "pale vesicles" have also been observed close or in contact with the plasma membrane of the Sertoli cell recesses and therefore, they may be involved in membrane recycling (see Fig. 61). Since these vesicles originate from a pre-lysosomal structure, they do not present acid phosphatase reaction.

Later, the tracers are seen in smaller spherical MVBs with a denser matrix (1 hour after injection) and in membrane bound granules showing an electron dense content (2 hours after injection); the last two structures show acid phosphatase activity and they are considered to be secondary lysosomes (Figs. 59, 61). The formation of multivesiclar bodies showing acid phosphatase activity has already been described as an intermediate step between the transformation of an endosome into a typical dense secondary

lysosome (Van Deurs et al., 1981; Geuze et al., 1983; Steinman et al., 1983). This seems to be the case in the Sertoli cell where the more spherical MVBs not only show a later labelling with the different markers compared to the endosomes, but also present acid phosphatase activity. In fact, Lalli et al.(1984), based on radioautographic observations, concluded that among the lysosomal elements, the large irregular multivesicular bodies incorporate first ^{3}H fucose, a precursor for glycoprotein synthesis, and seemingly transfer it to the dense MVBs and to the dense lysosomes in a sequence similar to the electron dense tracers used in this study (see Figs. 59, 61).

The "dense core vesicles" with a diameter of approximately 120-170 nm are also associated to the clusters. These structures have been shown to pinch off from the smaller and spherical MVBs showing a denser matrix and from the dense secondary lysosomes. The dense core vesicles show labelling after 1 hour of tracer injection and frequently show strong acid phosphatase activity. The dense core vesicles are believed to be "primary lysosomes" (Fawcett et al., 1975; Assaf, 1980). However, a primary lysosome is defined as a virgin structure carrying acid hydrolases, whereas a secondary lysosome is defined as an acid hydrolase rich vacuole that has already acquired substrates by endocytosis or by autophagy (Posner et al., 1982; Steinman et al., 1983). Although the dense core vesicles contain acid phosphatase activity, they also show labelling with the markers; consequently they should not be regarded as primary lysosomes. Furthermore, it has been shown herein that the "dense core vesicles" pinch off from either the smaller spherical MVBs of dense matrix and from the dense secondary lysosomes, whereas a primary lysosome by definition is the package of acid hydrolases that is formed by the concerted action of rER and Golgi

apparatus (Farqhuar et al., 1983; Steinman et al., 1983). Although the functional significance of the "dense core vesicles" remains to be elucidated, it is important to point out that membrane solutes and ligands may recycle not only from a pre-lysosomal compartment but also from the lysosomal compartment (Van Deurs and Nilausen,1982; Steinman et al., 1983; Widnell and Kitson,1983).

Our results indicate that fusion occurs between dense spherical MVBs and dense secondary lysosomes or between secondary lysosomes themselves (Fig. 61). The use of tracers permitted to pre-load several secondary lysosomes and it made possible to identify figures of fusion with other unlabelled spherical MVBs and secondary lysosomes. Figures of fusion have been observed at all stages of the cycle, although they appear to be more frequent between stages I to VII. Fusion between lysosomes along the endocytic pathway has already been reported by Steinman et al.(1983).

Although the "microvesicles" ranging in diameter between 25-35 nm forming clusters or neighbouring MVBs and secondary lysosomes are not reactive to CMPase and TMPase, Lalli (1982, 1983) has demonstrated that they are reactive to other acid hydrolases such as arylsulfatase and thiaminophosphatase and therefore, they may be considered as part of the lysosomal system. In addition, these structures have never been labelled with the endocytosed markers at any time interval after marker injection. This evidence suggests that microvesicles may be regarded as virgin structures that are not involved in digestive events and consequently, they may represent primary lysosomes directed toward MVBs and secondary lysosomes. However, more evidence is needed to confirm this speculation.

In conclusion, the pinocytic pathway in Sertoli cells presents the following steps in relation to time: fluid-phase pinocytosis of fluids and

solutes mediated by large non-coated vesicles, large irregular MVBs, dense spherical MVBs, dense secondary lysosomes (Figs. 59, 61). In addition, the large irregular multivesicular bodies are characterized as pre-lysosomal in nature and therefore, they are regarded as endosomes. Endosomes are involved in the formation of the "pale vesicles" which in turn seem to be involved in membrane recycling. "Dense core vesicles" are not primary lysosomes since they pinch off from spherical MVBs and dense secondary lysosomes and their fate is unclear. Finally, it is concluded that fusion between different types of secondary lysosomes occurs at all stages of the cycle, specially during stages I to VII.

(b) The phagocytic pathway

The ingestion of the cytoplasmic residual bodies is followed by the formation of a phagosome surrounded by two membranes separated by a constant interval of 100-150 Å. As in other phagocytes (Silverstein et al., 1977; Hart, 1979; Myagkaya and Daems, 1979; Myagkaya and Schellens, 1981), the phagosomes in the Sertoli cells are pre-lysosomal in nature as revealed by the absence of acid phosphatase activity. In Sertoli cell phagosomes undergo fusion with dense secondary lysosomes, as evidenced by morphological and cytochemical findings as well as by the subsequent delivery of endocytosed material by labelled secondary lysosomes directed toward this compartment (Figs. 60, 61). The lowest values in the number and volume of labelled secondary lysosomes registered at stage IX of the cycle are consistent with the merging and fusion of secondary lysosomes with the phagosomes containing the cytoplasmic residual bodies. Therefore, it can be concluded that secondary lysosomes merge with the cytoplasmic residual bodies in a common compartment releasing the hydrolases they still contain, which in turn contribute to the lysis of the content of the phagosomes.

Fusion between phagosomes and lysosomal elements leads to the formation of phagolysosomes which are characterized by a content of pH close to 5 and the presence of acid hydrolases (Hart, 1979). Such a process would consequently result in the rapid disappearance of both the residual bodies and most of the old secondary lysosomes in a common container. However, the contribution of acid hydrolases via primary lysosomes should be considered as another possible mechanism that contributes to the breakdown of residual bodies. Fusion between phagosomes and secondary lysosomes has been reported in the trophoblastic cell of the sheep placenta during erythrophagocytosis (Myagkaya and Daems, 1979; Myagkaya and Schellens, 1981) and in macrophages during phagocytosis of erythrocytes and leukocytes (Spors, 1970). Fusion between phagosomes and primary lysosomes has been well documented in macrophages (Silverstein et al., 1977; Hart, 1979; Steinman et al., 1983).

By the end of stage IX of the cycle, the phagolysosomes are observed deep within the Sertoli cell cytoplasm and the dissolution of the cytoplasmic residual bodies components coincides with the appearance of large lipid droplets. The process ends with the formation of a few lipid droplets of large sizes and the disappearance of the enclosing membranes (Assaf, 1980). These lipidic droplets are not considered to be lypofucsin inclusions, which is a non digestible product, since the lipidic droplets appear to be recycled by the Sertoli cell at the subsequent different stages of the cycle of the seminiferous epithelium (Lacy, 1962; Niemi and Kormano, 1965; Kerr and Krester, 1975; Assaf, 1980).

The conclusions of the present study are: 1) The demonstration for the first time of the interrelationship between the pinocytic pathway and the phagocytic pathway in Sertoli cells at stage VIII of the cycle which occurs as a consequence of the merging of the secondary lysosomes formed by pino-

FIGURE 59

Schematic drawing of a Sertoli cell showing the pinocytic pathway in relation to time after intraluminal injection of the markers for fluid-phase endocytosis (solid arrows).

1) Between 1-15 minutes the markers are found within endocytic invaginations and endocytic vesicles.
2) At 30 min the markers reach the endosomes (E) and are also seen within pale vesicles (pv).
3) One hour after injection, the markers are found in dense multivesicular bodies (MVB) and in dense core vesicles (dv).
4) At 2 hours the tracers are seen within dense secondary lysosomes (SL) and also in dense core vesicles (dv).

Other labels: N, nucleus; M, mitochondria; G, Golgi apparatus.

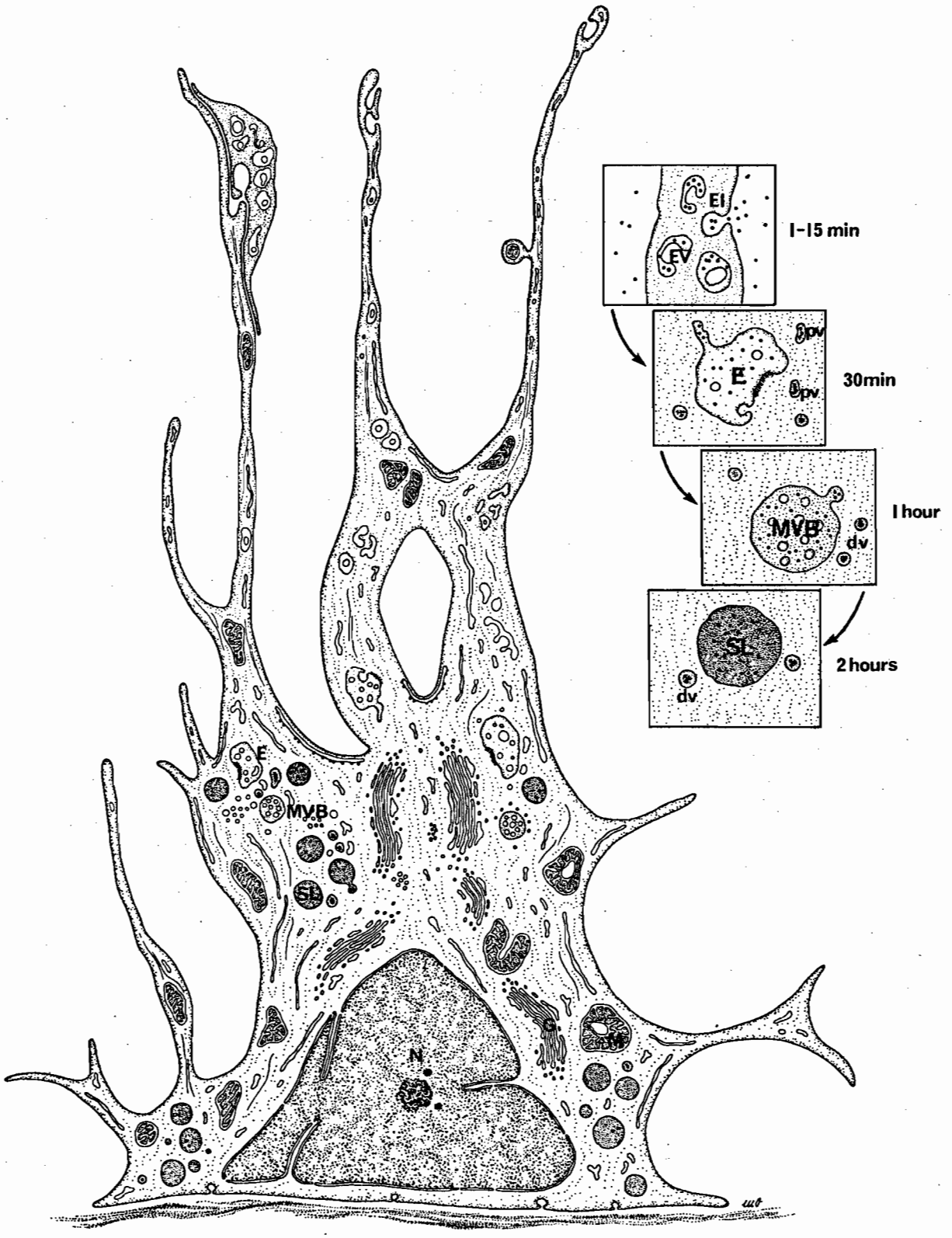
EI
EV
1-15 min
E
ipv
ipv
30min
MVB
dv
1 hour
SL
dv
2 hours
E
MVB
SL
N
G
M

FIGURE 60

Schematic drawing of a Sertoli cell describing the phagocytic pathway observed during the stages VIII and IX.

1) Attachment of spermatid's cytoplasmic residual body (RB) to the apical plasma membrane of the cytoplasmic processes of the Sertoli cell.
2) Engulfment of the RB and formation of a phagosome (PH) (prelysosomal compartment) enclosed by two membranes.
3) Fusion of SL with phagosomes leading to the formation of phagolysosomes (PL) which show different degrees of lysis of the cytoplasmic residual bodies.
4) Formation of lipidic droplets (Lip) which are accumulated in the basal aspect of the cell.

Other labels: G, Golgi complex; M, mitochondria; N, nucleus; ER, endoplasmic reticulum.

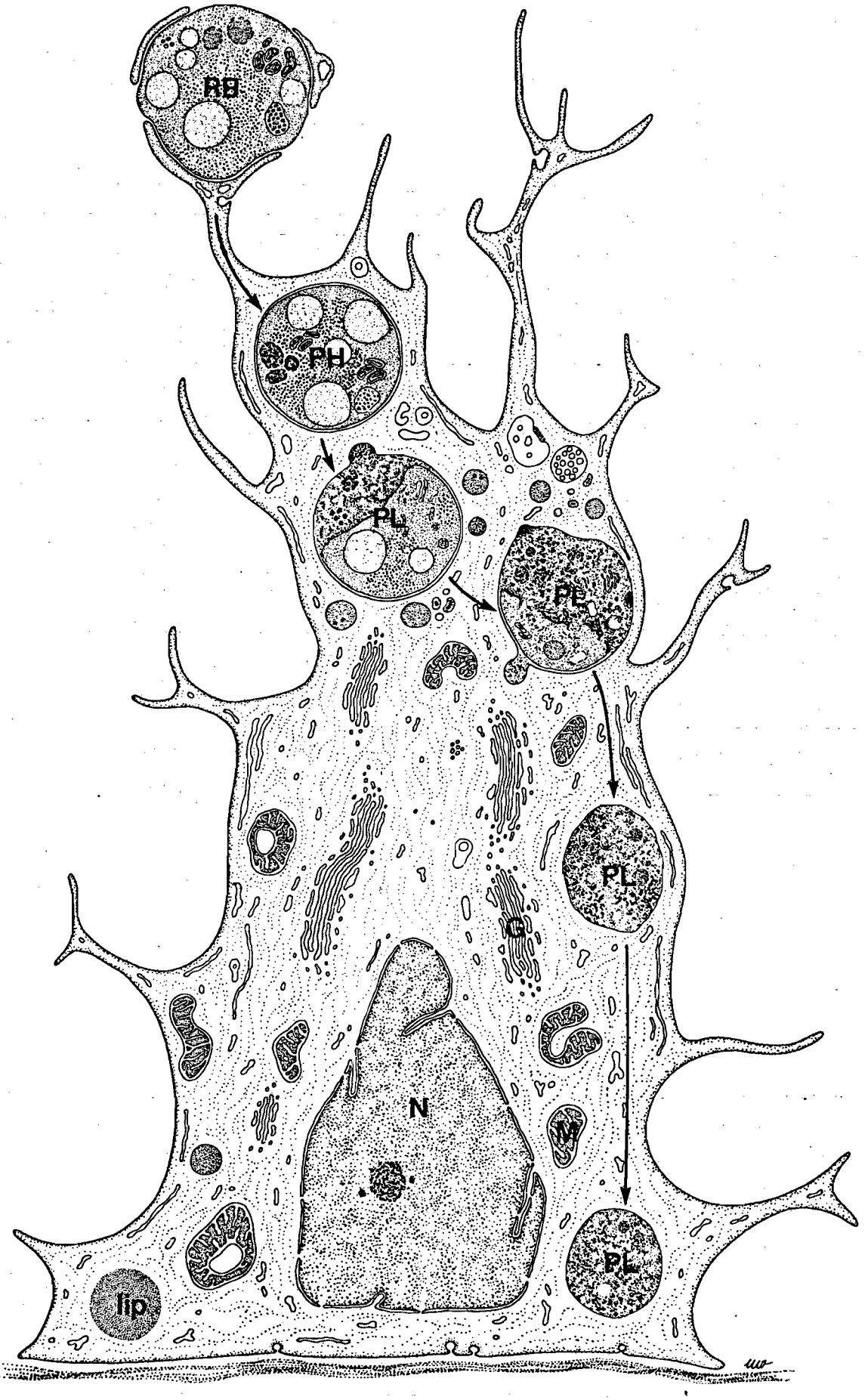
RB
PH
PL
PL
PL
PL
G
N
M
lip

FIGURE 61

Schematic drawing of the supranuclear region of the Sertoli cell showing the demonstrated pinocytic pathway and its integration with the phagocytic one as evidenced by tracer study (solid arrows). EI, endocytic invagination; EV, endocytic vesicle; E, endosome; LMVB and DMVB, light and dense multivesicular bodies respectively; SL, secondary lysosome; FS, figures of fusion between two secondary lysosomes, and between a phagosome (PH) and a secondary lysosome.

In addition, the broken lines and arrows show the hypothetical traffic of smaller vesicles:

1) Pale vesicles originated from both endosomes and light multivesicular bodies returning to the plasma membrane.
2) Microvesicles (mv) presumably primary lysosomes arising from the Golgi apparatus (G) which eventually would fuse with endosomes, LMVB, DMVB, SL or even with phagosomes.
3) Dense core vesicles originated from dense multivesicular bodies and secondary lysosomes whose fate remains unclear.

Other labels: N, nucleus of Sertoli cell; M,mitochondria.

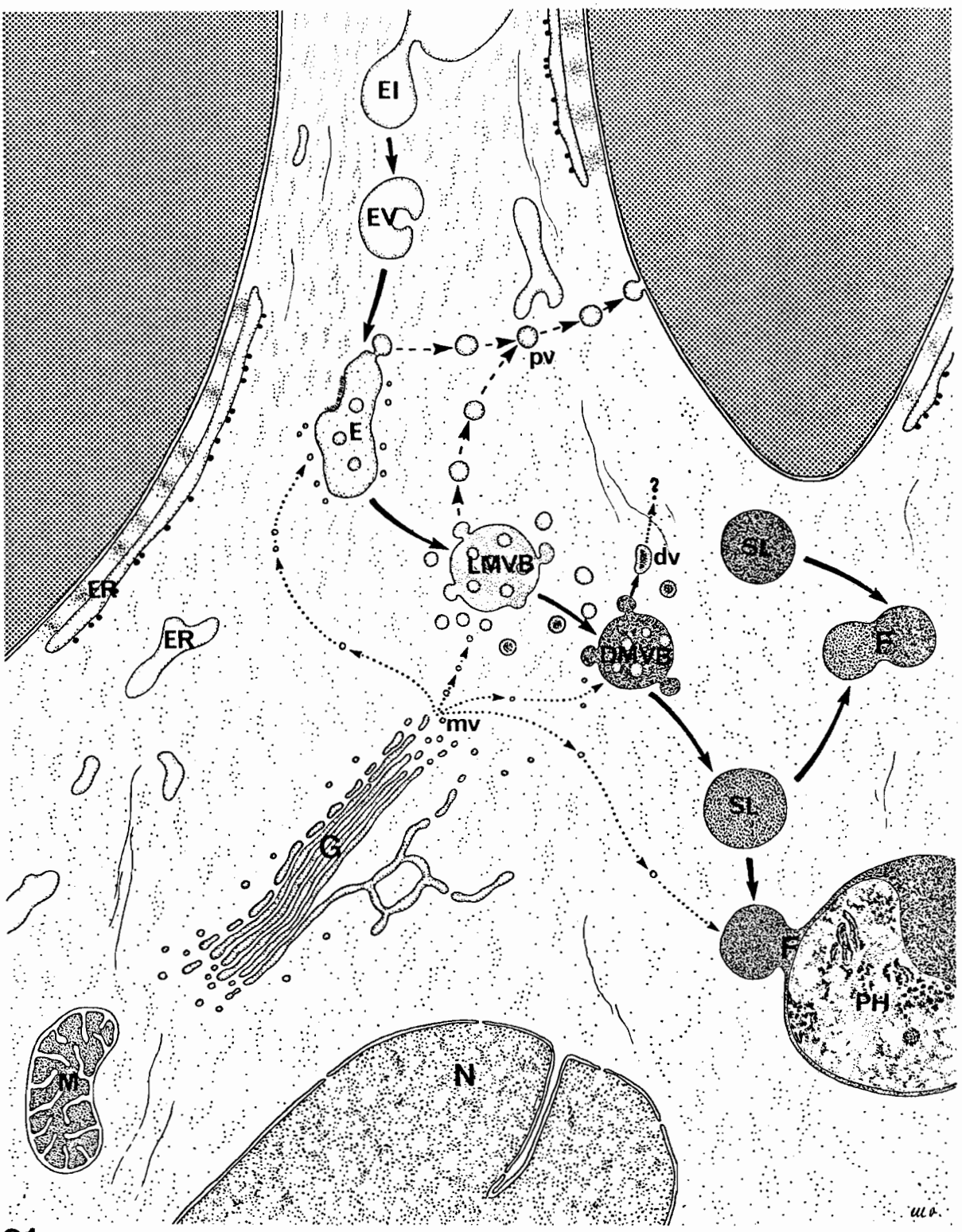

61

cytosis and the phagosomes containing the cytoplasmic residual bodies. 2) The elimination of the cytoplasmic residual bodies and the end of the life of the secondary lysosomes formed during one cycle of the seminiferous epithelium in a common compartment, i.e. in a phagolysosome. 3) All this evidence emphasizes the idea that the Sertoli cell is very well equipped to perform both pinocytosis and phagocytosis, and that these functions are not merely opportunistic events but well coordinated specific functions. Therefore, these observations are consistent with our suggestion to consider Sertoli cells as "professional endocytic cells", i.e. both professional phagocytic and professional pinocytic cells.

(3) Demonstration of cyclic endocytic activity in Sertoli cells

(a) Number, volume and percentage of labelled lysosomes per Sertoli cell

One of the main objectives of our quantitative analysis was to estimate the true number, the total volume and the percentage of labelled secondary lysosomes in the Sertoli cell at different stages of the cycle of the seminiferous epithelium of the rat, in order to determine if the endocytic activity of this cell is subject to cyclical variations.

The quantitative analysis reveals a substantial increase in the number of labelled secondary lysosomes per Sertoli cell from stage IX of the cycle of the seminiferous epithelium, reaching a peak at stage XIII. These values decrease abruptly from stage I until stage II of the cycle, remaining low until stage VIII. The statistical tests, i.e. the two-way analysis of variance and the "t" test, emphasized the validity of these results. As it has been shown in Section 6 of Material and Methods, the total volume of secondary lysosomes can be obtained multiplying the number of labelled lysosomes by the average volume of secondary lysosomes. Thus, the quantitative

analysis reveals that the total volume of labelled secondary lysosomes parallels the values of the number of labelled secondary lysosomes and therefore, both data indicate that the endocytic activity of Sertoli cells varies significantly during the cycle of the seminiferous epithelium of the rat.

When the percentages of labelled lysosomes used as an index of endocytic activity in Sertoli cells are compared from stage II to stage VIII, the values of labelled secondary lysosomes remain at a relatively low level (14.63%±0.55% SEM). Then, during stage IX the percentage of labelled lysosomes increases abruptly and remains at a high level until stage XIV of the cycle (56.26%±1.62% SEM). During stage I the percentage of labelled lysosomes decreases to return to the low value. Therefore, the present data reveal two distinct levels of pinocytic activity in Sertoli cells during the cycle of the seminiferous epithelium, i.e. a basal level from stage II to VIII and a high level from stage IX to stage XIV. These results are consistent with the increasing number and volume of labelled secondary lysosomes from stage IX to stage XIV and with the substantial diminution of these values during stages I to VIII.

Recently, Wing and Christensen (1982) analyzed several morphometric parameters of seminiferous tubules, such as the volume of the seminiferous epithelium and the volume of the seminiferous tubule per unit length of tubule at the various stages of the cycle. These authors found a significant increase in volume of the lumen from stages I - IV to stage VIII of the cycle leading up to spermiation. On the other hand, they found a prominent decrease in the volume of the lumen of the seminiferous tubule at stage IX remaining at low levels throughout stages X to XIV. The decrease in volume

of the lumen occurred simultaneously with a decrease in tubular diameter. Wing and Christensen (1982) concluded that the prominent decrease in the diameter of the seminiferous tubule is caused by the "depletion" of the luminal contents rather than by the loss of the germinal epithelial elements, since the latter remains relatively constant over the portion of the cycle in which the tubule diameter is decreasing.

The low values in volume of luminal content registered between stages IX - XIV are coincident with the high levels of endocytic activity found in this investigation. Thus, fluid-phase pinocytosis may play an important role in removing the fluids flowing toward the rete testis through the narrower tubular lumen of stages IX - XIV of the cycle (Setchell, 1980). Moreover, fluid-phase pinocytosis is a mechanism of uptake of both fluids and solutes (Silverstein et al., 1977) which does not modify substantially the composition of the fluids. In fact, the analysis of the tubular fluid from samples of cannulated seminiferous tubules reveals that this fluid is very characteristic in its ion, hormone and protein composition (Koskimies and Kormano, 1973; Setchell, 1980). In addition, Sertoli cell has been pointed out as the major source of the different components of the tubular fluid mainly of some proteins such as plasminogen activator, androgen binding protein, ceruloplasmin-like protein, transferrin, etc. (Lacroix et al., 1977; Skinner and Griswold, 1980; Wright et al., 1981; Kissinger et al., 1982; Parvinen, 1982; Skinner and Griswold, 1983), and may be responsible for the secretion of the cyclic proteins (Parvinen, 1982). Thus, it is likely that the composition of fluids is regulated by a secretory mechanism of the Sertoli cell, whereas the volume of the tubular fluid is regulated by fluid-phase pinocytosis.

Fluid-phase pinocytosis may also play an important role in the regulation

of the amount of PM in the adluminal compartment, facing the developing germ cells, specially the spermatids. For instance, during stages I to VIII there are two generations of spermatids (i.e. early and late spermatids); consequently the Sertoli cell would need more membranes to form the deep recesses that hold these germinal cells. Thus a low level of endocytic activity would ensure the disponibility of membrane in the adluminal compartment to form enough recesses. At the beginning of stage IX, one generation of spermatids is lost during the spermiation (i.e. late spermatids in step 19) persisting only one generation until stage XIV. Therefore, a high level of endocytic activity is consistent with the internalization of large amounts of apical plasma membrane that would ensure the diminution of the surface contact areas between Sertoli cell and spermatids. Further investigations are needed to substantiate these speculations.

In conclusion, the Sertoli cell shows two distinct levels of pinocytic activity, one low from stages II to VIII and one significantly high from stage IX to stage XIV. The quantitative analysis reveals further that the highest level of endocytic activity occurs at stage XIII of the cycle of the seminiferous epithelium.

(b) Total number and volume of secondary lysosomes per Sertoli cell

The quantitative data on the total number and total volume of secondary lysosomes emphasizes a cyclic behaviour of the lysosomal population of the Sertoli cell during the cycle of the seminiferous epithelium. Thus we have demonstrated that the total number of secondary lysosomes per Sertoli cell increases from stage X reaching a peak at stage XIV and decreases abruptly from stage I to stage III remaining low throughout stages IV to VIII. The lowest value was registered at stage IX of the cycle. These data correlate with the morphological images of fusion of

secondary lysosomes with the phagosomes at this stage. These results thus re-inforced the morphological, cytochemical and tracer data indicating the integration of the pinocytic and phagocytic processes at this particular stage of the cycle.

The decrease of the total number of secondary lysosomes per Sertoli cell registered from stage I to stage III of the cycle and the low values of the stages IV to VIII despite a constant low rate of pinocytic activity between stages II and VIII (see above), can be explained by the images of fusion which are particularly numerous at stage I of the cycle. This evidence has been further substantiated by the use of tracers which revealed the fusion of labelled and unlabelled secondary lysosomes. It is in accord with the view that membrane fusion occurs at many levels of the endocytic pathway. In some cases, as in the formation of endocytic vacuoles (endosomes), there is fusion of pinocytic vesicles; in other cases fusion occurs between pinocytic vesicles and lysosomes, and fusion also occurs between the protoplasmic faces of different lysosomes (Steinman et al, 1983).

Since the decrease in the number of secondary lysosomes between stages I to III is accompanied by a diminution of the total volume of secondary lysosomes, there must exist a process of shrinkage of the latter. Silverstein et al.(1977) have pointed out that an efflux of pinocytosed fluid and of low molecular-weight solutes occurs following fusion between elements involved in the degradation of endocytosed substances. The shrinkage process has been shown to be low in several cell types (hours to days), and there is not information on the fate of the ingested membrane (Steinman and Cohn, 1972; Silverstein et al, 1977). Based on stereological analysis, Assaf (1980) reported shrinkage of the cytoplasmic residual bodies from stage VIII to stage IX in which the phagosomes are converted into phagolysosomes after

their fusion with secondary lysosomes, confirming previous observations made by Nicander (1963) who attributed this condensation to a lysis of lipid material and ribonucleoproteins present in these elements.

In conclusion, the significant diminution in number and volume of secondary lysosomes between stages I - III may be explained by both figures of fusion and the shrinkage of the secondary lysosomes as a consequence of efflux of materials. The dramatic drop in the total number and total volume of secondary lysosomes at stage IX of the cycle of the seminiferous epithelium reflects, as stated above, the fusion of these elements with the phagosomes containing the cytoplasmic residual bodies.

(c) Average volume of secondary lysosomes

In general, the average volume of secondary lysosomes does not change throughout all stages of the cycle, except at stage XII in which the average volume has the tendency to be higher. This value remains high at stage XIII and abruptly decreases at stage XIV of the cycle. The "t" test emphasizes the statistical validity of these results. Although we do not have an explanation for the temporary increase in the average volume of secondary lysosomes, it is important to point out that it coincides with the period of high endocytic activity of the Sertoli cell (the peak is registered at stage XIII).

As it was previously discussed, the secondary lysosomes could undergo shrinkage as a consequence of efflux of fluids and low-molecular solutes (Silverstein et al, 1977). However, this process has been reported to be slow in most of the cell types studied, and it may take hours or days (Silverstein et al, 1977). Thus, it is possible that a higher endocytic activity may result temporarily in the formation of more secondary lysosomes of larger volumes.

(4) General Summary and Conclusions

The various observations made led to the following conclusions:

1) Sertoli cells are active endocytic cells which internalized by fluid-phase endocytosis various tracers infused into the lumen of seminiferous tubules; native ferritin, HRP-G, albumin-G, lactoalbumin-G and Con A-F in the presence of alpha-methyl-D-mannoside are firstly enclosed in large pinocytic vesicles (0.1-0.2 μm in diameter), then the tracers are transferred to large irregular multivesicular bodies, acid phosphatase-negative, identified as endosomes; these transform into acid phosphatase-positive dense, spherical multivesicular bodies which in turn evolve into dense secondary lysosomes which condense the tracers. This fluid-phase endocytosis appears to be a constitutive process that exists at all stages of the cycle of the seminiferous epithelium and independently of microtubule polymerization and microfilament gelation.

2) Sertoli cells appear to have a limited adsorptive pinocytic activity at their apex which is limited to stage VIII of the cycle.

3) Endosomes, dense multivesicular bodies, dense secondary lysosomes, small pale vesicles and dense core vesicles, plus microvesicles are usually seen in clusters located at the base of Sertoli cells from stages II to VIII of the cycle and in the supranuclear apical cytoplasm of Sertoli cells from stages IX to XIV-I of the cycle. Pale vesicles derive from endosomes and appear to be involved in membrane recycling, while the small dense vesicles derive from condensing, secondary lysosomes. The fate of these dense core vesicles remains to be elucidated.

4) Phagocytosis of spermatids cytoplasmic residual bodies by Sertoli cells takes place during stages VIII and IX of the cycle. It appears to be the result of a specific interaction between the plasma membrane delimiting

residual bodies and certain segments of the apical plasma membrane of the Sertoli cell. Phagocytosis of residual bodies is also dependent on the integrity of the microtubular system of the cell.

5) Tracer studies and morphometric quantitative analysis of the lysosomal population supported the notion that during stage IX of the cycle the secondary lysosomes fuse with the residual bodies transforming them into phagolysosomes which are rapidly lysed. In the process, both phagocytosed residual bodies and secondary lysosomes are eliminated from the Sertoli cell cytoplasm. Thus, in Sertoli cells both phagocytic and pinocytic processes are well integrated.

6) Data from the morphometric analysis, which yielded absolute numbers, total volumes, percentages of tracer-labelled lysosomes in Sertoli cells at various stages of the cycle of the seminiferous epithelium revealed the existence of two distinct levels of pinocytic activity of Sertoli cells during the cycle. From stage II to stage VIII of the cycle, the percentage of labelled lysosomes remains low (14.63%±0.55% SEM) while from stage IX to stage XIV of the cycle, these percentages are comparatively high (56.26%±1.62% SEM). During stage I the values decreased rapidly to return to a low value. While the exact functional significance of the phenomenon remains unclear, an attempt was made to correlate this activity with other histological processes taking place during the cycle of the seminiferous epithelium.

LITERATURE CITED

Abrahamson, D.R., D.T. Fearon 1983 Endocytosis of the C3b receptor of complement within coated pits in human polymorphonuclear leukocytes and monocytes. Lab. Invest. 48:162-168.

Abrahamson, D.R., R. Rodewald 1981 Evidence of the sorting of endocytic vesicle contents during the receptor-mediated transport of IgG across the newborn intestine. J. Cell Biol. 91:270-280.

Ackerman, G.A., W.H. Freeman 1979 Membrane differentiation of developing hemic cells of the bone marrow demonstrated by changes in concanavalin A surface labelling. J. Cytochem. Histochem. 27:1413-1423.

Anderson, E., B.E. Batten 1982 Surface distribution and uptake of cationic ferritin in a steroid producing cell. J. Cell Biol. 95 (Part 2):423a.

Anderson, R.G.W., J.L. Goldstein, M.S. Brown 1977 A mutation that impairs the ability of lipoprotein receptors to localize in coated pits on the cell surface of human fibroblasts. Nature 270:695-699.

Anderson, W.A., C. Burnett 1979 Reproductive tract peroxidase as end products of estrogen-specific gene expression. J. Histochem. Cytochem. 27:1363-1364.

Anderson, W.A., J. Tantalis, J.H. Kang 1975 Ultrastructural localization of endogenous mammary gland peroxidase during lactogenesis in the rat. Results after tannic acid-formaldehyde-glutaraldehyde fixation. J. Cytochem.Histochem. 23:295-302.

Andrews, P.M. 1981 Cationized ferritin binding to anionic surfaces in normal and aminonucleoside nephrotic kidneys. Am. J. Anat.162:89-106.

Aoki, A. 1980 Induction of sperm release by microtubule inhibitors in rat testis. Eur. J. Cell Biol. 22:467.

Aoki, A., D.W. Fawcett 1975 Impermeability of Sertoli cell junctions to prolonged exposure to peroxidase. Andrologia 7:63-76.

Askenase, P.W., B.J. Hayden 1974 Cytophilic antibodies in mice contact-sensitized with oxazolone. Immunochemical characterization and preferential binding to a trypsin-sensitive macrophage receptor. Immunology 27:563-576.

Assaf, A.A. 1980 Cyclic changes of cytoplasmic components in rat Sertoli cells. Master of Science Thesis, McGill University, Montreal, Canada.

Aulenbacher, P., N. Paweletz, E. Friedrich, R. Suss 1983 Studies on intravascular phagocytosis in the lung. Virchows Arch. Cell Pathol. 44: 57-64.

Axiline, S.G., E.P. Reaven 1974 Inhibition of phagocytosis and plasma membrane mobility of the cultivated macrophage by cytochalasin B. J. Cell Biol. 62:647-659.

Bainton, D.F., M.G. Farquhar 1968 Differences in enzyme content of azurophil and specific granules of polymorphonuclear leukocytes. II. Cytochemistry and electronmicroscopy of bone marrow cells. J. Cell Biol. 39:299-317.

Beguinot, L., R.B. Dickson, J.A. Hanover, N.D. Richert, M.C. Willingham, I. Paston 1983 Isolation and characterization of a highly enriched preparation of receptosome from human cultured epithelial cells. J. Cell Biol. 97(Part 2):102a.

Bendayan, M. 1981 Ultrastructural localization of nucleic acid by the use of enzyme gold complexes. J. Histochem. Cytochem. 29:531-541.

Bergeron, J.J.M., L. Resch, R. Rachubinski, B.A. Patel, B.I. Posner 1983 Effect of colchicine on internalization of prolactin in female rat liver. An in vivo radioautographic study. J. Cell Biol. 96:875-886.

Bergeron, J.J.M., R. Sikstrom, A.R. Hand, B.I. Posner 1979 Binding and uptake of ^{125}I-Insulin into rat liver hepatocytes and endothelium. An in vivo radioautographic study. J. Cell Biol. 80:427-443.

Besterman, J.M., J.A. Airhart, R.B. Low, D.E. Rannels 1983 Pinocytosis and intracellular degradation of exogenous protein:modulation by amino acids. J. Cell Biol. 96:1586-1591.

Bhishey, A.N., J.J. Freed 1971 Altered movement of endosomes in colchicine-treated cultured macrophages. Exp. Cell Res. 64:430-438.

Black, V.H. 1971 Gonocytes in fetal guinea-pig testes: Phagocytosis of denervating gonocytes by Sertoli cells. Am. J. Anat. 131:415.

Blok, J., A.A. Mulder-Stapel, L.A. Ginsel, W.Th. Daems 1981 Endocytosis in absorptive cells of cultured human small intestinal tissue: Horseradish peroxidase, lactoperoxidase, and ferritin as markers. Cell Tissue Res. 216:1-13.

Blok, J., B.A.A. Scheven, A.A. Mulder-Stapel, L.A. Ginsel, W. Th. Daems 1982 Endocytosis in absorptive cells of cultured human small intestinal tissue: effect of cytochalasin B and D. Cell Tissue Res. 222:113-126.

Blouin, A., R.P. Bolender, E.R. Weibel 1977 Distribution of organelles and membranes between hepatocytes and nonhepatocytes in the rat liver parenchyma. J. Cell Biol. 72:441-455.

Brac, T. 1983 Charged sieving by the basal lamina and the distribution of anionic sites on the external surfaces of fat body cells. Tissue and Cell 15:489-498.

Brokelmann, J. 1961 Surface modifications of Sertoli cells at the various stages of spermatogenesis in rat. Anat. Rec. 139:211a.

Brown, J.C., R. Hunt 1978 Lectins. In: International Review of Cytology. Vol. 52, G.H. Bourne and J.F. Danielli, eds., Academic Press, New York, pp. 277-349.

Brown, M.S., J.L. Goldstein 1976 Receptor-mediated control of cholesterol metabolism. Science 191:150-154.

Bruns, R.R., G.E. Palade 1968 Studies on blood capillaries. I. General organization of blood capillaries in muscle. J. Cell Biol. 37:244-276.

Burton, G.J. 1982 Placental uptake of maternal erythrocytes: a comparative study. Placenta 3:407-434.

Burton, G.J., C.A. Samuel, D.H. Steven 1976 Ultrastructural studies of the placenta of the ewe: phagocytosis of erythrocytes by the chorionic epithelium of the central depression of the cotyledon. Quart. J. Exp. Physiol. 61:275-286.

Bustos-Obregon, E. 1970 On Sertoli cell number and distribution in rat testis. Arch. Biol. (Liege) 81:99-108.

Byers, S.W., P.K. Qasba, H.L. Paulson, M. Dym 1984 Immunocytochemical localization of alpha lectoalbumin in the male reproductive tract (in press).

Cantin, M., Y. Gutawska, M.B. Anand-Srivastava, S. Ledoux, C. Bianchi, P. Carriere, J. Genest 1982 Binding and internalization of ^{125}I-angiotensin II in the rat adrenal. An ultrastructural radioautographic study. J. Cell Biol. 95(Part 2):411a.

Carr, I., E.J. Clegg, G.A. Meek 1968 Sertoli cells as phagocytes: An electron microscopy study. J. Anat. 102:501-509.

Chalkly, H.W. 1943 Method for the quantitative morphologic analysis of tissues. J. Nat. Cancer Inst. 4:47.

Chavez, D.J., A.C. Enders 1982 Lectin binding of mouse blastocysts: appearance of dolichos biflorus binding sites on the trophoblast during delayed implantation and their subsequent disappearance during implantation. Biol. Reprod. 26:545-552.

Ciechanover, A.J., A.L. Schwartz, H.F. Lodish 1982 Kinetics of internalization and recycling of the surface receptor for asialoglycoproteins. J. Cell Biol. 95(Part 2):428a.

Ciechanover, A.J., A.L. Schwartz, H.F. Lodish 1983 The asialoglycoprotein receptor internalizes and recycles independently of the transferrin and insulin receptors. Cell 32:267-275.

Clegg, E.J., E.W. McMillan 1965 The uptake of vital dyes and particulate matter by Sertoli cells of the rat testis. J. Anat. 99:219-220.

Clermont, Y. 1972 Kinetics of spermatogenesis in mammals: seminiferous epithelium cycle and spermatogonial renewal. Physiol. Rev. 52: 198-235.

Clermont, Y., S.C. Harvey 1965 Duration of the cycle of the seminiferous epithelium of normal, hypophysectomized and hypophysectomized-hormone treated albino rats. Endocrinology 76:80-89.

Clermont, Y., C.P. Leblond, B. Messier 1959 Durée du cycle de l'epithelium seminale du rat. Archiv. d'Anat. Microsc. Morphol. Exper. 48:37-56.

Clermont, Y., J. McCoshen, L. Hermo 1970 Evolution of the endoplasmic reticulum in the Sertoli cell cytoplasm encapsulating the heads of late spermatids in the rat. Anat. Rec. 196:83-99.

Clermont, Y., A. Rambourg 1978 Evolution of the endoplasmic reticulum during rat spermiogenesis. Am. J. Anat. 151:191-212.

Danon, D., L. Goldstein, Y. Marikovsky, E. Skutelky 1972 Use of cationized ferritin as a label of negative charges. J. Ultrastruct. Res. 38: 500-510.

Daukas, G., D.A. Lauffenburger, S. Zigmond 1983 Reversible pinocytosis in polymorphonuclear leukocytes. J. Cell Biol. 96:1642-1650.

Davis, B.D., R. Dulbecco, H. Eisen, H.S. Ginsberg, W.B. Wood, M. McCarty 1973 In: Microbiology, pp. 633-634. New York: Harper and Row.

de Duvé, C., Rh. de Barsy, B. Poole, A. Trouet, P. Tulkens, F. Van Hoof 1974 Lysosomotropic agents. Biochem. Pharmacol. 23:2495-2531.

Denef, J.F., R. Ekholm 1980 Membrane labelling with cationized ferritin in isolated thyroid follicles. J. Ultrastruct. Res. 71:203-221.

Dickson, R.B., R. Schlegel, M. Willingham, I.H. Pastan 1982 Involvement of Na^+ and HCO_3^- in receptor-mediated endocytosis of alpha 2 - macroglobulin, epidermal growth factor, and vesicular stomatitis virus. J. Cellular Physiol. 113:353-358.

Dietert, S.E. 1966 Fine structure of the formation and fate of the residual bodies of mouse spermatozoa with evidence for the participation of lysosomes. J. Morph. 120:317-346.

Doty, S.B., C.E. Smith, A.R. Hand, C. Oliver 1977 Inorganic trimeta-phosphatase as a histochemical marker for lysosomes in light and electron microscopy. J. Histochem. Cytochem. 25:1381-1384.

Douglas, C.G., B.F. King 1982 Endocytosis and subsequent processing of IgG by guinea pig yolk sac in vitro. J. Cell Biol. 95(Part 2):419a.

Dunn, W.A., A.L. Hubbard 1982 Receptor-mediated endocytosis of epidermial growth factor (EGF) by liver. J. Cell Biol. 95(Part 2):425a.

Dym, M. 1972 The fine structure of the monkey Sertoli cell and its role in establishing the blood-testis barrier. Biol. Reprod. 7:129a.

Dym, M. 1976 Mammalian Rete Testis - A morphological examination. Anat. Rec. 186:493-524.

Dym, M., D.W. Fawcett 1970 The blood-testis barrier in the rat and the physiological compartmentation of the seminiferous epithelium. Biol. Reprod. 3:308-326.

Elias, H., D.M. Hyde 1980 An elementary introduction to stereology (Quantitative Microscopy). Am. J. Anat. 159:411-446.

Farquhar, M.G. 1978 Recovery of surface membrane in anterior pituitary cells. J. Cell Biol. 77:R35-R42.

Farquhar, M.G. 1983 Multiple pathways of exocytosis, endocytosis, and membrane recycling: validation of a Golgi route. Fed. Proc. 42:2407-2413.

Fawcett, D.W. 1975 Ultrastructure and Function of the Sertoli Cell. In: Handbook of Physiology. Sec. 7, Endocrinology, Vol. 5. Male Reproductive System. Ed. by D.W. Hamilton and R.O. Greep. Amer. Phys. Soc., Washington. pp. 21-55.

Fawcett, D.W. 1977 The ultrastructure and Function of the Sertoli Cell. In: Frontiers in Reproduction and Fertility Control. Sec. 28, Part 2. Ed. by R.O. Grup and M.A. Koblinsky. pp. 302-320.

Fawcett, D.W., S. Doxey 1982 The entry of sporozoites of Theileria parva into bovine lymphocytes in vitro. Electron microscopic observations. Eur. J. Cell Biol. 27:10-21.

Fehlmann, M., J.L. Carpentier, E.V. Obberghen, P. Freychet, P. Thamm, D. Saunders, D. Branderburg, L. Oci 1982 Internalized insulin receptors are recycled to the cell surface in rat hepatocytes. Proc. Natl. Acad. Sci. USA 79:5921-5925.

Flickinger, C.J., D.W. Fawcett 1967 Junctional specializations of the Sertoli cells in the seminiferous epithelium. Anat. Rec. 158:207-222.

Galbraith, R.M., P. Wermer, P. Armand, G.M.P. Galbraith 1980 Transferrin binding to peripheral blood lymphocytes activated by phytohemagglutinin involves a specific receptor: ligand interaction. J. Clin. Invest. 66:1135-1143.

Geiger, B. 1983 Membrane-cytoskeleton interaction. Biochim. Biophys. Acta 737:305-341.

Geoghegan, W.D., G.A. Ackerman 1977 Adsorption of horseradish peroxidase, ovomucoid and anti-immunoglobulin to colloidal gold for the indirect detection of concanavalin A, wheat germ agglutinin and goat anti-human immunoglobulin G on cell surfaces at the electron microscopic level. A new method, theory and application. J. Histochem. Cytochem. 25:1187-1200.

Geuze, H.J., J.W. Slot, J.A.M. Strous, H.F. Lodish, A.L. Schwartz 1983 Intracellular site of Asialoglycoprotein receptor-ligand uncoupling: Double label immunoelectron microscopy during receptor-mediated endocytosis. Cell 32:277-287.

Gillouzo, A., G. Feldmann 1977 Surface and intracellular localization of concanavalin A binding sites in rat liver cells. J. Histochem. Cytochem. 25:1303-1310.

Goldstein, I.J. 1975 Studies of the combining sites of Concanavalin A. In: Advances of Experimental Medicine and Biology, no. 55. Ed. by T.K. Chowhdury and A.K. Weiss. pp. 35-54.

Gonella, P., T. Hall, D. Abrahamson, M. Neutra 1982 Sorting of soluble and membrane-bound protein in prelysosomal compartments of epithelial cells in suckling rat ileum. J. Cell Biol. 95 (Part 2); 421a.

Gordon-Weeks, P.R., D.H. Jones 1983 Binding and uptake of concanavalin A into rat brain synaptosomes: evidence for synaptic vesicle recycling. Proc. R. Soc. Lond. B 219:413-422.

Goud, B., J.C. Antoine, N.K. Gonatos, A. Stieber, S. Avrameas 1981 A comparative study of fluid-phase and adsorptive endocytosis of horseradish peroxidase in lymphoid cells. Exp. Cell Res. 132: 375-386.

Graham, R.C., M.J. Karnovsky 1966 The early stages of adsorption of injected horseradish peroxidase in the proximal tubules of mouse kidney. Ultrastructural cytochemistry by a new technique. J. Histochem. Cytochem. 14:291-301.

Griffin, F.M., J.A. Griffin, J.E. Leider, S.C. Silverstein 1975 Studies on the mechanism of phagocytosis. I. Requirements for circumferential attachment of particle-bound ligands to specific receptors on the macrophage plasma membrane. J. Exp. Med. 142:1263-1282.

Griffin, F.M., J.A. Griffin, S.C. Silverstein 1976 Studies on the mechanism of phagocytosis. II. The interaction of macrophages with anti-immunoglobulin IgG-coated bone marrow-derived lymphocytes. J. Exp. Med. 144:788-809.

Griffin, F.M., S.C. Silverstein 1974 Segmental response of the macrophage plasma membrane to a phagocytic stimulus. J. Exp. Med. 139:323-336.

Gronblad, M., K.E.O. Ackerman, O. Eranko 1982 Endocytic uptake of cationized ferritin tracer into glomus cells and dissociated from the adult rat carotid body. Cell Tissue Res. 226:37-49.

Haigler, H., J.A. McKanna, S. Sohen 1979 Direct visualization of the binding and internalization of ferritin conjugate of epidermal growth factor in human carcinoma cells. J. Cell Biol. 81 (Part 2); 382a.

Hamilton, T.A. 1983 Receptor-mediated endocytosis and exocytosis of transferrin in concanavalin A - stimulated rat lymphoblasts. J. Cellular Physiol. 114:222-228.

Hamilton, T.A., H.G. Wada, H.H. Sussman 1979 Identification of transferrin receptors on the surface of human cultured cells. Proc. Natl. Acad. Sci. USA 76:6406-6410.

Hand, A.R. 1979 Cytochemical detection of peroxisomal oxidases. J. Histochem. Cytochem. 27:1367-1370.

Handley, D.A., C.M. Arbeeny, L.D. Witte, D.S. Goodman, S. Chien 1983 Ultrastructural visualization of low-density lipoproteins during receptor binding and cellular endocytosis. J. Ultrastruct. Res. 83:43-47.

Harding, C., J. Heuser, P. Stahl 1983 Receptor-mediated endocytosis of transferrin and recycling of the transferrin receptor in rat reticulocytes. J. Cell Biol. 97:329-339.

Hart, P.D. 1979 Phagosome-lysosome fusion in macrophages: Hinge in the fate ingested microorganism? In: Lysosomes in Applied Biology and Therapeutics. J.T. Dingle, P.J. Jacques, I.H. Scharr (eds.), Vo. 6. Amsterdam, North Holland Co., p. 409.

Hermo, L. 1972 Quantitative study of the spermatogonial stem cell population of the rat. Master of Science Thesis, McGill University, Montreal, Canada.

Hermo, L., Y. Clermont, M. Lalli, A. Rambourg 1978 Distribution of lysosomes in Sertoli cells during the cycle of the seminiferous epithelium of the rat. In: 9th Int. Cong. on Elect. Microscop. Ed. by H.M. Sturgess, Imperial Press, Ontario. p. 690 (Abstract).

Hermo, L., C.R. Morales, Y. Clermont 1982 Endocytic activity of Sertoli cells in the rat. J. Cell Biol. 95 (Part 2): 434a.

Hermo, L., C.R. Morales, Y. Clermont 1983 Endocytosis in epithelial cells lining the rete testis of the rat. J. Cell Biol. 95 (Part a): 100a.

Herzog, V. 1979 The secretory process as studied by the localization of endogenous peroxidase. J. Histochem. Cytochem. 27:1360-1370.

Herzog, V. 1983 Trancytosis in thyroid follicle cells. J. Cell Biol. 97:607-617

Hewit, K., A.E. Beer, F. Grinnell 1979 Disappearance of anionic sites from the surface of the rat endometrial epithelium at the time of blastocyst implantation. Biol. Reprod. 21:691-707.

Ichev, K., W. Ovtscharroff 1981 Concanavalin A binding sites on the intestinal microvillus membrane of rat. Acta histochem. 69:119-124.

Imamura, T., M. Beppu, T. Terao, T. Osawa 1981 Valence-dependent internalization of lectins into Balb/c 3T3 cells. Cell Struct. Funct. 6:1-10.

Jacques, P.J. 1969 Endocytosis. In: Lysosomes in Biology and Pathology, Vol. 2 (J.T. Dingle and H.B. Fell, eds.), Academic Press, New York, pp. 395-420.

Jakoi, E.R., R.B. Marchase, M.C. Reddy 1981 Distribution of anionis sites on surfaces of retinal cells: A study using cationized ferritin. J. Ultrastruct. Res. 76:96-106.

Jersild, R.A. 1982 Restricted mobility and endocytosis of anionic sites on newborn rat jejunal brush border membranes. Anat. Rec. 202:61-71.

Jesaitis, A.J., C.G. Cochrane 1983 Receptor-mediated endocytosis, host defence and inflammation. Lab. Invest. 48:117-119.

Johansson, B.R. 1983 Distribution of anionic binding sites in extravascular space of skeletal muscle demonstrated with policationized ferritin. J. Ultrastruct. Res. 83:176-183.

Karnovsky, J. 1971 The use of ferrocyanide osmium tetroxide in electron microscopy. Proc. 11th Am. Soc. Cell Biol., Nov. 17-20, 1971, New Orleans, Louisiana, Abstract 284, p. 146.

Kerr, J.B., D.M. de Krester 1975 Cyclic variations in Sertoli cell lipid content throughout the spermatogenic cycle in the rat. J. Reprod. Fert. 43:1-8.

King, F.B. 1982 Absorption of peroxidase-conjugated immunoglobulin G by human placenta: an in vitro study. Placenta 3:395-406.

Kissinger, C., M.K. Skinner, M.D. Griswold 1982 Analysis of Sertoli cell secreted proteins by two-dimensional gel electrophoresis. Biol. Reprod. 27:233-240.

Kolb-Bachofen, V., J. Schelepper-Schaffer, W. Vogell, H. Kolb 1982 Electron microscopic evidence for an asialoglycoprotein receptor on Kupffer cells: Localization of lectin-mediated endocytosis. Cell 29:859-866.

Kormano, M., A.I. Koskimies, R.L. Hunter 1971 The presence of specific proteins in the absence of many serum proteins, in the rat seminiferous tubule fluid. Experientia 27:1461-1463.

Koskimies, A.I., M. Kormano 1973 The proteins in fluids from the seminiferous tubules and rete-testis of the rat. J. Reprod. Fert. 34:433-444.

Lacroix, M., M. Parvinen, I.B. Fritz 1981 Localization of testicular plasminogen activator in discrete portions (Stages VII and VIII) of the seminiferous tubule. Biol. Reprod. 25:143-146.

Lacroix, M., F.E. Smith, I.B. Fritz 1977 Secretion of plasminogen activator by Sertoli cell enriched cultures. Mol. Cell Endocrinol. 9:227-236.

Lacy, D. 1962 Certain aspects of testis structure and function. Brit. Med. Bull. 18:205-208.

Lalli, M.F. 1983 The use of thiamine monophosphate for cytochemical localization of acid phosphatase activity in Sertoli cells of rat testis. In: 10th Annual Meeting of the Microscopical Society of Canada, Chalk River, Ontario, pp. 32-33 (Abstract).

Lalli, M.F. 1983 Ultrastructural localization of phosphatases and arylsulfatase activities in the Golgi apparatus and lysosomes of Sertoli cells in the rat. Anat. Rec. 205:105a.

Lalli, M.F., X.M. Tang, Y. Clermont 1984 Glycoprotein synthesis in Sertoli cells during the cycle of the seminiferous epithelium of adult rats: a radioautographic study (In press).

Leak, L.V., D.C. Sun 1983 Con A stimulation of endocytic cisternae in isolated lymph node cells. J. Cell Biol. 95 (Part 2):101a.

Leblond, C.P., Y. Clermont 1952a Spermiogenesis of rat, mouse, hamster and guinea pig as revealed by the "periodic acid-fuchsin sulfurous acid technique". Am. J. Anat. 90:167-216.

Leblond, C.P., Y. Clermont 1952b Definition of the stages of the cycle of the seminiferous epithelium of the rat. Ann. N.Y. Acad Sci. 55:548-573.

Marikovsky, Y., L. Wang, M. Imbar 1983 Distribution of surface anionic sites on mouse hybrid myelomas. Exp. Cell Biol. 51:242-249.

Maupin, P., T.D. Pollard 1983 Improved preservation and staining of hela cell actin filaments, clathrin-coated membranes, and other cytoplasmic structures by tannic acid-glutaraldehyde-saponin fixation. J. Cell Biol. 96:51-62.

McLean, I.M., E.J. Sanders 1983 Cationized ferritin and phosvitin uptake by coated vesicles of the early chick embryo. Anat. Embryol. 166:385-397.

Michl, J., D.J. Ohlbaum, S.C. Silverstein 1976 2-Deoxiglucose selectively inhibits Fc and complement receptor-mediated phagocytosis in mouse peritoneal macrophages. II. Dissociation of the inhibitory effects of 2-deoxyglucose on phagocytosis and ATP generation. J. Exp. Med. 144: 1484-1493.

Moller, P.C., J.P. Chang 1978 Internalization of cationized ferritin receptors by rat hepatoma ascites cells. Exp. Cell Res. 114:39-45.

Morales. C., H.A. Domitrovic, J.C. Sampietro 1982 Influence of colchicine on lactating mammary gland of the cow and rat with special reference to the exocytosis and to the milk fat globule secretion. Zbl. Vet. Med. C. Anat. Histol. Embryol. 11:56-64.

Morales, C., L. Hermo 1983 Demonstration of fluid-phase endocytosis in epithelial cells of the male reproductive system by means of horseradish peroxidase-colloidal gold complex. Cell Tissue Res. 230:503-510.

Morales, C., L. Hermo, Y. Clermont 1983 Endocytosis and the lysosomal apparatus of epithelial cells of the ductuli efferentes in the rat. Anat. Rec. 205:133A-134A.

Morales, C., L. Hermo, Y. Clermont 1984 Endocytosis in epithelial cells lining the rete testis of the rat. Anat. Rec. (In press).

Muller, W.A., R.M. Steinman, Z.A. Cohn 1980 The membrane proteins of the vacuolar system. II. Bidirectional flow between secondary lysosomes and plasma membrane. J. Cell Biol. 86:304-314.

Muller, W.A., R.M. Steinman, Z.A. Cohn 1983 Membrane proteins of the vacuolar system. III. Furhter studies on the composition and recycling of endocytic vacuole membrane in cultured macrophages. J. Cell Biol. 96: 29-36.

Myagkaya, G., W. Th. Daems 1979 Fusion of erythrolysosomes in epithelial cells of the sheep placenta. Cell Tissue Res. 203:209-221.

Myagkaya, G., J.P.M. Schellens 1981 Final stages of erythrophagocytosis in the sheep placenta. Cell Tissue Res. 214:501-518.

Nicander, L. 1963 Some ultrastructural features of mammalian Sertoli cells. J. Ultrastruct. Res. 8:190 (abstract).

Nicander, L. 1969 An electron microscopical study of cells in the seminiferous tubules of some mammals. Z. Zellforsch. Mikroskop. Anat. 83:375-397.

Nichols, B.A. 1982 Uptake and digestion of horseradish peroxidase in rabbit alveolar macrophages. Formation of a pathway connecting lysosomes to the cell surface. Lab. Invest. 43:235-246.

Nicolson, G.L. 1972 Topography of membrane concanavalin A sites modified by proteolysis. Nature 239:193-197.

Nicolson, G.L. 1974 The interaction of lectins with animal cell surfaces. In: International Review of Cytology. Vol. 39. G.H. Bourne and J.F. Danielli, eds. Academic Press, New York, pp. 89-190.

Nicolson, G., M. Lacorbiere, R. Yamagimachi 1972 Quantitative determination of plant agglutinin membrane sites on mammalian spermatozoa (36847). Proc. Soc. Exp. Biol. Med. 141:661-663.

Niemi, M. M. Kormano 1965 Cyclical changes in and significance of lipids and acid phosphatase in the seminiferous tubules of the rat testis. Anat. Rec. 151:159-170.

Nilsson, J.R., B. Van Deurs 1983 Coated pits and pinocytosis in tetrahymena. J. Cell Sci. 63:209-222.

Novikoff, A.B. 1963 Lysosomes in the physiology and pathology of cells: Contributions of staining and methods. In: Ciba Foundation Symposium on Lysosomes. A.V.S. de Reuck and M.P. Cameron, Eds. Little Brown, Boston, pp. 36-77.

Ockner, R.K., R.A. Weisiger, J.L. Gollan 1983 Hepatic uptake of albumin-bound substances: albumin receptor concept. Am. J. Physiol. 245:613-618.

Orci, L., Y. Lemarchand, A. Singh, F. Assimicopoulos-Jeannet, C. Rouiller, B. Jeanrenaud 1973 Role of microtubules in lipoprotein secretion by the liver. Nature 244:20-32.

Orth, J., A.K. Christensen 1977 Localization of ^{125}I-labeled FSH in the testes of hypophysectomized rats by autoradiography at the light and electron microscope levels. Endocrinology 101:262-278.

Orth, J., A.K. Christensen 1978 Autoradiographic localization of FSH-binding sites on Sertoli cells and spermatogonia in testes from hypophysectomized rats. In: Structure and Function of the Gonadotrophins. McKerns, K.W., ed. Plenum Press, New York, pp. 111-137.

Paavola, L.G., J.F. Strauss 1983 Uptake of lipoproteins in situ perfused rat ovaries: identification of binding sites for high density lipoproteins. J. Cell Biol. 97:593-606.

Palade, G.E. 1956 The endoplasmic reticulum. J. Biophys. Biochem. Cytol. Suppl. 2:85-98.

Palade, G.E. 1960 Transport in quanta across the endothelium of blood capillaries. Anat. Rec. 136:254.

Parvinen, M. 1982 Regulation of the seminiferous epithelium. Endocrine Reviews 3:404-417.

Pastan, I.H., M.C. Willingham 1981 Journey to the center of the cell: Role of receptosome. Science, 214:504-509.

Patton, S. 1974 Reversible suppression of lactation by colchicine. FEBS Letters, 1:85-87.

Peress, N.S., D. Tompkins 1981 Effect of molecular charge on choroid-plexus permeability: Tracer studies with cationized ferritins. Cell Tissue Res. 219:425-431.

Pinto da Silva, P., S.M. Torrisi, B. Kachar 1981 Freeze-fracture cytochemistry of wheat-germ agglutinin and concanavalin A binding sites on freeze-fractured pancreatic cells. J. Cell Biol. 91:361-372.

Pool, R.R., K.M. Maurey, B. Storrie 1982 Processing steps in pinocytic content transfer into lysosomes in CHO cells. J. Cell Biol. 95 (Part 2):437a.

Posner, B.I., J.J.M. Bergeron, Z. Josefsberg, M.N. Khan, R.J. Khan, B.A. Patel, R.A. Sikstrom, A.K. Verma 1981 Polypeptide hormones: Intracellular receptors and internalization. Recent Prog. Horm. Res. 37:539-582.

Posner, B.I., N. Nassod, N. Khan, J.J.M. Bergeron 1982 Endocytosis of peptide hormones and other ligands. Endocrine Reviews 3:280-298.

Posner, B.I., A.K. Verma, B.A. Patel, J.J.M. Bergeron 1982 Effect of colchicine on the uptake of prolactin and insulin into Golgi fractions of rat liver. J. Cell Biol. 93:560-567.

Raikhel, A.S., A.O. Lea 1982 Internalization of specific and non-specific proteins by mosquito oocyte. J. Cell Biol. 95 (Part 2):441a.

Rambourg, A., Y. Clermont, L. Hermo 1979 Three-dimensional architecture of the Golgi apparatus in Sertoli cells of the rat. Am. J. Anat. 154: 455-475.

Rabinovitch, M. 1968 Phagocytosis: the engulfment stage. Seminars Hemat. 5:134-155.

Reaven, E.P., M.G. Reaven 1975 A quantitative ultrastructural study of microtubule content and secretory granule accumulation in parathyroid glands in phosphate and colchicine-treated rats. J. Clin. Invest. 1: 49-55.

Reddy, K.H., D.J. Svoboda 1967 Lysosomal activity in Sertoli cells of normal and degenerating germinal epithelial cells of rat testis. Am. J. Pathol. 51:1-18.

Regaud, C. 1901 Etudes sur la structure des tubes séminifères et sur la spermatogénèse chez les mammifères. Arch d'Anat. Microscop. 4:101-156, 231-380.

Reston, R.H., A.L. Jones, W.D. Christiansen, G. Hradek 1980 Evidence for a vesicular transport mechanism in hepatocytes for biliary secretion of immunoglobulin A. Science 208:1276-1278.

Ritzen, E.M., C. Boitani, M. Parvinen, F. French, M. Feldman 1982 Stage dependent secretion of ABP by rat seminiferous tubules. Mol. Cell Endocrinol. 25:25-33.

Rodewald, R. 1972 Intestinal transport of antibodies in the newborn rat. J. Cell Biol. 58:189-211.

Rodewald, R. 1980 Distribution of immunoglobulin G receptors in the small intestine of the young rat. J. Cell Biol. 85:18-32.

Rodewald, R., J.P. Kraehenbuhl 1982 IgG receptors of intestinal brush borders from neonatal rats. J. Cell Biol. 95 (Part 2):416a.

Roth, J., M. Wagner 1977 Peroxidase and gold complexes of lectins for double labeling of surface-binding sites by electron microscopy. J. Histochem. Cytochem. 25:1181-1184.

Russell, L.D. 1977 Observations on rat Sertoli ectoplasmic ("junctional") specializations in their association with germ cells of the rat testis. Tissue and Cell 9:475-498.

Russell, L.D., Y. Clermont 1976 Anchoring device between Sertoli cells and late spermatids in rat seminiferous tubules. Anat. Rec. 185:259-277.

Russell, L.D., Y. Clermont 1977 Degeneration of germ cells in normal, hypophysectomized and hormone treated hypophysectomized rats. Anat. Rec. 187:347-366.

Russell, L.D., J.P. Mallone, D.S. MacCurdy 1981 Effect of the microtubule disrupting agents, colchicine and vinblastine, on seminiferous tubule structure in the rat. Tissue and Cell 13:349-367.

Salhanick, A.I., J.P. Wiebe 1970 FSH receptors in isolated Sertoli cells: changes in concentration of binding sites at the onset of sexual maturation. Life Sci. 26:2281-2288.

Salisbury, J.L., J.S. Condielis, N.J. Maihle, P. Satir 1981 Calmodulin localization during capping and receptor-mediated endocytosis. Nature 294:163-166.

Sapsford, C.S., C.A. Rae, K.W. Cleland 1969 Ultrastructural studies on maturing spermatids and on Sertoli cells in the bandicoot (Perameles nasuta) . Austr. J. Zool. 17:195-292.

Schwartz, A.L., S.E. Fridovich, H.F. Lodish 1982 Kinetics of internalization and recycling of the asialoglycoprotein receptor in a hepatoma cell line. J. Biol. Chem. 257:4230-4237.

Setchell, B.P. 1967 The blood testis barrier in sheep. J. Physiol. 189:63-65.

Setchell, B.P. 1969 Do the Sertoli cells secrete the rete testis fluid? J. Reprod. Fert. 19:391-392.

Setchell, B.P. 1980 The functional significance of blood-testis barrier. Andrology 1:3-10.

Setchell, B.P., G.M.H. Waites 1975 The blood-testis barrier. In: Hamilton, D.W., Greep, R.O., eds. Male Reproductive System; Section 7, Endocrinology Handbook of Physiology, Vol. 5. Washington, D.C.: American Physiology Society, pp. 143-172.

Silverstein, S.C., R.M. Steinman, Z.A. Cohn 1977 Endocytosis. Ann. Rev. Biochem. 46:669-722.

Simon, G.T., S. Burke 1970 Electron Microscopy of the spleen. III. Erythro-Leukophagocytosis. Am. J. Pathol. 58:451-469.

Simionescu, N. 1979 The microvascular endothelium: segmental differentiations, trancytosis, selective distribution of anionic sites. Adv. Inflammation Res. 1:64-70.

Simionescu, N., M. Simionescu 1978 Differential distribution of anionic sites on the capillary endothelium. J. Cell Biol. 79 (Part 2):59a.

Skinner, M.K., M.D. Griswold 1980 Sertoli cells synthesize and secrete transferrin-like protein. J. Biol. Chem. 255:9523-9525.

Skinner, M.K., M.D. Griswold 1983 Sertoli cells synthesize and secrete a ceruloplasmin-like protein. Biol. Reprod. 28:1225-1229.

Skutelky, E., D. Danon, M. Wilchek, E.A. Boyer 1977 Localization of sialyl residues on cell surfaces by affinity cytochemistry. J. Ultrastruct. Res. 61:325-335.

Sly, W.S., P.D. Stahl 1978 In: Transport of Macromolecules in Cellular Systems (Dahlem Konferenzen) (S.C. Silverstein, ed.), Abakon Verlaggesell, Berlin, pp. 229-244.

Smith, R.M., L. Jarett 1983 Quantitative ultrastructural analysis of receptor-mediated insulin uptake into adipocytes. J. Cellular Physiol. 115:199-207.

Solari, R., L. Fabiani, L.C. Kuhn, J.P. Kraehenbuhl 1982 Cleavage of a membrane receptor is required for the translocation of polymeric IgA antibodies across epithelia. J. Cell Biol. 95 (Part 2):413a.

Southwick, S., T.P. Stossel 1983 Contractile proteins in leukocyte function. Seminars in Hematology 20:305-321.

Spicer, S.S., P.L. Sannes, M. Eguchi, P.E. McKeever 1979 Fine structural and cytochemical aspects of the development of macrophages and of their endocytic and secretory activity. J. Reticuloendothel. Soc. 26: 49-65.

Spors, S. 1970 Electron microscopic study on acid phosphatase of macrophages during the breakdown of erythrocytes in the spleen of the rat. Blut XXI:244-250.

Starling, D., R. Duncan, J.B. Lloyd 1983 The role of microtubules on pinocytosis. Inhibition of fluid-phase pinocytosis in the rat visceral yolk sac by mitoclasic and related agents. Cell Biol. Internat. Rep. 7:593-602.

Stein, O., Y. Stein 1973 Colchicine-induced inhibition of very low density lipoprotein release by rat liver in vitro. Biochem. Biophys. Acta 306: 142-147.

Steinman, R.M., S.E. Brodie, Z.A. Cohn 1976 Membrane flow during pinocytosis. A stereologic analysis. J. Cell Biol. 68:665-687.

Steinman, R.M., Z.A. Cohn 1972 The uptake, distribution and fate of soluble horseradish peroxidase in mouse peritoneal macrophage in vitro. J. Cell Biol. 55:186-204.

Steinman, R.M., I.S. Mellman, W.A. Muller, Z.A. Cohn 1983 Endocytosis and the recycling of plasma membrane. J. Cell Biol. 96:1-27.

Steinman, R.M., J.M. Silver, Z.A. Cohn 1974 Pinocytosis in fibroblasts: quantitative studies in vitro. J. Cell Biol. 63:949-969.

Steinman, R.M., J.M. Silver, Z.A. Cohn 1978 Fluid-phase pinocytosis. In: Transport of Macromolecules in Cellular Systems. S.C. Silver, ed. Dahlem Konferenzen, Berlin, pp. 167-179.

Storrie, B., M. Sachdeva, V.S. Viers 1983 CHO cells lysosomes labeled by fluid-phase pinocytosis retain pinocytozed horseradish peroxidase and in situ radioiodinated proteins. J. Cell Biol. 95 (Part 2):100a.

Strauss,W. 1957 Segregation of an intravenously injected protein by droplets of cells of rat kidneys. J. Biophys. Biochem. Cytol. 3:1037-1040.

Strauss, W. 1983 Mannose specific binding sites for horseradish peroxidase in various cells of the rat. J. Cytochem. Histochem. 31:78-84.

Sung, J.S., R.S. Nelson, S.C. Silverstein 1983 The role of mannose/N-acetyl glucosamine receptor in pinocytosis of horseradish peroxidase by mouse peritoneal macrophages. J. Cellular Physiol. 116:21-25.

Taylor, R.B., W.P.H. Duffus, M.C. Raff, S. de Petris 1971 Redistribution and pinocytosis of lymphocyte surface immunoglobulin molecules induced by anti-immunoglobulin molecules induced by anti-immunoglobulin antibody. Nat. New Biol. 233:225-227.

Tietze, C., P. Schlesinger, P. Stahl 1982 Mannose-specific endocytosis receptor of alveolar macrophages: demonstration of two functionally distinct intracellular pools of receptor and their roles in receptor recycling. J. Cell Biol. 92:417-424.

Tsubakio, T., Y. Kurata, Y. Kanayama, T. Yonezawa, S. Tarui, T. Kitani 1983 In vitro platelet phagocytosis in idiopathic thrombocytopenic purpura. Acta Hemat. 70:250-256.

Tuck, R.R., B.P. Setchell, G.H. Waites, J.A. Young 1970 The composition of fluid collected by micropuncture and catheterization from the seminiferous tubules and rete testis of rats. Pfleugers Arch. 318:225-243.

Tulkens, P. 1979 The role of lysosomes and plasma membrane in the intracellular accumulation of exogenous substances. Physiological, pharmacological and toxical studies in cultured cells. These presentee en vue de l'obtention du grade d'agrege de l'enseignement superiur. Université Catholique de Louvain, France.

Turner, T.T., J.L. Plesums, C.L. Cabot 1979 Luminal fluid proteins of the male reproductive tract. Biol. Reprod. 21:883-890.

Tycko, B., F.R. Maxfield Endocytic vesicle acification and asialoglycoprotein receptor reutilization in Hep G2 human hepatoma cells. J. Cell Biol. 95 (Part 2):435a.

Van Deurs, B. 1978a Microperoxidase uptake into the rat choroid plexus epithelium. J. Ultrastruct. Res. 62:168-180.

Van Deurs, B. 1978b Horseradish peroxidase uptake into the rat choroid plexus epithelium, with special reference to the lysosomal system. J. Ultrastruct. Res. 62:155-167.

Van Deurs, B., K. Nilausen 1982 Pinocytosis in mouse L-fibroblasts: ultrastructural evidence for a direct membrane shuttle between the plasma membrane and the lysosomal compartment. J. Cell Biol. 94:279-286.

Van Deurs, B., F. Von Bulow, M. Moller 1981 Vesicular transport of cationized ferritin by the epithelium of the rat choroid plexus. J. Cell Biol. 89:131-139.

Vasile, E., M. Simionescu, N. Simionescu 1983 Visualization of the binding, endocytosis, and trancytosis of low-density lipoprotein in the arterial endothelium in situ. J. Cell Biol. 96:1677-1689.

Venkatachalam, M.A., M.H. Soltani, H.D. Fahimini 1970 Fine structural localization of peroxidase activity in the epithelium of large intestine of rat. J. Cell Biol. 46:168-173.

Virtanen, I., A. Miettinen, J. Wartiovaaha 1978 Lectin-binding sites are found in rat liver cell plasma membrane only on its extracellular surface. J. Cell Sci. 29:287-296.

Wada, H.G., P.E. Hass, H.H. Sussman 1979 Transferrin receptor in human plascenta brush border membranes: studies on the binding of transferrin to placental membrane vesicles and the identification of a placental brush border glycoprotein with high affinity for transferrin. J. Biol. Chem. 254:12629-12635.

Wall, D.A., A.L. Hubbard 1981 Galactose-specific recognition system of mammalian liver: receptor distribution on the hepatocyte cell surface. J. Cell Biol. 9:687-696.

Wall, D.A., G. Wilson, A.L. Hubbard 1980 The galactose-specific recognition of mammalian liver: the route of ligand internalization in hepatocytes. Cell 21:79-93.

Weibel, E.R., R.P. Bolender 1973 Stereological techniques for electron microscopy morphometry. In: Principles and Techniques of Electron Microscopy. Vol. 3. Ed. by M.A. Hayat, Van Mostrand Reinhold Company, New York, pp. 238-296.

Weibel, E.R., H. Elias 1965 Quantitative methods in morphology. In: Proc. of Symp. in Quant. Methods in Morph. during the 8th Int. Cong. of Anatomy. Ed. by E.R. Weibel, H. Elias, Springer-Verlag, Weisbaden.

Weibel, E.R., W. Staubli, H.R. Gnagi, F.A. Hess 1969 Correlated morphometric and biochemical studies on the liver cell. I. Morphometric model, Sstereologic methods and normal morphometric data for rat liver. J. Cell Biol. 42:69-91.

Welsch, V., U. Schumacher 1983 In vivo binding and effects of concanavalin A (con A) on rat and mouse pulmonary alveolar epithelial cells and macrophages. Virchows Arch. (Cell Pathol.) 44:45-56.

Widnell, C.C., R.P. Kidson 1983 Origin of vacuoles formed during the inhibition of pinocytosis in rat embryo fibroblasts treated with monensin. J. Cell Biol. 95 (Part 2):101a.

Willingham, M.C., H.T. Haigler, D.J.P. Fitzgerald, M.G. Gallo, A.V. Rutherford, I.H. Pastan 1983 The morphologic pathway of binding and internalization of epidermal growth factor in cultured cells. Exp. Cell Res. 146:163-175.

Willingham, M.C., I.H. Pastan 1982 The transit of epidermal growth factor through coated pits of the Golgi. J. Cell Biol. 94:207-212.

Willingham, M.C., A.V. Rutherford, M.G. Gallo, J. Wehland, R.B. Dickson, R. Schlegel, I.A. Pastan 1981 Receptor-mediated endocytosis in cultured fibroblasts: Cryptic coated pits and the formation of receptosomes. J. Histochem. Cytochem. 29:1003-1013.

Wilson, L., M. Friedkin 1966 The biochemical events of mitosis. I. Synthesis and properties of colchicine labeled with tritium in its acetyl moiety. Biochemistry 5:2463-2468.

Wing, T.Y., A.K. Christensen 1982 Morphometric studies on rat seminiferous tubules. Am. J. Anat. 165:13-25.

Wright, W.W., N.A. Musto, J.P. Mather, G.W. Bardin 1981 Sertoli cells secrete both testis-specific and serum proteins. Proc. Natl. Acad. Sci. 78:7265-7269.

Wright, W.W., M. Parvinen, N.A. Musto, G.L. Gunsalus, D.M. Phillips, J.P. Mather, C.W. Bardin 1983 Identification of stage-specific proteins synthesized by rat seminiferous tubules. Biol. Reprod. 29:257-270.

Yahara, I., F. Kakimoto-Sameshima 1978 Microtubule organization of lymphocytes and its modulation by patch and cap formation, Cell 15:251-259.

Yokoyama, M., J.P. Chang, P.C. Moller 1980 Cytochemical study of concanavalin A binding sites and their mobility in normal cystic fibrosis and SV40 transformed human fibroblast in vitro. J. Histochem. Cytochem. 28: 543-551.

Zaman, Z., M.J. Heynen, R.L. Verwilghen 1980 Studies on the mechanism of transferrin iron uptake by rat reticulocytes. Biochim. Biophys. Acta 632:553-561.

Zinsmeister, V.A.P., G.A. Ackerman 1983 Surface localization of wheat germ agglutinin and concanavalin A binding sites on normal human blood cells: An ultrastructural histochemical study. Tissue and Cell 15:673-681.

ORIGINAL CONTRIBUTIONS

1) Demonstration of fluid-phase pinocytosis by the Sertoli cell at the 14 stages of the cycle of the seminiferous epithelium with the use of markers infused into the lumen of the seminiferous tubules

2) Description of the intracellular pathways taken by the tracers after their internalization by Sertoli cells (e.g. endocytic vesicles, endosomes, multivesicular bodies and secondary lysosomes).

3) Demonstration of adsorptive pinocytosis at stage VIII of the cycle after intraluminal injection with CF and Con A-F.

4) Demonstration of the role of the secondary lysosomes of Sertoli cells in the degradation of phagocytosed cytoplasmic residual bodies of the spermatids.

5) Determination of two different levels of endocytic activity by Sertoli cells during the cycle of the seminiferous epithelium.

APPENDIX

Volumetric changes of Sertoli cells during the cycle of the seminiferous epithelium

Introduction

The present appendix deals with the volumetric determinations of Sertoli cells in relation to the stages of the cycle of the seminiferous epithelium. Since these values were estimated from ratios obtained by Wing and Christensen (1982), and from experimental data obtained as described in Materials and Methods, one of the goals of this chapter is to describe the approach used by these authors to obtain their values. Therefore, this appendix will be divided into the following: (1) Description of the ratios used in the present study, (2) Description of the morphometric estimations obtained by Wing and Christensen (1982), (3) Estimation of the volume of Sertoli cells in relation to the stages of the cycle, and (4) Comments on the volume of Sertoli cells reported by Wong and Russell (1983).

(1) Description of the ratios used in the present study

Table I-A contains the estimations of the absolute areas in given sections of seminiferous epithelium and Sertoli cells obtained by using a MOP-3 instrument in four similar experiments (see Materials and Methods, sections 2 and 6). In addition, the corresponding values of absolute areas of secondary lysosomes, the total number and total number of labelled secondary lysosomes per Sertoli cell in given sections, and the average area of secondary lysosomes expressed in MOP units are similarly represented. Finally, the values obtained by Wing and Christensen (1982), i.e. number of Sertoli cells and volume of epithelium per given length of seminiferous tubules are also expressed in this table. The Roman numerals represent the stages of the cycle and the capital letters represent the type of estimations.

This enumeration was used to simplify the operational program of the computer that performed the calculations according to the formulas used in this investigation (See Materials and Methods, section 6). where:

A = Number of labelled lysosomes per given area of section.

B = Total number of lysosomes per given area of section.

C = Volume of lysosomes per given area of section expressed in MOP units.

D = Volume of Sertoli cells per given area of section expressed in MOP units.

E = Average area of lysosomes expressed in MOP units.

F = Volume of epithelium per given area of section expressed in MOP units.

G = Volume of epithelium per length of tubule*

H = Number of Sertoli cells per length of tubule*

(2) Description of the morphometric estimations obtained by Wing and Christensen (1982).

Since the volume of the Sertoli cell in relation to the stages of the cycle of the seminiferous epithelium was calculated using some estimations obtained by Wing and Christensen (1982), such as the volume of the epithelium per length of tubule and the number of Sertoli cells per length of tubule, it has been decided to analyze the experimental approach used by these authors.

Thus, from 150-200 tubular profiles for each one of the four animals examined, Wing and Christensen (1982) obtained measurements on individual seminiferous tubule profiles, stored in computer files and processed with statistical package, MIDAS (Michigan Interactive Data Analysis System, Fox and Guire, 1976). Calculations and transformations were carried out in MIDAS, and stage differences in seminiferous tubule diameter, luminal ratio and "epithelial or luminal volume" per unit length of the seminiferous tubule

---

*From Wing and Christensen (1982).

were compared by using one-way ANOVA and Scheffe's test in MIDAS (Snedecor and Cochram, 1980). Assuming that the seminiferous tubule was a round tube with a radius (r), a length (L) and a basement membrane surface area (S), Wing and Christensen (1982) applied the standard equation for a cylinder where the volume (V) equals $\pi R^2 L$, while $S = 2\pi rL$. Since they were able to measure the volume and to derive the radius from the measured average diameter of the seminiferous tubule, it was possible to calculate the length of the seminiferous tubule. These authors also considered the presence of hairpin turns of the seminiferous tubule depicted by Clermont and Huckins (1961). By defining a hairpin turn as a segment of a torus with a radio of curvature (R) and with r, S and L defined as above, the volume of a torus was $V = 2\pi^2 r^2 R$, the surface area was $S = 4\pi^2 rR$, while the length was $L = 2\pi R$. From the last equation it was clear that $R = L/(2\pi)$, and so $V = \pi r^2 L$ and $S = 2\pi rL$ which was the same as for a cylinder.

In order to obtain the number of germ cells and Sertoli cells per unit volume of the seminiferous tubules, Wing and Christensen (1982) applied the Floderus (1944) equation $N_V = N_A/(T+D-2h)$, where N_V represents the numerical density, N_A is the number of nuclei or nucleoli counter per unit area, T is the thickness of the section, D is the diameter of the object, and h is the height of the smallest cap sections. Since the specific gravity of fresh testis is near to the unity, 1,040 (Mori and Christensen,1980), the volumes in terms of "cm^3" can be expressed in "grams" (Wing and Christensen,1982). Therefore, these authors were able to describe the numerical densities in terms of number per gram of testis tissue.

The number of cells of a given type per unit length of the seminiferous tubule (N_L) was derived by multiplying the numerical density of the cell in the seminiferous tubule (N_V) by the average cross-sectional area of the

seminiferous tubule of that stage, of $N_L = N_V \pi r^2$, Wing and Christensen (1982) derived this relationship as follows: if r was the average radius of the tubule, n was the cell number in the seminiferous tubule segment, V was the volume and L the length of the segment, then by definition $N_V = n/V$ and $N_L = n/L$, yielding $VN_V = LN_L$ or $N_L = N_V (V/L)$. Since for a cylinder, $V = \pi r^2 L$ or $V/L = \pi r^2$, then $N_L = N_V \pi r^2$.

Based on these analyses, Wing and Christensen (1982) observed a significant increase in the volume of the lumen per centimeter of seminiferous tubule between stages V and VIII, leading up to spermiation, and followed by a dramatic decrease in the luminal volume which occurs simultaneously with the decrease in tubular diameter. These authors found that the prominent decrease in the diameter of the seminiferous tubule was caused by the depletion of the luminal content instead of by the loss of the germinal epithelium, since the latter remained relatively constant over the portion of the cycle in which the tubule diameter was decreasing.

The results obtained by Wing and Christensen (1982) also showed that the number of Sertoli cells and major germ-cell types per unit length of seminiferous tubule remained essentially constant throughout all stages of the cycle of the seminiferous epithelium. This data was consistent with those presented by Bustos-Obregon (1970), from Sertoli cell counts in whole mounts of seminiferous tubule at stages II, IV, V and VII, and later extended to all stages of the cycle by Hermo (1972) in counts of Sertoli cells per unit area of a whole mount tubule.

The estimation of the volume of the seminiferous epithelium and the number of Sertoli cells per length of seminiferous tubule are both expressed in columns G and H of Table I-A, respectively.

(3) Estimation of the volume of Sertoli cells in relation to the stages of the cycle

The volume of the Sertoli cell at the 14 stages of the cycle was calculated applying the following formula:

$$\text{Mean volume of Sertoli cell} = \frac{\text{Volume of Sertoli cell/given area of section}}{\text{Volume of epithelium/given area of section}} \quad (1)$$

$$\times \frac{\text{Volume of epithelium/length of tubule}}{\text{Nr of Sertoli cells/length of tubule}}$$

The statistical analysis by the "two-way analysis" of variance showed that there were significant differences in the volume of Sertoli cells among the stages of the cycle of the seminiferous epithelium ($p \leqslant 0.0005$).

The quantitative analysis revealed that the mean volume of the Sertoli cell was subject to cyclical variations with a low value of 0.53 $\mu m^3 \times 10^3$ (at stage VIII) and with a high value of 0.68 $\mu m^3 \times 10^3$ (at stages X and XIII). Three peaks of high values were registered at stage V (0.66 $\mu m^3 \times 10^3$), and at stages X and XIII (both with 0.68 $\mu m^3 \times 10^3$).

The "t" test demonstrated no statistical differences between stages II and IV, whereas it did show statistical differences between stages XIII and II ($p \leqslant 0.005$), IV and V ($p \leqslant 0.001$), V and VIII ($p \leqslant 0.001$), VIII and X ($p \leqslant 0.005$), X and XI ($p \leqslant 0.001$) and XII and XIII ($p \leqslant 0.001$). Thus, the "t" test clearly showed that the three peaks produced at stages V, X and XIII were statistically significant. The lowest values were registered during stage I late, IV, VII, VIII and XI (see Table IIA and Fig. 1A). The analysis of the variance also indicated no statistical differences among the four experimental groups. Therefore, these results demonstrated that the volume of the Sertoli cells present variations during the cycle of the seminiferous epithelium.

(4) Comments on the volume of Sertoli cells reported by Wong and Russell (1983)

Recently, Wong and Russell (1983) reported that the volume of Sertoli cell at stage V of the cycle of the seminiferous epithelium of the rat was equal to 6,012 μm^3. This estimation was obtained from a three dimensional reconstruction of one Sertoli cell whose volume was calculated by dividing the mean water displacement of the model by "magnification^3". Our results showed that the average volume of the Sertoli cell at stage V was less, approximately 660 μm^3. To analyse this discrepancy, it is emphasized that the absolute values for the volume of Sertoli cells derived in this work depended on data supplied by Wing and Christensen (1982). In fact, the value for the proportion of volumes of seminiferous epithelium occupied by Sertoli cells (obtained experimentally in this research) was multiplied by the volume of seminiferous epithelium per Sertoli cell (obtained from data supplied by Wing and Christensen, 1982). We rely on the latter data because these authors also calculated the number of Sertoli cells per unit surface area of tubule, and their conclusions have been confirmed by others. Thus, Wing and Christensen (1982) calculated that there is approximately one Sertoli cell per 763 μm^2 of tubule surface which is close to the value obtained by Bustos-Obregon (1970) (one Sertoli cell per 549 μm^2 of tubule surface) and to the value obtained by Hermo (1972) (one Sertoli cell per 400 μm^2 of tubule surface) who scored Sertoli cells in whole mounts of fixed tubules. The relatively higher values of Wing and Christensen (1982) reflect the fact that their data were corrected to correspond to values in the fresh testis. In fact, conventional histological fixation by immersion would tend to shrink the tubules, which could give rise to a larger number of nuclei per unit area of tubule surface (Wing and Christensen, 1982).

Moreover, our results show that the proportion of volume of seminiferous epithelium occupied by Sertoli cells corresponds to 23-27%, and are in agreement with the earlier calculations obtained by Assaf (1980) using stereological methods.

Thus, knowing the proportion of epithelium occupied by Sertoli cells calculated from both the volume of Sertoli cells and the seminiferous epithelium per given area of section, plus the number of Sertoli cells and volume of epithelium per length of tubule (calculated by Wing and Christensen, 1982), it was possible to estimate the absolute volume of Sertoli cells at the 14 stages of the cycle of the seminiferous epithelium.

The volume of the Sertoli cell obtained by Wong and Russell (1983) remains unexplained. Notwithstanding, confidence in the volume derived in this work is based on the data presented by Wing and Christensen (1983) which yields other conclusions in agreement with the findings of other workers (Bustos-Obregon, 1970; Hermo, 1972).

---

(1) Volume of any structural entity in a section is equal to the product of the area occupied by that structure in the section times the thickness of the section. Since the thickness of the section is the same for Sertoli cell and epithelium, the ratio of volume of Sertoli cell and volume of epithelium in any section is also proportional to the ratio of the areas occupied by these entities in the section.

Example: $\frac{\text{Volume of Sertoli cell/given area of section}}{\text{Volume of epithelium/given area of section}} =$

$\frac{\text{Area occupied by Sertoli cell/given area of section}}{\text{Area occupied by epithelium/given area of section}}$

TABLE I-A

Estimations used for the calculations of the present investigation

Experiment 1

	A	B	C	D	E	F	G	H
I e	19	46	1017	63206	22.1	269600	3.96	1.61
I l	11	35	805	46868	22.94	203841	3.96	1.61
II	4	31	743	48171	23.96	208385	3.96	1.61
III	4	24	648	44915	27	177723	3.96	1.61
IV	3	13	436	34201	27.25	153601	3.96	1.61
V	8	42	1104	82757	26.28	328585	4.37	1.64
VI	4	24	539	33090	22.45	140935	3.91	1.62
VII	3	20	540	41022	27	163484	3.5	1.58
VIII	6	32	736	72846	23	294077	3.38	1.6
IX	5	9	217	50707	24.11	200833	3.35	1.36
X	25	42	1060	72605	25.23	280493	3.42	1.62
XI	22	39	960	62434	24.61	261390	3.12	1.5
XII	27	45	1236	60619	27.46	235338	3.54	1.54
XIII	45	76	2165	69171	28.48	242633	3.73	1.46
XIV	32	54	1294	50122	23.96	195368	3.44	1.36

Experiment 2

	A	B	C	D	E	F	G	H
I e	18	45	1110	62709	24.66	257714	3.96	1.61
I l	6	23	537	31245	23.34	136847	3.96	1.61
II	4	27	684	49474	25.33	212930	3.96	1.61
III	3	22	352	41633	29.63	182526	3.96	1.61
IV	4	26	702	44713	27	192612	3.96	1.61
V	6	33	821	57923	24.87	234760	4.37	1.64
VI	4	28	680	45506	24.28	187847	3.91	1.62
VII	3	23	606	40595	26.34	180250	3.5	1.58
VIII	4	27	705	50853	26.11	214200	3.38	1.6
IX	6	11	270	55025	24.54	214303	3.35	1.36
X	19	33	773	57711	23.42	202554	3.42	1.62
XI	19	35	879	56330	25.11	235423	3.12	1.5
XII	26	46	1457	57826	31.67	229968	3.54	1.54
XIII	36	53	1581	52596	29.83	219059	3.73	1.46
XIV	29	59	1473	58452	24.98	206297	3.44	1.36

Experiment 3

	A	B	C	D	E	F	G	H
I e	22	45	1203	62212	26.73	239829	3.96	1.61
I l	7	27	667	47266	24.7	180949	3.96	1.61
II	2	16	416	29566	26	138927	3.96	1.61
III	2	20	452	38788	22.6	174289	3.96	1.61
IV	3	21	569	39457	27.09	173106	3.96	1.61
V	3	19	509	38809	26.78	180296	4.37	1.64
VI	4	21	567	44256	27	186514	3.91	1.62
VII	2	21	544	33016	25.9	150760	3.5	1.58
VIII	4	25	630	39102	25.2	170090	3.38	1.6
IX	1.5	3	69	27721	23	120302	3.35	1.36
X	17	32	798	50227	24.93	209456	3.42	1.62
XI	20	36	931	50719	25.86	181456	3.12	1.5
XII	30	56	1706	68566	30.46	239731	3.54	1.54
XIII	46	67	1957	59568	29.2	226546	3.73	1.46
XIV	25	49	1114	41793	22.73	184439	3.44	1.36

Experiment 4

	A	B	C	D	E	F	G	H
I e	13	32	892	50737	27.87	187875	3.96	1.61
I l	6	22	599	35629	27.22	167037	3.96	1.61
II	3	23	610	38198	26.52	163786	3.96	1.61
III	3	20	451	35651	22.55	168975	3.96	1.61
IV	3	23	640	38088	27.82	170090	3.96	1.61
V	2	20	552	48030	27.6	186004	4.37	1.64
VI	3	24	672	55063	28	191001	3.91	1.62
VII	3	24	576	37532	24	167741	3.5	1.58
VIII	3	29	741	44827	25.55	184742	3.38	1.6
IX	8	15	400	40843	26.66	168008	3.35	1.36
X	16	32	860	46985	26.87	181435	3.42	1.32
XI	17	30	968	56002	26.88	192503	3.12	1.5
XII	22	40	1174	57564	29.57	194658	3.54	1.54
XIII	33	55	1561	54798	28.38	196500	3.73	1.46
XIV	32	60	1652	55557	27.53	197007	3.44	1.36

Table II-A

Volume of Sertoli cell at different stages of the cycle x 10^3 μm^3

Stagesof the cycle	Number of experiment				Average (± SEM)
	1	2	3	4	
I early	0.66	0.58	0.60	0.64	0.62±0.02
I late	0.52	0.57	0.56	0.64	0.57±0.02
II	0.57	0.57	0.57	0.52	0.56±0.01
III	0.52	0.62	0.56	0.55	0.56±0.02
IV	0.55	0.55	0.57	0.56	0.56±0.00
V	0.70	0.68	0.67	0.58	0.66±0.03
VI	0.69	0.57	0.58	0.57	0.60±0.03
VII	0.61	0.56	0.50	0.49	0.54±0.03
VIII	0.61	0.52	0.50	0.49	0.53±0.03
IX	0.60	0.62	0.63	0.57	0.61±0.01
X	0.67	0.67	0.74	0.62	0.68±0.02
XI	0.61	0.50	0.50	0.58	0.55±0.03
XII	0.68	0.59	0.58	0.66	0.63±0.02
XIII	0.71	0.73	0.61	0.67	0.68±0.03
XIV	0.71	0.65	0.72	0.57	0.66±0.03

FIGURE 1A

Mean volume of Sertoli cell at the 14 stages of the cycle of the seminiferous epithelium.

The volume of the Sertoli cell presents cyclical variations characterized by 3 prominent peaks of high values at the stages V, X and XIII which have been shown to be statistically significant.

The lowest values are registered during stage I (late), IV, VII, VIII and XI of the cycle of the seminiferous epithelium.

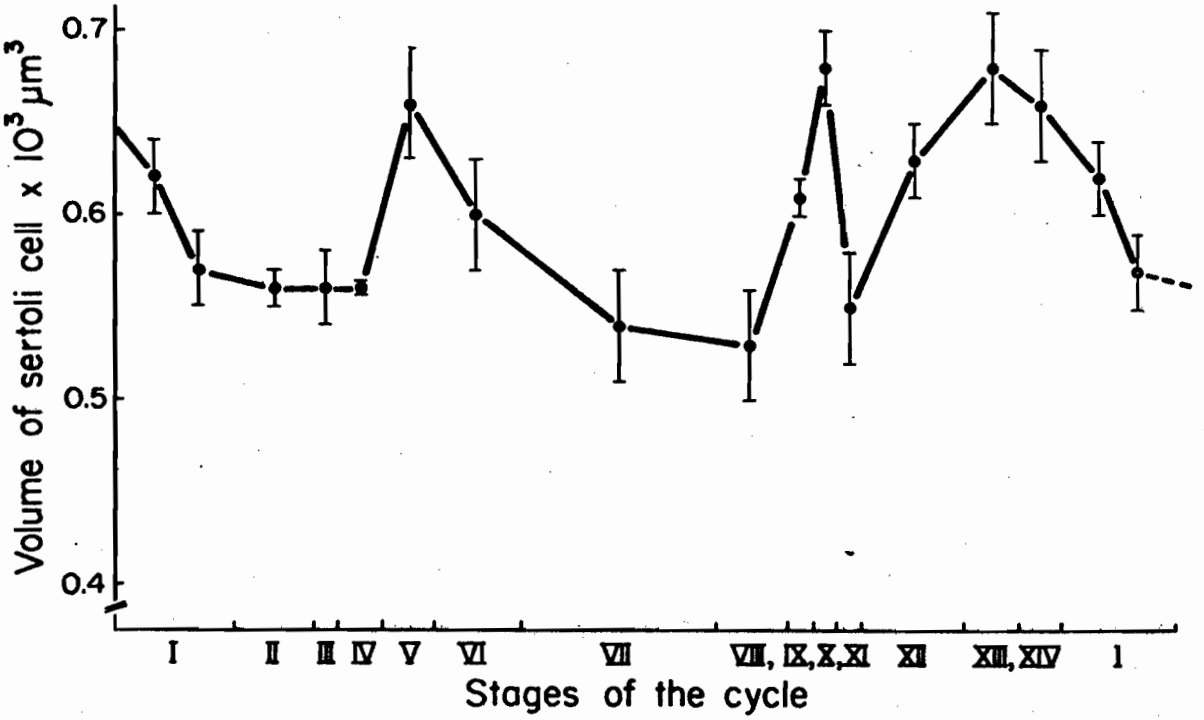
Volume of sertoli cell x $10^3 \mu m^3$
0.7
0.6
0.5
0.4
I
II
III
IV
V
VI
VII
VIII, IX, X, XI
XII
XIII, XIV
1
Stages of the cycle

1A

Literature Cited

Assaf, A.A. 1980 Cyclic changes of cytoplasmic components in rat Sertoli cells. Master of Science Thesis, McGill University, Montreal, Canada.

Buston-Obregon, E. 1970 On Sertoli cell number and distribution in rat testis. Arch. Biol. (Liege) 81:99-108.

Clermont, Y., C. Huckins 1967 Microscopic anatomy of the sex cords and seminiferous tubules in growing and adult male albino rats. Am. J. Anat. 108:79-98.

Hermo, L. 1972 Quantitative study of the spermatogonial stem cell population of the rat. Master of Science Thesis, McGill University, Montreal, Canada.

Floderus, S. 1944 Untersuchungen uber den Bau der menschlichen hypophyse mit besonderer Berucksichtifung der quantitativen mikromorphologischen Verhaltnisse. Acta path. microbiol. Scand. Suppl. 53:1-276.

Fox, D.J., K.E. Guire 1976 Documentation for MIDAS, 3rd ed. Statistical Research Laboratory, Univ. Michigan, Ann Arbor.

Mori, H., A.K. Christensen 1980 Morphometric analysis of Leydig cells in the normal rat testis. J. Cell Biol. 84:340-354.

Snedecor, G.W., W.G. Cochran 1980 Statistical Methods. 7th ed. Iowa State Univ., Ames,Iowa.

Wing, T.Y., A.K. Christensen 1982 Morphometric studies on rat seminiferous tubules. Am. J. Anat. 165:13-25.

Wong, V., L.D. Russell 1983 Three-dimensional reconstruction of a rat stage V Sertoli cell. I. Methods, basic configuration and dimensions. Am. J. Anat. 167:143-161.